Anne Mäkiranta

Renewable thermal energy sources

Sediment and asphalt energy applications in an urban northern environment

ACTA WASAENSIA 454

Vaasan yliopisto
UNIVERSITY OF VAASA

ACADEMIC DISSERTATION

To be presented, with the permission of the Board of the School of Technology and Innovations of the University of Vaasa, for public examination on the 18th of December, 2020, at noon.

Reviewers

Professor Andres Annuk
Estonian University of Life Sciences, Institute of Technology
Kreutzwaldi 1
51014 TARTU
ESTONIA

Dr. Jean-Nicolas Louis
Water, Energy and Environmental Engineering
P.O.Box 4300
FI-90014 UNIVERSITY OF OULU
FINLAND

Julkaisija Vaasan yliopisto	**Julkaisupäivämäärä** Joulukuu 2020	
Tekijä(t) Anne Mäkiranta	**Julkaisun tyyppi** Artikkeliväitöskirja	
ORCID tunniste https://orcid.org/0000-0002-8931-3155	**Julkaisusarjan nimi, osan numero** Acta Wasaensia, 454	
Yhteystiedot Vaasan yliopisto Tekniikan ja innovaatiojohtamisen akateeminen yksikkö Energiatekniikka PL 700 FI-65101 VAASA	**ISBN** 978-952-476-934-1 (painettu) 978-952-476-935-8 (verkkoaineisto)	
	http://urn.fi/URN:ISBN:978-952-476-935-8	
	ISSN 0355-2667 (Acta Wasaensia 454, painettu) 2323-9123 (Acta Wasaensia 454, verkkoaineisto)	
	Sivumäärä 131	**Kieli** englanti

Julkaisun nimike

Uusiutuvat lämpöenergialähteet – sedimentti- ja asfalttienergian sovellutukset urbaanissa pohjoisessa ympäristössä

Tiivistelmä

Tämä väitöskirja arvioi, ovatko uudet geoenergialähteet sedimentistä ja asfaltin alta mahdollisia ja käyttökelpoisia Suomen ilmasto-olosuhteissa. Tutkimus koostuu tapaustutkimuksista, jotka on tehty kahdella kenttätutkimusalustalla pohjoisessa kaupunkiympäristössä: Suvilahden sedimenttilämpökohteessa ja asfalttienergiakentällä Vaasan yliopiston kampusalueella. Sedimenttilämmön käytettävyyttä on tutkittu pitkäaikaisilla lämpötilamittauksilla selvittäen, onko sedimenttilämpö vuosittain uusiutuvaa energiaa. Pitkäaikaisia lämpötilamittauksia on tehty myös asfalttikentällä, jotta voitaisiin määrittää lämpöenergian riittävyys hyödyntämistä varten. Tutkimus sisältää lämpöenergiamäärän arvion molempien urbaanien lämpöenergialähteiden osalta. Tähän väitöskirjaan on sisällytetty yhteensä seitsemän julkaistua artikkelia.

Lämmön palautumisen havaittiin olevan täydellinen sedimenttikerroksessa kesän aikana. Sedimenttilämpöön perustuvan matalaenergiaverkoston energiansäästökyky todennettiin myös. Tarkoituksenmukaisen lämmönkeruuverkoston suunnittelun ja mitoituksen havaittiin olevan tärkeää sedimenttilämmön käytettävyydelle. Asfalttikerroksen osalta tulokset osoittavat, että asfaltin alla on riittävästi energiaa käytettäväksi lämmönlähteenä. Keskimääräisen nettolämpövuon mitattiin olevan vähemmän kuin 15 % saatavilla olevasta säteilyvoimakkuudesta yön aikaisten lämpöhäviöiden vuoksi.

Merenpohjasedimentti on luonnollinen lämpövarasto, joka on uusiutuvaa ja vuosittain täysin auringon lataamaa energiaa. Asfalttilämpö on sopiva lämmönlähde, jopa pohjoisissa oloissa. Havaitut lämpötilat 0,5 m syvyydessä asfaltin alla ovat positiivisia huhtikuusta joulukuuhun. Asfaltti on urbaani geoenergialähde, joka on rakennetun ympäristön sivutuote. Asfalttilämmön käytettävyyttä voitaisiin lisätä optimoimalla maaperän rakennetta pinnan paremman lämmönjohtokyvyn aikaansaamiseksi ja päivittäisellä lämmön keräämisellä kausivarastoon.

Asiasanat

geoenergia, sedimenttilämpö, asfalttilämpö, uusiutuva energia, hajautettu lämpötilojen mittaus

Publisher Vaasan yliopisto	Date of publication December 2020	
Author(s) Anne Mäkiranta	**Type of publication** Doctoral thesis by publication	
ORCID identifier https://orcid.org/0000-0002-8931-3155	**Name and number of series** Acta Wasaensia, 454	
Contact information University of Vaasa School of Technology and Innovations Energy Technology P.O. Box 700 FI-65101 Vaasa Finland	**ISBN** 978-952-476-934-1 (print) 978-952-476-935-8 (online) http://urn.fi/URN:ISBN:978-952-476-935-8 **ISSN** 0355-2667 (Acta Wasaensia 454, print) 2323-9123 (Acta Wasaensia 454, online)	
	Number of pages 131	**Language** English

Title of publication

Renewable thermal energy sources - sediment and asphalt energy applications in an urban northern environment

Abstract

This thesis evaluates if novel shallow geothermal energy, specifically geoenergy sources under sediment and asphalt layer, are viable and usable in Finnish climate conditions. The research consists of case studies implemented in two urban northern open-air study platforms: Suvilahti sediment heat installation and an asphalt energy field at the University of Vaasa (UVA) campus site. The usability of sediment heat is studied by long-term temperature measurements clarifying if sediment heat is annually renewable energy. Long-term temperature measurements are used also in the asphalt field to determine sufficiency of thermal energy in the ground. The research includes an estimation of available thermal energy from both urban heat energy sources. In total, the thesis includes seven published articles.

Recovery of heat in the sediment layer during the summer was observed to be complete. The energy-saving ability of the sediment heat based low-energy network is also verified. Correct planning and sizing of the heat-collection network are considered important elements for the usability of sediment heat energy. With regard to the asphalt layer, results show there is sufficient thermal energy under the asphalt for utilization as a heat source. The average net heat flux density was measured at less than 15 % of the available irradiance due to the night time heat losses.

Sediment heat is natural heat storage which is renewable and annually fully reloaded by the Sun. Asphalt heat is an appropriate heat source, even in higher latitude. Observed temperatures 0.5 m under the asphalt are positive from April to December. Asphalt is an urban geoenergy source which is a by-product of the built environment. The usability of asphalt heat could be increased by optimizing the ground structure for better conductivity of the surface and by daily collection and transfer of heat to seasonal storage.

Keywords

Shallow geothermal energy, sediment heat, asphalt heat, renewable energy, distributed temperature sensing

ACKNOWLEDGEMENT

This study has been conducted in the School of Technology and Innovations at the University of Vaasa. Our Renewable Energy research group is part of the Energy Technology Unit in that school. The research work was carried out over several years until 2020, and the results are based on the data from years 2013–2017. I have been honored to be part of a great research team. That team´s composition has changed over the years, so there are several people who have contributed to this study. I am grateful to you all for making this dissertation possible.

I am most grateful to my supervisors emeritus, Research Manager Dr. Erkki Hiltunen and Professor Seppo Niemi. Dr. Hiltunen has guided and encouraged me during these nine years, first with my second master´s degree and then with this dissertation. We have made a long, productive and fruitful journey. Professor Niemi has always supported and trusted me. Thanks go to both you gentlemen: I have learned a lot from you.

I want to thank my colleagues; Dr. Birgitta Martinkauppi for her contribution in articles, accompanying me in conferences and supporting my research; Dr. Katriina Sirviö for her great company in conferences and assisting me in the first studies; Dr. Carolin Nuortila, Dr. Jukka Kiijärvi and Dr. Petri Välisuo for supporting and counselling me as a researcher; Mr. Tapio Syrjälä, Mr. Janne Suomela and Mr. Thileepan Paulraj for assisting in the studies; Mr. Teemu Ovaska for his peer support; and Mrs. Sonja Heikkilä for being such a kind and handy workmate. I want to express my thanks to all co-authors who have contributed in the publications. As mentioned, my thanks go to our whole research team and also to Levón Institute’s former energy team.

My employer, the University of Vaasa, deserves the greatest thanks for awarding me a doctoral student position for two years. It accelerated and smoothed the dissertation process.

I am grateful to Mr. Mauri Lieskoski of GeoPipe GP Oy for his and his company´s valuable contribution to this study. I want to thank Mr. Pertti Reinikainen retired from Vaasan Vesi for providing the opportunity to take measurements in Suvilahti. I wish to thank Mr. Asmo Huusko and Mr. Ilkka Martinkauppi from Geological Survey of Finland. The collaboration with them has been effortless.

Thanks to my friends and close relatives for being part of my life.

I am thankful for my late mother Leena, my father Teuvo, my sister Mari and my mother-in-law Sisko for their continual help and support. My warmest thanks go my children Ella and Eetu for their patience and giving joy to my life. My dear husband Mika, I want to thank you for your eternal love, support and encouragement!

Vaasa, August 2020

Anne Mäkiranta

Contents

Figures

Tables

Abbreviations

ASHP Air Source Heat Pump

AWHP Air-Water Heat Pump

CO_2 Carbon Dioxide

CST Constant Soil Temperature

DTS Distributed Temperature Sensing

EAHP Exhaust Air Heat Pump

GSHP Ground Source Heat Pump

HDD Horizontal Directional Drilling

Pt100 Platinum resistance thermometer

PVGIS Photo Voltaic Geographical Information System

UVA University of Vaasa

Publications

This doctoral dissertation is based on the following seven refereed publications:

I Hiltunen, E.; Martinkauppi, B.; Zhu, L.; Mäkiranta, A.; Lieskoski, M.; Rinta-Luoma, J. (2015). Renewable, carbon-free heat production from urban and rural water areas. Journal of Cleaner Production, 153: 397-404. ISSN: 0959-6526.

II Mäkiranta, A.; Martinkauppi, J.B.; Hiltunen, E. (2016). Correlation between temperatures of air, heat carrier liquid and seabed sediment in renewable low energy network. Agronomy Research, 14: 1191-1199. ISSN 1406-894X.

III Mäkiranta, A.; Martinkauppi, B.; Hiltunen, E.; Lieskoski, M. (2018). Seabed sediment as an annually renewable heat source. Applied Science, 8(2), 290. ISSN 2076-3417.

IV Mäkiranta, A.; Martinkauppi, B.; Hiltunen, E. (2017). Seabed sediment – a natural seasonal heat storage feasibility study. Agronomy Research, 15(S1): 1101-1106. ISSN 1406-894X.

V Mäkiranta, A.; Martinkauppi, B.; Hiltunen, E. (2016). Design of Asphalt Heat Measurement in Nordic Country. SDEWES 2016 conference. Book of abstracts SDEWES2016, digital proceedings. ISSN 1847-7178.

VI Mäkiranta, A.; Hiltunen, E. (2019). Utilizing Asphalt Heat Energy in Finnish Climate Conditions. Energies, 12, 2101. ISSN 1996-1073.

VII Çuhac, C.; Mäkiranta, A.; Välisuo, P.; Hiltunen, E.; Elmusrati, M. (2020). Temperature Measurements on a Solar and Low Enthalpy Geothermal Open-Air Asphalt Surface Platform in a Cold Climate Region. Energies, 13, 979. ISSN 1996-1073.

Author`s contribution

Paper I: Mäkiranta is the fourth author. Mäkiranta implemented the site measurements in Suvilahti and analyzed the data. She wrote the description of the installation site, sediment heat harvesting system and measurement method.

Paper II: Mäkiranta is the main author. She implemented the site measurements in Suvilahti and did most of the data analysis. She wrote most of the paper.

Paper III: Mäkiranta is the main author. She implemented the long-term measurements in Suvilahti and analyzed the data. She wrote the paper. Mäkiranta conceived and designed the experiments with Hiltunen.

Paper IV: Mäkiranta is the main author. She implemented the long-term measurements in Suvilahti and analyzed the data. She wrote the paper.

Paper V: Mäkiranta is the main author. She designed and performed the background work for planning and chose the research methods on the measurement sites. Mäkiranta planned and implemented two measurement sites on the University of Vaasa (UVA) campus area. She wrote the majority of the paper.

Paper VI: Mäkiranta is the main author. She proposed the research topic and prepared the original draft. Mäkiranta implemented the measurements at the UVA campus site. She analyzed the data. Mäkiranta reviewed and edited the paper, together with Hiltunen.

Paper VII: Mäkiranta is the second author. She implemented the DTS measurements in the asphalt field at UVA campus. She analyzed the data and wrote about those parts of the study. She reviewed and edited the paper, together with Hiltunen.

1 INTRODUCTION

Eliminating the practice of burning of oil and coal is a reasonable objective in the quest for a sustainable future. Geothermal energy is both cleaner and renewable energy. Its use also helps to slow down climate change.

Finland´s heating energy demand could be covered by renewable domestic solutions. This strategy would also improve energy self-sufficiency.

Geothermal energy is thermal energy generated by the Earth. Actually, the continuous cooling of the Earth emits heat. The liquid mass erupting from the outer core of the Earth sets free thermal energy in the form of hot wells, volcanic eruptions and earthquakes. However, the main source of geothermal energy is the decay of long-lived radioactive isotopes. (Lowrie 2007, Boden 2016.)

Pure geothermal energy plays a minor role in Finland and other non-volcanic regions. Instead, shallow geothermal energy i.e. geoenergy, mainly originating from the Sun, is a feasible heat source. (Bertermann et al. 2015, Lund et al. 2016, Zohuri 2018). Geoenergy is low-enthalpy geothermal energy by nature. It is utilized via heat pumps to heat and cool houses (Stober & Bucher 2013, Eicker 2014, Quaschning 2014, Bertani 2017, Rosen 2017).

There is abundant thermal energy in urban environments. Part of it exists due to roads and parking place pavements. Urban geoenergy accumulates in surface layers of the ground, in shallow watercourses and sediment layers beneath the water. This study concentrated on two sources of shallow geothermal energy and their potential to provide renewable urban heat: seabed sediment and asphalt fields.

1.1 Background

It has been observed that geothermal heating systems may malfunction after several years of use if their geothermal bedrock wells are not drilled deep enough. (Nordell & Ahlström 2007, Andersen & Gehlin 2018). There is incomplete recovery of heat balance in the borehole due to the overuse of heat. Seabed sediment heat is shallow geothermal energy but its potential for annual reloading still needs to be studied. This thesis investigates if sediment heat is annually renewable energy and evaluates the extent of recovery of heat balance that is achieved in the sediment layer before autumn.

Shallow geothermal boreholes can function properly if they can be loaded with some excess heat from another source. Asphalt heat could be one such solution. Asphalt has been studied as a solar collector by many researchers and companies (Sheeba & Rohini 2014, Mallick et al. 2012, ICAX ltd. 2012, Zhou et al. 2015, Ooms Produkten 2020). Bobes-Jesus et al (2013) have researched many applications concerning asphalt heat and seasonal storing. Qin & Hiller (2014) noticed that daily cumulative heat storage in deeper ground is only 5 % of the solar absorption. Hermans et al. (2014) has reviewed several methods, including DTS (distributed temperature sensing), to monitor spatial and temporal temperature changes in the subsurface with shallow geothermal applications. This thesis assesses if there is appropriate heat under the asphalt layer to be utilized in Finnish climate conditions, and if the thermal energy is directly usable, or, for instance, should be sent to bedrock storage.

Other key aspects that need to be addressed in determining the potential of sediment heat as a heat source are its energy-saving ability and how to plan and size the heat-collection network. This thesis considers these issues.

The estimation of the amount of available energy from both sediment and asphalt sources is also studied in this thesis. When selecting shallow geothermal sources it is important to be able to assess their available energy potential and long-term sustainability.

1.2 Objectives and scope

The objective of this research was to evaluate if novel shallow geothermal energy sources are viable and usable in Finnish climate conditions with four seasons. The scope of the thesis was sediment and asphalt heat. To achieve its objective this research needed 1) to verify the usability of seabed sediment and asphalt heat and 2) to estimate the available energy from both sources. This work studied the thermal behavior of these heat sources in a high latitude. The amount of thermal energy was clarified and in which conditions it could be utilized.

1.3 Research approach

This was empirical research, implemented by a quantitative experimental research method. The study consisted of case studies implemented in two study platforms: Suvilahti sediment heat installation and an asphalt energy field including a comparable field with lawn cover at the University of Vaasa (UVA) campus site.

This study explains the reason and consequence relationships and defines the phenomena which are described by the measured numerical data and calculated values. The research material was produced by measurements on study platforms with chosen methods and by analyzing data. The seabed sediment temperature data was measured in Suvilahti every month in the years 2013–2016. The temperature data of an asphalt and lawn field was measured in the UVA campus every month in the years 2014–2017. The frequency of measurements was raised above once a month during summers at the UVA campus site.

1.4 Research questions, included publications and dissertation structure

From the main research objective of the thesis, the following research questions (RQ) arose.

The usability of new thermal energy sources:

RQ 1. The usability of sediment heat

- Is sediment heat annually renewable energy? How good is the recovery of heat during summer? (Papers I, II, III, IV)

RQ 2. The usability of asphalt heat

- Is there sufficient thermal energy in the ground under the asphalt layer to be a viable heat source? Is asphalt heat usable with the normal asphalt building structure (gravel, sand and clay)? (Papers V, VI, VII)

RQ 3. How much thermal energy is available from renewable urban heat sources: sediment and asphalt? (Papers IV, VI)

In order to answer these research questions, experimental studies were carried out and seven publications were produced. Four publications cover seabed sediment heat (Papers I, II, III and IV) and three publications address asphalt heat (Papers V, VI and VII). Taken together, these papers provide a unique approach to urban geoenergy applications and their usability in Finnish climate conditions. The long-term measurements are a key element in both research platforms. This dissertation introduces the advantages of urban geoenergy sources but also reveals the critical points of sediment and asphalt heat usability. The novelty of the dissertation is its exploitation of unique open-air research platforms (both sediment and asphalt heat) in a high latitude in order to thoroughly examine the feasibility and usability of these partially researched energy sources.

The objective of Paper I “Renewable, carbon-free heat production from urban and rural water areas” was to describe the sediment heat energy system in Suvilahti and analyze the heat energy consumption and energy-saving ability of a single family house in Suvilahti´s low-energy network.

In Paper II “Correlation between temperatures of air, heat carrier liquid and seabed sediment in renewable low-energy network” the objective was to study the adequacy of network sizing with the help of possible correlations between ambient air, heat carrier liquid and sediment temperatures.

In Paper III “Seabed sediment as an annually renewable heat source” the objective was to verify the possible cooling or annual renewability of a sediment heat source. The effects of long-term usage of heat for a low-energy network´s usability were studied, with the help of the comparison between autumn months with the highest sediment temperature and months with the lowest sediment temperature during the following winter in 2008–2009, 2013–2014 and 2014–2015.

The objective of Paper IV “Seabed sediment – a natural seasonal heat storage feasibility study” was to estimate the annual amount of thermal energy charged into the sediment by the Sun. The estimation was compared with the amount of exploited energy. Additionally, the annual loading of sediment heat was studied with the help of long-term temperature measurements by comparing sediment temperature differences between the warmest and the coldest months of the year.

Paper V “Design of asphalt heat measurement in Nordic country” presented the design and implementation of a unique site measurement field for monitoring solar radiation, heat flux and temperatures under asphalt cover. The design and implementation of a comparable measurement field in the lawn yard was also introduced.

The objective of Paper VI “Utilizing asphalt heat energy in Finnish climate conditions” was to measure temperatures under (depths 0.5–10.0 m) the asphalt layer over a three-year period, determine the depth of constant soil temperature (CST) and compare available energy at a depth of 0.5 m under the lawn layer with that available under the asphalt field. The aim was to determine if asphalt is an appropriate heat source in high latitude.

In Paper VII “Temperature measurements on a solar and low-enthalpy geothermal open-air asphalt surface platform in a cold climate region” the objective was to define the amount of energy absorbed by asphalt, the energy conducted through the asphalt layer and the energy conducted to ground beneath the asphalt.

The dissertation structure is as follows:

Chapter 1 introduces the topic and clarifies the background. It defines the scope of the research and sets the objectives. It presents the research approach, questions and structure.

Chapter 2 presents shallow geothermal energy, urban energy, the Finnish weather conditions and the technical issues of heat-collection.

Chapter 3 introduces the research´s two study platforms and methods. One platform is a residential community with a sediment heat based, low-energy network and the other is an asphalt-paved parking lot at the UVA campus site, with a comparable lawn field to study the usability of asphalt heat. The end of the chapter addresses the validity of the research and evaluation of its methods.

Chapter 4 is presents the results from Papers I–VII, concentrating on those that answer the research questions. First, the usability of sediment heat is clarified, followed by that of asphalt heat. The available energy of sediment and asphalt heat sources is addressed at the end of this chapter.

Chapter 5 discusses the results and suggests future research topics.

Chapter 6 presents the final conclusions and the novel findings of this thesis.

Chapter 7 is a summary of the chapters 1–6.

2 SHALLOW GEOTHERMAL ENERGY

Renewable energy has a central role in mitigating climate change. The discussion is often concentrated on electricity production, but heating, and nowadays also cooling, are critical aspects of life in higher latitudes like Finland. Several renewable energy solutions for heating already exist, such as bioenergy, solar energy and geothermal energy. This thesis examines the new concept of shallow geothermal energy as a heat source, especially in urban areas under Finnish climate conditions. Harnessing locally available existing heat is a modern way to implement beneficial climate actions and reduction of CO_2 emissions. Smart cities are using local renewable energy (Picon 2015, Song et al. 2017, Bhatia et al. 2018).

2.1 Urban energy

Urban areas generate heat locally due to traffic, people, buildings, different pavements (Santamouris 2013) and lack of flora. (Oke 1982, Chen et al. 2017, Mohajerani et al. 2017). Francesco Musco et al. 2016 point out that waste heat generated by energy consumption (heating and cooling plants, industrial activities, transport etc.) is one of the key factors increasing ambient air temperature. This urban energy, including urban geoenergy, accumulates in surface layers of the ground and in sediment layers under shallow water courses. This thesis makes a more detailed study of asphalt heat and sediment heat. Sediment and water courses can be seen as natural heat energy sources (Fang et al. 1996, Banks 2012, Jones et al. 2016, Bush 2018) whereas asphalt heat originates from the built environment. The collection of heat depends on the weather conditions.

2.2 Weather conditions in Finland

The Finnish climate has characteristics of both maritime and continental climates. Therefore, it is called an intermediate climate. The Gulf Stream influences the Finnish climate by continuously warming the region. Winters in Scandinavia and Fennoscandia would be much colder without that stream. (Climate guide 2020). The weakening of the Gulf Stream may mean very severe winters for Finland (Caesar et al 2018). However, summer heatwaves may become more common with the global rise of average ocean temperatures. Anomalies of sea surface temperature may still occur. (Duchez et al 2016).

Due to the northern location, with latitudes from about 60° to about 70°, Finland has four distinct seasons. The northern hemisphere is exposed to more direct sunlight during May, June, and July. The Earth's axial tilt means the Sun is higher in the sky during the summer months, increasing the solar flux in the north. When coupled with seasonal lag of heat transfer, this means June, July, and August are the warmest months in the hemisphere (see Table 1.)

Table 1. Average ambient air temperatures [°C] in Vaasa, Helsinki and Utsjoki in April 2013–March 2017. (Finnish Meteorological Institute 2020).

		VAASA	HELSINKI	UTSJOKI
2013	April	2.4	3.1	-2.4
	May	12.7	12.6	8.1
	June	15.6	17.5	13.9
	July	16.4	18.1	14.0
	August	16.1	17.2	13.1
	September	11.9	12.6	8.6
	October	6.3	7.5	-0.1
	November	2.6	4.7	-6.3
	December	0.8	2.3	-8.7
2014	January	-8.0	-5.9	-17.5
	February	0	0.2	-4.8
	March	1.3	2.1	-5.1
	April	4.2	5.9	-1.0
	May	9.3	10.6	3.4
	June	12.6	13.5	9.2
	July	20.0	20.1	15.4
	August	16.5	17.9	12.2
	September	11.5	13.0	6.2
	October	5.0	6.7	-0.2
	November	1.0	3.2	-7.9
	December	-0.7	0.1	-10.8
2015	January	-3.1	-0.9	-16.1
	February	-0.2	0.9	-8.0
	March	1.1	2.4	-3.3
	April	4.0	5.3	0.8
	May	8.4	9.3	5.1
	June	12.1	13.3	9.2
	July	15.2	16.4	10.9
	August	16.5	17.5	12.7
	September	12.1	13.7	8.4
	October	5.9	6.4	-0.2
	November	3.9	5.6	-4.4
	December	1.2	3.3	-9.1
2016	January	-9.7	-8.8	-19.2
	February	-2.3	0.3	-8.6

	March	0.1	0.9	-4.8
	April	3.3	4.8	-0.2
	May	11.0	13.8	8.2
	June	14.0	15.3	9.8
	July	17.2	17.8	14.8
	August	14.6	16.4	10.5
	September	11.9	13.3	7.8
	October	4.0	5.6	2.3
	November	-1.1	0	-6.8
	December	-0.5	0.2	-9.0
2017	January	-2.3	-1.9	-10.1
	February	-3.9	-2.0	-10.7
	March	-0.3	1.2	-6.5

Frozen ground and frost heave are phenomena which are part of a Finnish winter. However, permafrost, as experienced in Siberia for example, does not occur in Finland. Frozen ground makes the availability and usability of asphalt heat slightly challenging and even questionable in higher latitudes. However, applications already exist in cold environments (Gordon 2005, ICAX 2020, Morita&Tago 2000).

2.3 Technical issues of heat collection

Utilization of thermal energy from asphalt or other cover materials is possible with current ground source heat-collection systems. Sediment heat harvesting is also possible via current coaxial heat-collection pipes and liquids. Horizontal directional drilling (HDD) is used to install the pipes into the sediment layer (Xufeng et al. 2018). The temperature of the collected heat must be raised by a heat pump before it is usable for house heating.

Heat pumps have been used in Finland since 1970. According to Sulpu ry (2020), there were over one million heat pumps sold by the end of 2019. Finnish environmental policy has affected the popularity of heat pumps. (Majuri 2016). They are commonly used either as a main (ground source heat pump GSHP, air-water heat pump AWHP) or secondary heat source (air source heat pump ASHP, exhaust air heat pump EAHP) in single family houses. Centralized heat-pump systems for several buildings with a semi-deep (2 000–4 000 m) borehole are a new and upcoming trend in the field of Finnish geothermal energy (YLE Uutiset 20.1.2020, Helsingin Sanomat 2.6.2020). Innovative applications will be seen, for example, keeping a canal fluid in winter (YLE Uutiset 27.1.2020). An even more ambitious project is seen in Espoo, where the aim is to use deep geothermal heat (6 000–7 000 m) for a district heating network. Geothermal energy is sure to be part of Finnish district heating in the future. (YLE Uutiset 28.11.2014, Länsiväylä 29.5.2020)

3 RESEARCH PLATFORMS, METHODS AND VALIDITY

Rather than use simulations, this study chose to build open-air platforms to acquire data in real Finnish conditions from both asphalt and sediment sources. As a comparison for the asphalt field, similar measurement conditions were made for the lawn field nearby. Sediment temperature measurements could be compared with ones made by the Geological Survey of Finland in 2008–2009.

3.1 The feasibility study of sediment heat: Suvilahti case

Suvilahti is a suburb located only 3 km south of Vaasa city center. The suburb was built in 1969, with additional building completed nearly 40 years later. This later development includes 20 private single-family houses, 28 semi-detached houses and three apartment buildings, totaling 130 apartments, located next to the coast. These buildings were part of a housing fair in 2008. One of the fair´s themes was ecology and renewable energy. (Suomen Asuntomessut 2008). The energy system for the whole fair area was implemented in a totally new way. One part of that system was a seabed sediment heat based low-energy network (Fig. 1). Seabed sediment heat was harnessed to heat and cool houses. This was an innovative method of energy collection in Finland, never before tested.

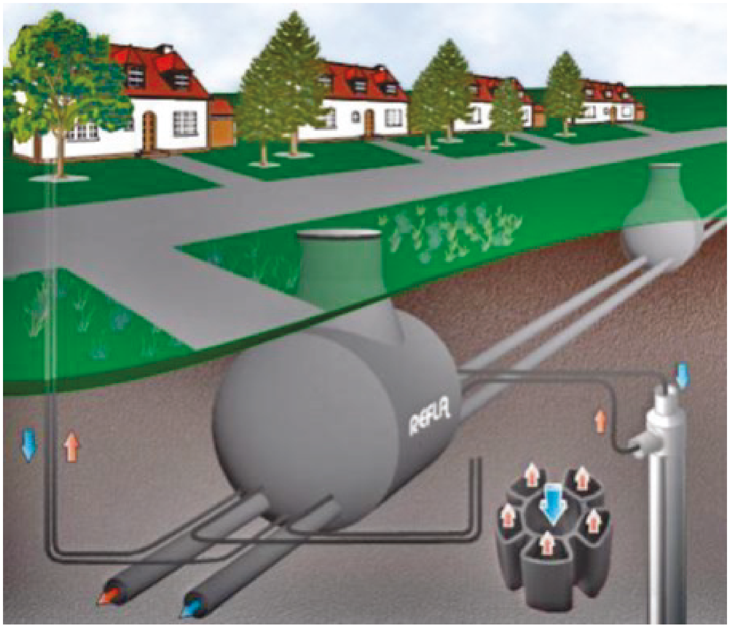

Figure 1. Distribution well in heat-collection network and a profile of “flower” pipe, Refla. (Vaasan Ekolämpö Oy).

3.1.1 Distributed temperature monitoring

The energy conducted to the sediment was studied by means of distributed temperature monitoring. Distributed temperature sensing (DTS) is based on optical light scattering. The DTS measurement device emits short pulses of laser light into a glass fiber cable. Part of that light pulse is backscattered and the intensity of these backscattered bands is acquired by the DTS measurement device. The estimated temperatures are calculated from the temperature-dependent part of this Raman scattering, i.e. Anti-Stokes band. (Selker 2006, McDaniel 2018). The double-ended measurement method was chosen to acquire more data simultaneously. In double-ended measurement, both ends of the fiber cable are connected to the device (Sensornet 2007, van de Giesen et al. 2012). The measurements were made using a Sensornet Oryx DTS device, which has a temperature accuracy of ±0.5 °C. The spatial resolution of the measurements was 1 m.

In Suvilahti, the novel heat source was monitored by measuring sediment temperatures with an optical cable as a linear sensor. A 300 m-long optical cable was attached to each of two heat-collection pipes (also 300 m-long), drilled and installed inside the seabed sediment layer. One pipe with the attached optical cable starts from Liito-oravankatu, the other from Ketunkatu (Fig. 2). Both Liito-oravankatu and Ketunkatu have a well for a splice box with connectors to enable the measurements. Suvilahti´s sediment heat-collection network is a unique open-air research platform and so provides an opportunity for novel research results. Assembly and implementation of this sediment temperature platform was carried out in 2007.

Sediment temperature measurements were taken only once per month because of relatively slow temperature changes in the sediment layer. The results were obtained over a distance of 0–300 m, starting from the shore. One measurement took 10 minutes during which time there was a total of 20 measurements by each measurement channel. The final sediment temperatures were calculated as an average of eight temperatures measured in the same 10-minute period.

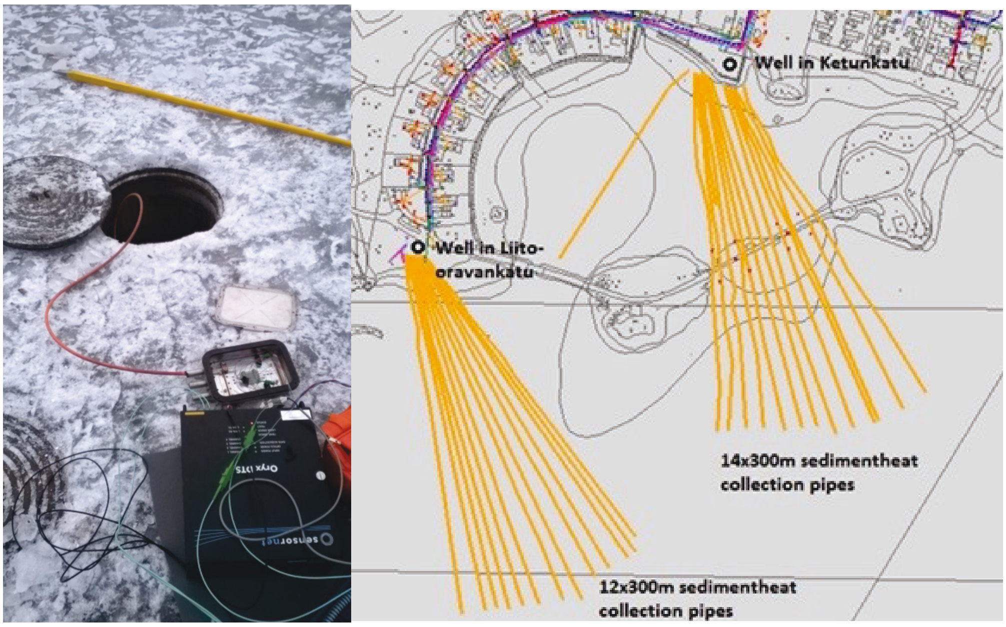

Figure 2. Seabed sediment heat field, comprising 7800 m of heat-collection pipes.

3.1.2 Site measurements implemented by one house owner

One household in Suvilahti collected and saved all the data concerning energy consumption in their single-family house for several years. Data included electricity usage from the grid and electricity needed by the heat pump. The inlet and outlet temperatures of the heat-collection fluid also were acquired.

3.2 The feasibility study of asphalt heat: UVA campus case

An urban environment collects an enormous amount of heat energy from sunlight to the ground due to the different pavements e.g. concrete, asphalt, buildings, people, vehicles and lack of flora. On the other hand, an urban area also has many consumers of heat energy. Harvesting asphalt heat energy for heating and cooling houses offers an opportunity to utilize the urban energy locally. Evaluating if this is possible even in a high latitude, with frozen ground for part of the year, entailed studying ground temperatures beneath the asphalt layer. The unique open-air platform of the asphalt heat measurement field was planned and implemented in the parking lot at the UVA campus site (Fig. 3). A comparable measurement field with lawn cover was established close to the asphalt field at the campus. The aim was to investigate the amount of energy absorbed by asphalt, the energy conducted through the asphalt layer and the energy conducted to the ground beneath the asphalt. The measurement fields were equipped with optical cables buried beneath the asphalt and lawn layers. Additionally, a heat flux plate was included in the asphalt measurement field. A pyranometer was located on the roof of the University´s library building, near both measurement fields. The planning and drilling started in 2013 and the final connections were made in spring 2014.

Figure 3. Drilling of measurement field at UVA campus area in November 2013.

3.2.1 Distributed temperature measurements on asphalt and lawn field

Distributed temperature measurements were used to study the energy conducted to ground beneath the asphalt. The optical cable was installed in the ground to act as a distributed sensor for measuring soil temperatures. Five holes were drilled: two to the depth of 10 m, two to the depth of 3 m and one to the depth of 5 m. Cables were set in the holes to gain the measurement data with 1 m spatial resolution. Wired cable tubes were inserted into the 3 m-deep holes to achieve a measurement spatial resolution of just 0.02–0.03 m (Fig. 4). The splice box with connectors was mounted on a lamppost in the parking lot.

Figure 4. Cables were wired around drainpipes (diameter 100 mm) in the 3 m-deep holes.

The similar design of measurement field was implemented in the lawn yard at the UVA campus shore site (Fig. 5).

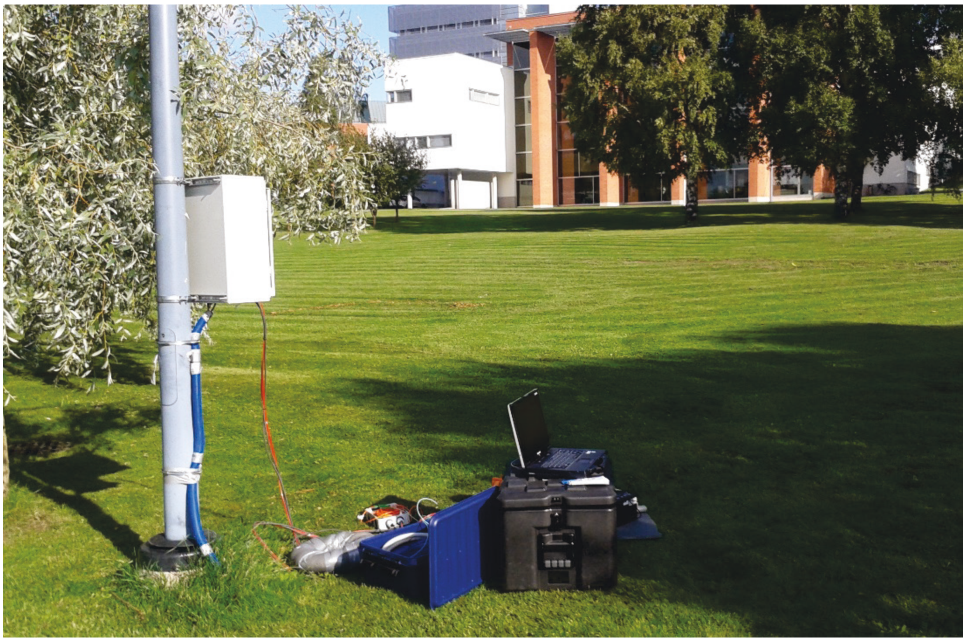

Figure 5. Reference field at the UVA lawn yard.

DTS measurements were made once per month, using a Sensornet Oryx DTS device. However, the measurement frequency was increased to twice per month in summer months because that was seen as more appropriate. The temperature accuracy of the DTS device was ± 0.5 °C. The spatial resolution of the measurements was 1 m. The measurements were always taken on the same date in both measurement fields. Each measurement action took 10 minutes, during which the DTS device made two measurements per minute per channel. The total temperature data consist of 20 measurements per channel. The final asphalt temperatures were calculated as an average of eight temperatures measured at the same 10-minute period on each measurement date. The same principle was used to determine the final temperature in the lawn field too.

3.2.2 Heat flow measurements

Heat flow measurements taken from a heat flux plate were applied to study the energy conducted through the asphalt layer. A heat flux plate is a sensor which consists of a number of thermocouples. The plate detects the positive (towards the ground) and negative (from the ground to the surface) heat flows, thus making it possible to determine the net heat flow during the day (Hoeksema 2015). The heat flux plate in the UVA measurement site was buried in the soil layer, set close to the bottom of the asphalt. This position allowed it to measure the heat flow through the soil layer under the asphalt. The data collection system with wireless gateway was planned and implemented by Cuhac (Cuhac 2019).

3.2.3 Solar irradiance monitoring

The amount of energy absorbed by the asphalt was studied by means of solar irradiance monitoring. This entailed a solar irradiance sensor called a pyranometer. It is designed to measure the solar radiation flux density (W/m^2) from a plane surface with a 180° hemispherical field of a view angle. It measures total, direct and diffuse solar radiation on a surface. (Goswami 2015). The pyranometer was located in an open space as high as possible on the roof of the UVA´s library building, close to both the asphalt and lawn measurement fields. The data were collected via data logger.

3.3 Validity of research and evaluation of methods

The double-ended DTS method was observed to be the most appropriate technique. Temperatures were acquired from two holes under the asphalt and data from both holes were almost identical in long-term measurements. DTS measurements were calibrated during each measurement with the help of Pt100 (accuracy ±0.25 °C) point sensors. In both asphalt and lawn fields at the UVA campus, these sensors were attached to an isolated cable coil, which was part of the actual measurement cable. In the Suvilahti platform, a separate patch cable was used to make the connection for calibrations. The patch cable was routed into an ice-bath to ensure the temperature data validity in double-ended measurements (van de Giesen et al. 2012).

The sensor cables in the seabed sediment were connected to the outside of the system´s heat-collection pipes that contain the heat carrier fluid. The validity of the sediment temperature data can still be regarded as reasonable due to the fact that the fluid´s influence on the surrounding sediment temperature can be expected to be quite small.

Higher vertical spatial resolution (0.02–0.03 m) in the UVA platform was achieved in the 3 m-deep holes by wiring the DTS fiber cable around a 100 mm-diameter drainpipe. Despite thorough preparation and planning, one malfunction was detected in a 3 m-deep hole in the lawn field, possibly due to some tension in the fiber cable during installation. The same configuration worked properly in the asphalt field.

The solar irradiance measured by the pyranometer on a continuous basis was found to be highly accurate, although part of the required data from the pyranometer was missing. Nevertheless, the estimation of irradiance by the pyranometer was found to correlate very well with that provided by the European Union´s Photo Voltaic Geographical Information System (PVGIS), an open source of solar radiation data (Huld et al. 2012).

The data from the heat flux plate were observed to correlate with the pyranometer data and thus heat flux measurement was deemed adequate.

4 RESULTS

4.1 Usability of sediment heat energy

The usability of sediment heat energy was studied in Papers I–IV. The key elements of usability are availability and renewability. Papers III–IV investigate whether sediment heat is annually renewable energy and how thoroughly the recovery of heat balance in the sediment layer takes place during the summer. A further aspect of sediment heat´s feasibility as a heat source is its energy-saving ability. This hinges on correct planning and sizing of the heat-collection network. These issues are clarified in Papers I and II.

Results of paper I:

The novelty of Paper I “Renewable, carbon-free heat production from urban and rural water areas” was that it was the first scientific article presenting the sediment heat energy system in Suvilahti and its new approach to renewable energy production. It also introduced the innovative “flower” pipe (later Refla). Paper I´s objective was to describe the sediment heat system and provide an analysis of the heat energy consumption and energy-saving ability.

The sediment heat energy system´s capability to extract heat from the sediment was verified by the optical short-term temperature measurements (DTS) which clearly indicated a drop in the sediment temperature from the normal temperature of 8 °C during the period of heating. The heat extraction rate from the sediment heat-collection pipes was evaluated to be 40–50 W/m (Aittomäki 2001). The sediment heat based low-energy system worked properly.

The annual heating-related energy consumption (including the hot water) of one household (floor area 234.5 m^2) connected to the low-energy network in Suvilahti was 9 000 kWh. The energy consumption per square meter was 38 kWh/m^2. The average annual energy consumption of a new, low-energy, single family house (140 m^2, 4 people, house location in temperature zone I or II) in Finland is 15 000 kWh for heating and hot water (Motiva 2019). This equates to an average energy consumption per square meter of 107 kWh/m^2, more than double the figure for the Suvilahti sediment energy house. Therefore, the sediment energy system provides evident energy-saving capabilities.

Paper I compared the sediment heat system with other ground source heat systems. Its comparison is summarized here in Table 2 (modified from Table 1 in Paper I). Sediment heat is mainly generated by solar energy. A sediment heat system is not sensitive to damage due to the position of its pipes in the sediment layer. The heat extraction rate of sediment heat system is at a very competent level compared with other ground source heat systems. Sediment heat is suitable for urban areas.

Results of paper II:

The novelty of Paper II “Correlation between temperatures of air, heat carrier liquid and seabed sediment in renewable low-energy network” was its evaluation of the adequacy of pipeline sizing by means of temperature correlations. Studying the delay of temperature changes in the sediment layer was also novel. This work underpinned Paper II´s objective of studying the adequacy of network sizing with the help of possible correlations between ambient air, heat carrier liquid and sediment temperatures, based on the measured data during 2014.

The high correlation between the heat carrier liquid temperature and sediment temperature was observed in Paper II. In particular, there was strong correlation between the liquid temperature and the next month´s sediment temperature, as well as between the liquid and sediment temperature of the same month. This correlation was seen to indicate that the low-energy system was working correctly. In winter, the sediment was getting cooler due to the usage for heating. In summer, the sediment was warming due to the cooling of the houses and the warmer ambient air temperatures.

Table 2. Comparison of different ground source heat systems (GSHS).

System	Water course heat	Ground source heat	Bedrock heat	Sediment heat
Main heat source	Solar energy	Solar energy	Geothermal energy	Solar energy
Annual renewal	Yes	Yes	No	Yes
Number of heat collector units > 20	Yes	Yes	Typically not	Yes
Pipeline`s sensitivity to damage	Yes	Not very	No	No
Main direction of pipe(s)	Horizontal	Horizontal	Vertical	Horizontal
Vertical depth of pipes	In the bottom of a water body	1.2–2 m	100–300 m	3–4 m inside the sediment layer (from the bottom of a water body) (Lieskoski 2014)
Approximate heat extraction rate W/m	15–28 W/m (Banks 2012)	100 W/m (Banks 2012)	20–92 W/m (Stober et al. 2013)	40–50 W/m (Aittomäki 2001)

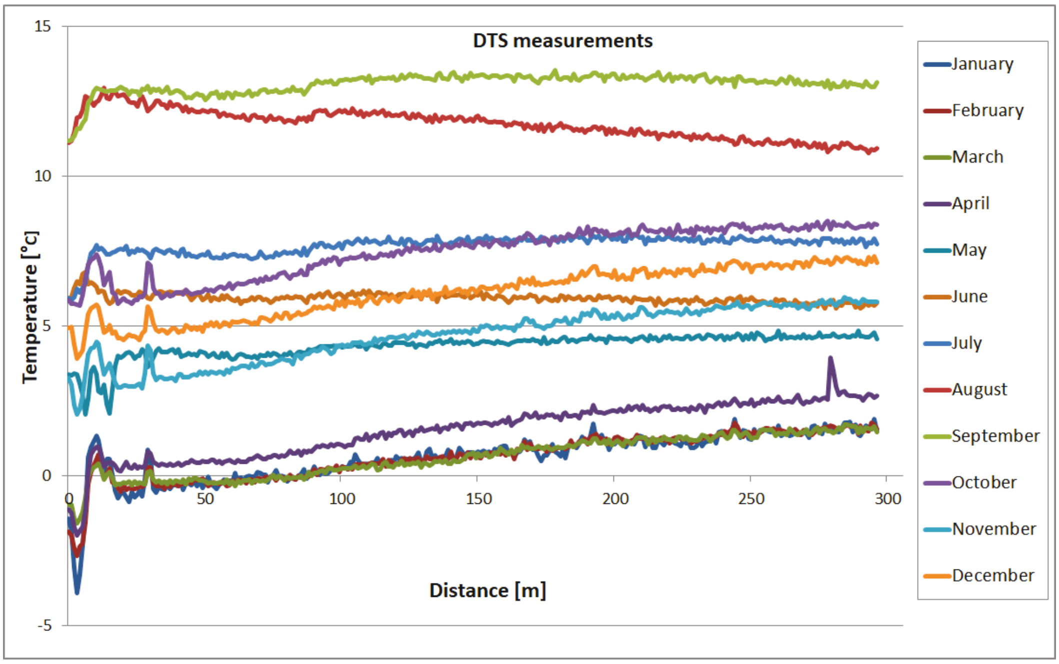

Figure 6. The original temperature data of DTS measurements from seabed sediment in year 2014.

Except in August, the sediment temperature curve (Fig. 6) was noticed to rise slightly up to the end of the pipe (300 m distance from the shore), even in winter. This might indicate that this network is over-sized for its energy demand. The recovery of sediment heat was observed using temperature curves for one year.

The inlet temperature of the heat carrier liquid is higher than the sediment temperature during June and July due to the cooling of houses (Fig. 7). Conversely, house heating reduced the heat carrier liquid temperature compared with the sediment temperature. The cooling of houses is observed as a peak in sediment temperatures in September. Although the ambient air temperature is falling after July, the sediment continues to warm up until September.

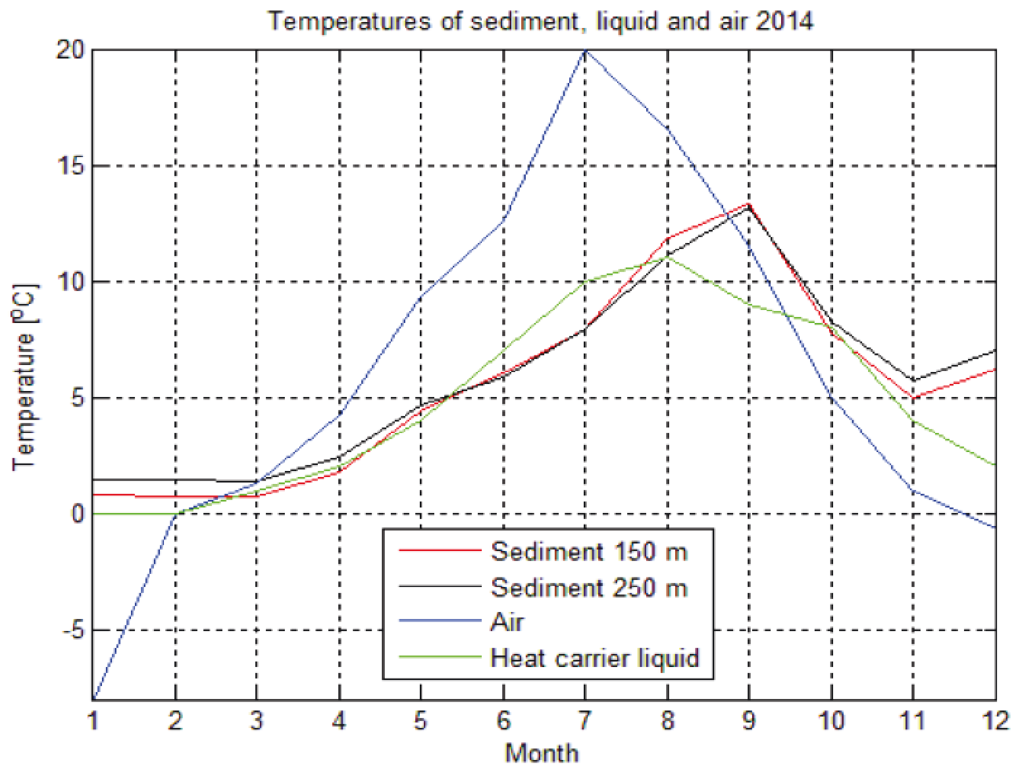

Figure 7. Temperature data from January to December 2014.

The high and significant correlation between the ambient air temperature and temperature of sediment one or two months later was also observed. The sediment temperature was indicating the previous weather conditions (Fig.7.) This delay reveals the heat loading and it has to be taken into account when utilizing sediment heat.

Results of Paper III:

The novelty of Paper III "Seabed sediment as an annually renewable heat source" was its study of sediment heat renewability. It is the first time that long-term measurements have been made and analyzed. Paper III´s objective was to verify annual renewability of sediment heat or the possible cooling of the sediment. The effects of long-term usage of heat for a low-energy network were studied.

The follow-up sediment temperature measurements (Fig. 8 and 9) showed that sediment had been fully reloaded every year. The highest values of sediment temperatures were measured in every autumn. This indicated the annual accumulation of heat.

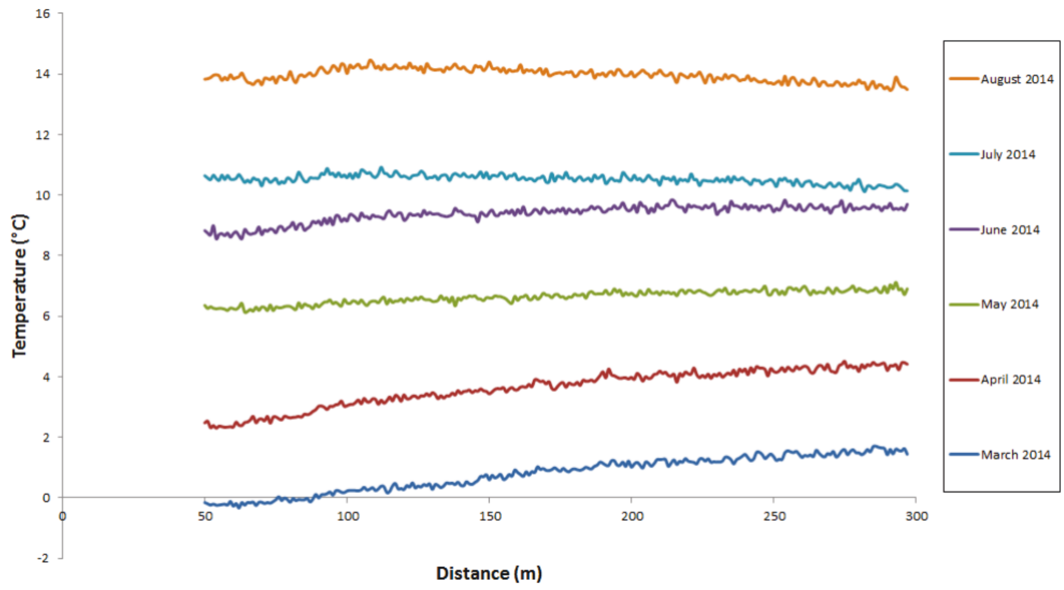

Figure 8. Seabed sediment temperatures against the distance from shore from March 2014 to August 2014 in Liito-oravankatu. Temperatures increased after the winter months.

Within the first 200 m distance from the shore, the slope of the temperature curve was bigger in March and April due to the energy intake. However, from May to August, the sediment was loaded by heat. It could be observed in the temperature curves, which became more horizontal.

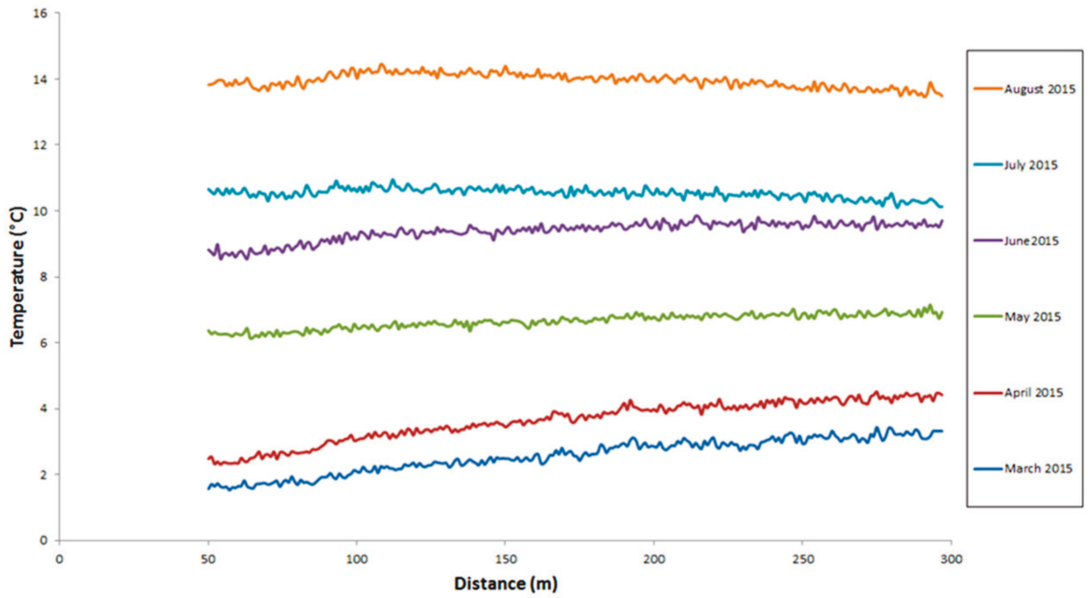

Figure 9. Seabed sediment temperatures measured versus distance from shore from March 2015 to August 2015 in Liito-oravankatu. Heat loading observed as increased temperatures in the sediment layer.

Paper III studied the influence of energy usage on sediment temperatures in the long term. The comparison was made in heating years of 2008–2009, 2013–2014 and 2014–2015. Temperatures were compared between the month with the highest sediment temperature value (in autumn) and the month with the coldest sediment temperature (in winter). The temperature differences during the three studied years were 9.7 °C, 11.1 °C and 11.2 °C respectively (Fig. 10). The use of the energy did not cause a permanent decrease in the temperature rate of the sediment during the several years period of the Vaasa Housing Fair area.

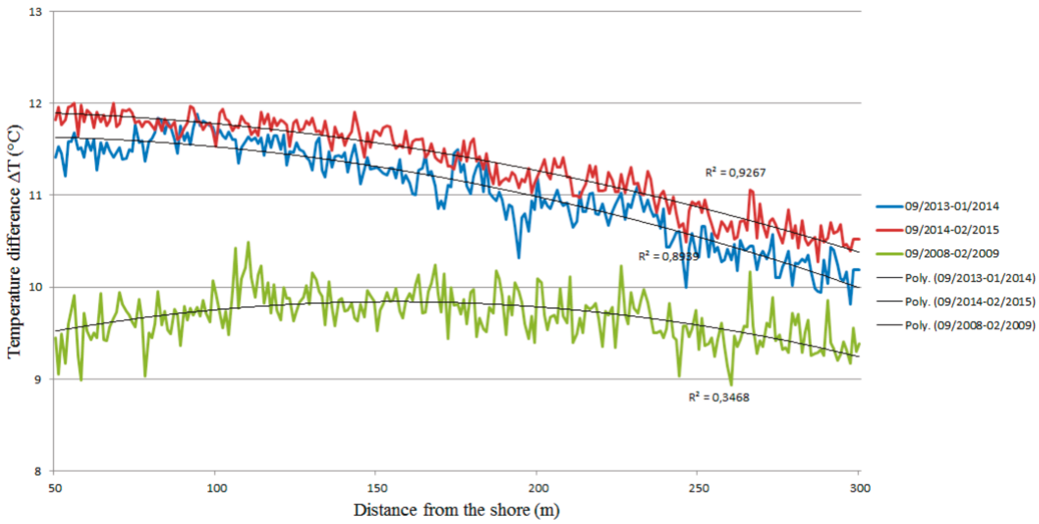

Figure 10. The between-month difference in sediment temperatures for the months with the highest and the lowest temperature values in the periods 2008–2009, 2013–2014 and 2014–2015. The polynomials of second degree are drawn as trend lines.

Results of Paper IV:

The novelty of Paper IV "Seabed sediment – a natural seasonal heat storage feasibility study" was its study of natural seasonal heat storage. Its objective was to estimate the annual amount of thermal energy charged into the sediment by the Sun. The estimation was compared with the amount of energy that was exploited (see 4.3). In addition, the annual loading of sediment heat was studied with the help of long-term temperature measurements.

A three-year measurement period indicated such regular sediment temperature differences between the warmest and the coldest months of the year that it was apparent there was distinct natural loading of heat energy (Fig. 11).

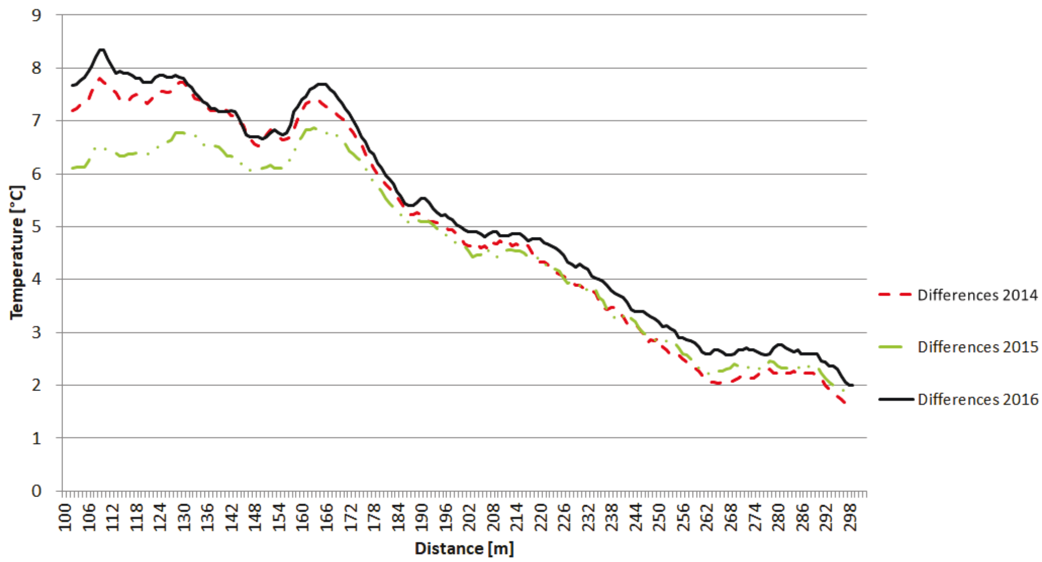

Figure 11. Sediment temperature differences between the warmest and the coldest months during three annual loading periods in 2014, 2015 and 2016 in Ketunkatu as a function of length and distance of the cable from the shore.

Papers I–IV provide the answer to RQ1: sediment heat energy was found to be annually renewable and the recovery of heat in the sediment layer during summer was observed to be complete. The energy-saving ability of the sediment heat based low-energy network was also verified. Correct planning and sizing of the heat-collection network were observed to be important elements for the usability of sediment heat energy.

4.2 Usability of asphalt heat energy

The usability of asphalt heat energy was studied in Papers V–VII. The objective was to find out if there is sufficient heat under the asphalt layer in Finnish climate conditions to be utilized. The papers examined if the thermal energy is directly usable or instead should be steered to an intermediate stage, such as bedrock storage. It was also clarified if a normal asphalt building layer structure (gravel, sand and clay) would be suitable when considering thermal energy utilization.

Results of Paper V:

The novelty of Paper V "Design of asphalt heat measurement in Nordic country" was the use of an open-air research platform for evaluating a possible new energy source in a region with four seasons. The objective was to present the design and implementation of a unique site measurement field for monitoring solar radiation, heat flux and temperatures under asphalt cover. This objective was supported by the design and implementation of a parallel measurement field in the adjacent lawn for comparison of results.

Both measurement fields were planned and implemented successfully. However, one malfunction was detected in a 3 m-deep hole in the lawn field, likely caused by too much tension, either mechanical or some stone exerting pressure on the wired fiber (Fig. 4). The same configuration worked faultlessly in the asphalt field and cable in deeper wells also functioned properly in both fields. Overall, it was possible to take measurements and compare results in both fields.

The monitoring of temperatures under the asphalt started in April 2014. Initial measurements showed temperatures were varying from 18 °C in the topmost layer near the asphalt surface to 8 °C at a depth of 10 m. Temperatures were measured once per month, except in summer months when they were taken twice per month. The design of the monitoring system was found to be unique and is appropriate for application in any northern country. At the planning stage of the measurement field it is important to survey if there are existing cables, pipelines or tunnels under the asphalt. At the installation stage it is recommended to use brand new or unused cable in wired 3 m-deep special installations. A splice box with sufficient capacity should be chosen to facilitate storage and measuring.

Results of Paper VI:

The novelty in Paper VI "Utilizing asphalt heat energy in Finnish climate conditions" was to demonstrate that asphalt-paved areas can act as passive solar collectors and function as a heat source in northern conditions. The objective was to measure temperatures under an asphalt layer (depths 0.5–10.0 m) over a three-year period. This would enable evaluation of the depth of constant soil temperature (CST) and a comparison between available energy under the lawn layer at 0.5 m depth and energy under the asphalt field at the same depth (See 4.3). The aim was to determine if asphalt is an appropriate heat source in high latitudes with four seasons.

The temperatures measured at 0.5 m under the asphalt layer showed a seasonal variation from -3.9 °C to 26.0 °C (Fig. 12). Data from two different measurement holes in each field were almost identical throughout the whole period of 2014–2017 for both the asphalt-covered (Fig. 12) and lawn-covered areas (Fig. 13). The temperatures at 0.5 m under the lawn-covered field (Fig. 13) were lower in the summer than in the asphalt-covered area.

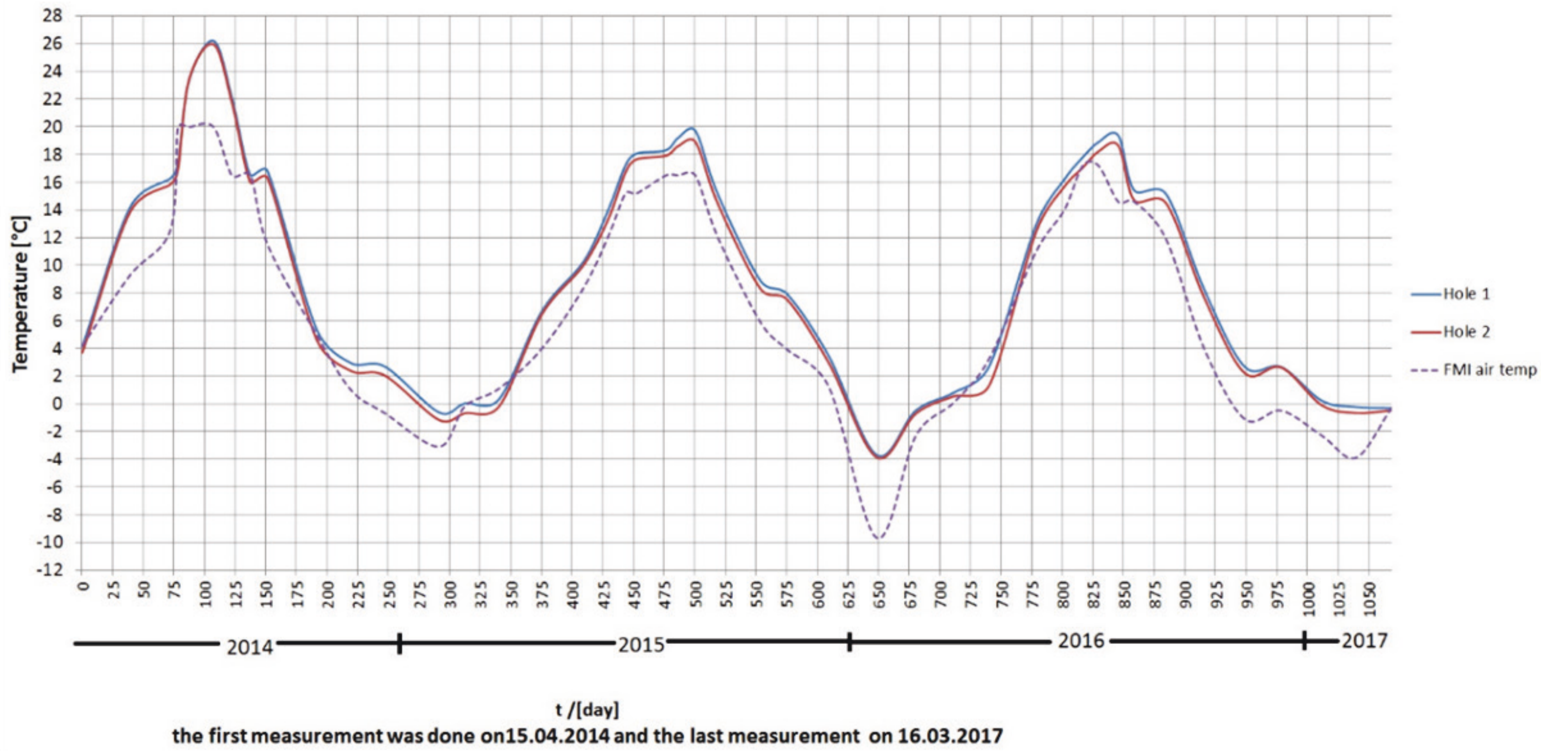

Figure 12. The temperature at 0.5 m under the asphalt layer in two different holes, and the average ambient air temperature of the month.

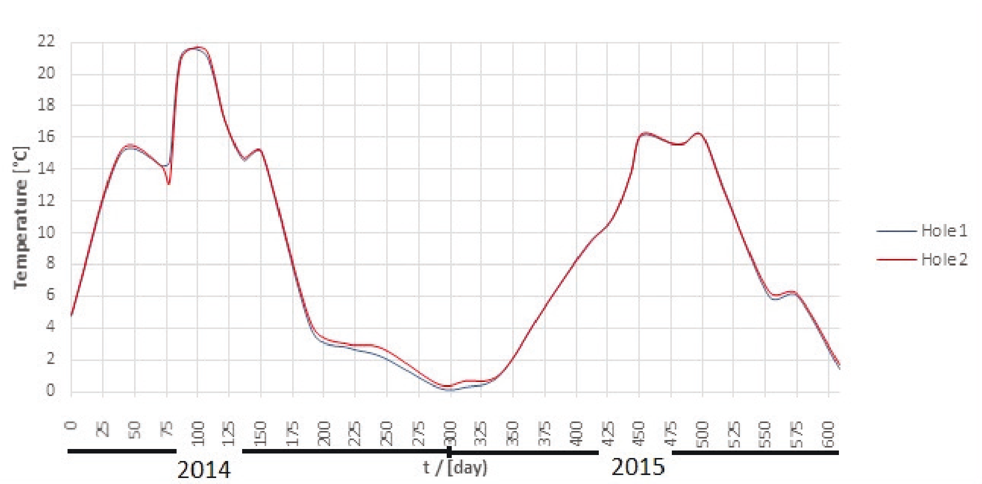

Figure 13. The temperatures in the soil at 0.5 m under the lawn cover.

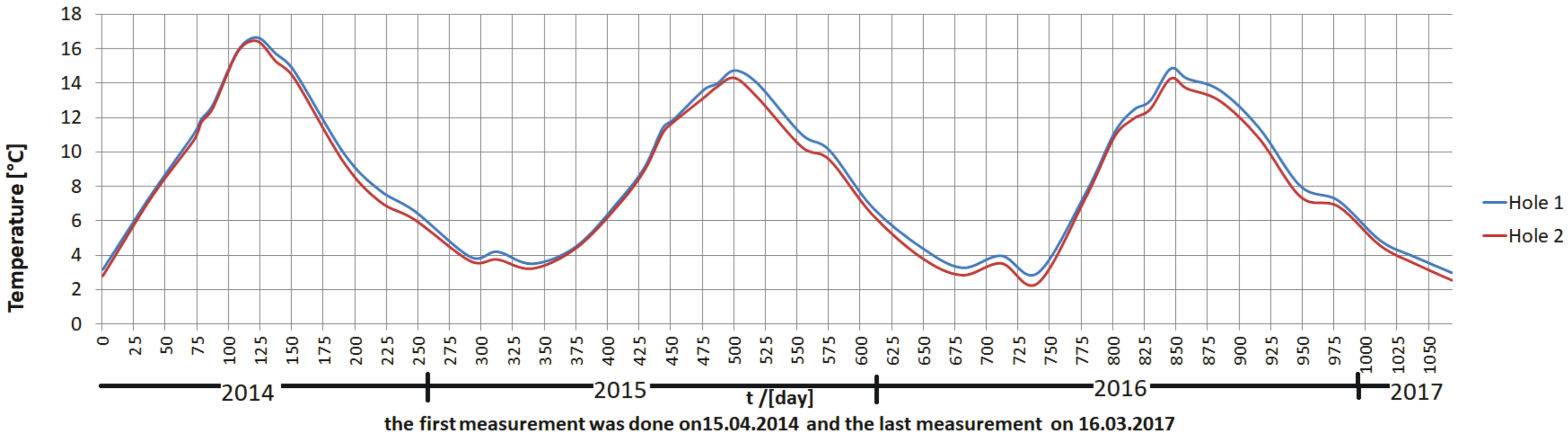

Figure 14. The temperatures in the soil at 1.5 m under the asphalt layer.

The temperature graph at a depth of 1.5 m (Fig. 14) under the asphalt layer shows that the seasonal temperature variation was about 13–14 °C. The lowest temperatures were monitored from January to April, when they varied from 2.4 °C to 4.8 °C. The highest temperatures were in August of each year. Temperatures were quite low during winter and at the beginning of spring. Once again, the data from both measurement holes under the asphalt were almost identical throughout the whole period of 2014–2017.

Temperatures at the depth of 0.5 m (Fig. 12) under the asphalt layer were very promising for heat collection from May until as late as September. Temperatures in May were 10–14 °C: they reached 26 °C in July and were 15–16 °C in September. This five-month period from late spring to autumn can be utilized to collect heat. However, heating demand is quite low in summer, even in Finland, so it is recommended that heat harvested in late spring and summer should be stored.

At the depth of 1.5 m, the temperature fell to just below 3 °C. During a hard and snowless winter this layer is frozen, at least in northern Finland. However, at a depth of 3 m under the asphalt layer the ground remains unfrozen year-round. The temperatures are from 4 to 12 °C, which is actually a very suitable temperature level for utilizing asphalt heat continuously for heating or cooling houses.

The depth of constant soil temperature (CST) was observed to be 10 m. The stabilization of the temperature to 8 °C at this depth, regardless of the season, was recorded in the periods of April 2014–March 2015, April 2015–March 2016 and April 2016–March 2017.

Results of Paper VII:

The novelty of Paper VII "Temperature measurements on a solar and low-enthalpy geothermal open-air asphalt surface platform in a cold climate region" was in studying the thermal energy absorption of the asphalt surface and soil layers beneath the asphalt in a cold climate region by using daily and annual temperature variation data measured in an open-air research platform. The objective was to define the amount of energy absorbed by asphalt, the energy conducted through the asphalt layer and the energy conducted to ground beneath the asphalt.

The measured average heat flux was 140 Wh/m^2 during the daytime. That was 60 % of the daytime solar irradiance. The absorption rate for the entire 24 hours was 14 Wh/m^2, which is only 6 % of the solar irradiance. Heat loss during the night caused this reduction.

The temperature distributions shown in Fig. 15 and Fig. 16 reveal a higher gradient in the topmost gravel layer than in the deeper layers such as clay from about 0.7 m downwards and bedrock from about 3 m downwards. The heat was not flowing efficiently through the asphalt to deeper layers in ground because part of it was dissipated back into the atmosphere from the surface during the night.

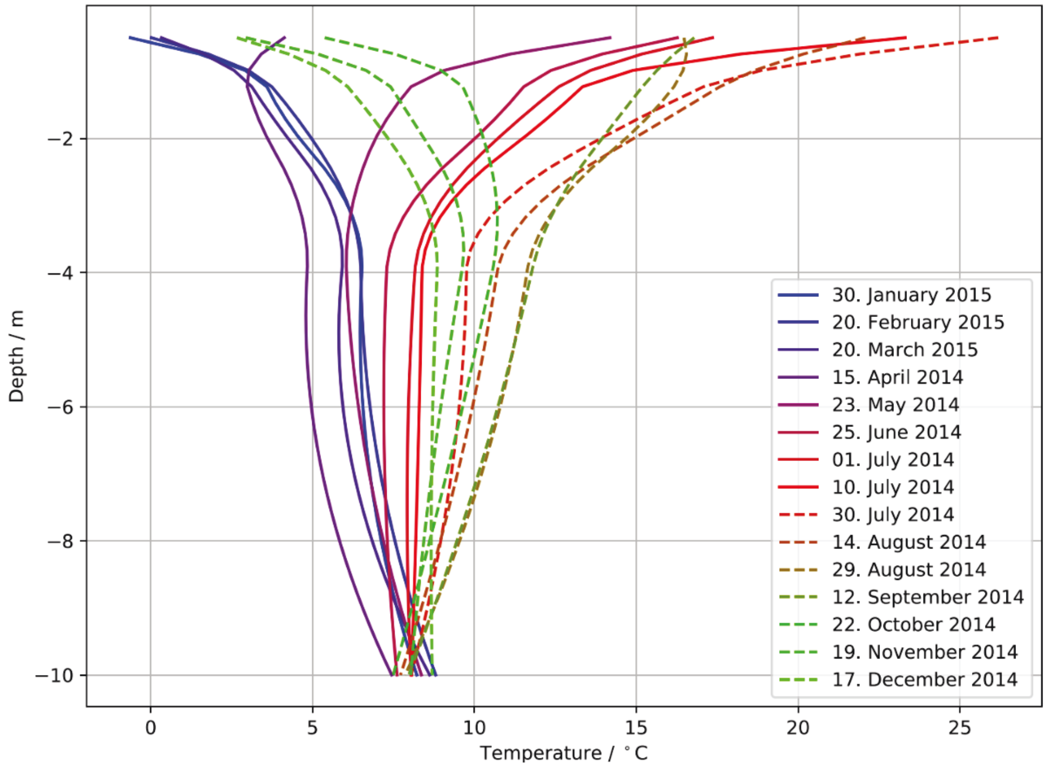

Figure 15. Seasonal soil temperatures in UVA campus area.

The heat conduction speed between studied layers differed, depending on the soil type and heat conductivity. The ground structure could be optimized by increasing the conductivity of the surface by changing the materials or by irrigation.

The average net heat flux density was measured at less than 15 % of the available irradiance due to the night time heat losses, while the average positive heat flux was 64 % of the irradiance. The positive heat flux could be more efficiently utilized by reducing night time losses, which were 3/4 of the positive heat flux during spring and summer, and even higher during autumn (Table 3).

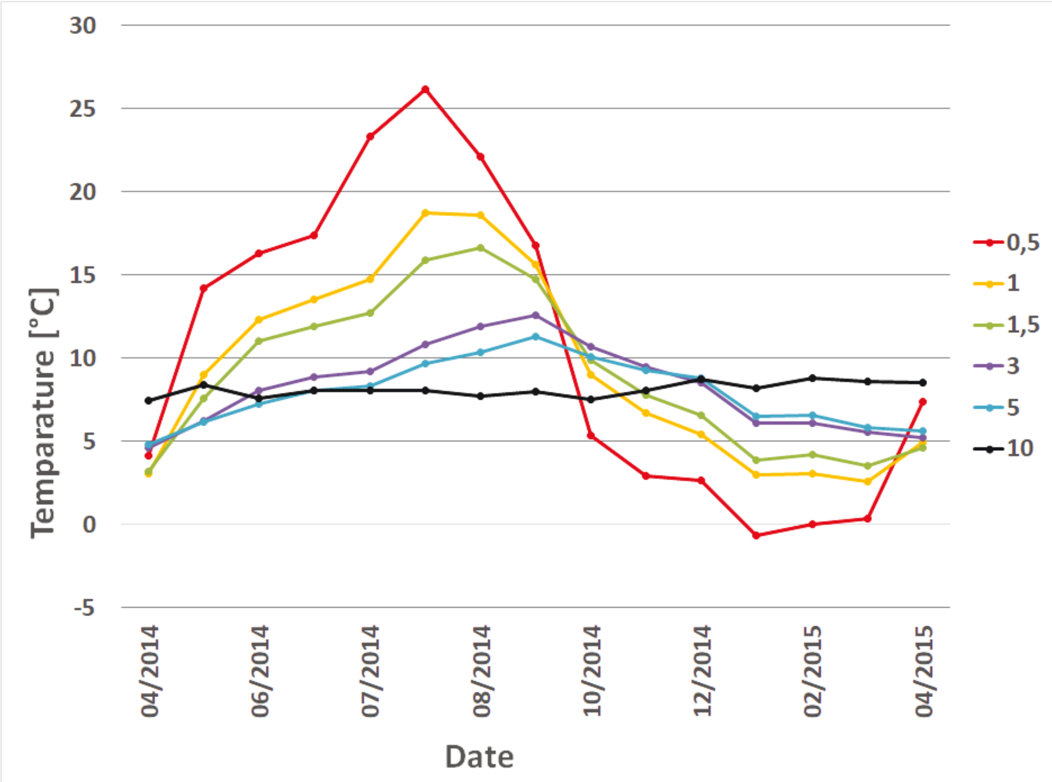

Figure 16. Soil temperatures measured at different depths (from 0.5 m to 10 m) under asphalt layer.

Table 3. Average solar irradiance, heat flux and absorption ratios over five-day periods in all seasons. The first three rows represent the average net heat-collection values over the whole period and the next two rows represent the corresponding data for positive values.

Parameter	*Autumn*	*Winter*	*Spring*	*Summer*	*Yearly average*
Average solar irradiance $\bar{E}_e$	92 W/m^2	11 W/m^2	230 W/m^2	260 W/m^2	148 W/m^2
Average net heat flux $\overline{\varphi}$	-28 W/m^2	-1.9 W/m^2	42 W/m^2	8.4 W/m^2	9.5 W/m^2
Absorption ratio σ	-30 %	-18 %	18 %	3.3 %	6.4 %
Average positive heat flux $\overline{\varphi}_p$	60 W/m^2	16 W/m^2	150 W/m^2	190 W/m^2	104 W/m^2
Absorption ratio, positive flux σ_p	65 %	145 %	65 %	73 %	70 %

Because heat loss due to radiation and convection also occurs during daylight, the positive heat flux could be further improved by lowering the temperature of the surface during daylight hours. This could be achieved, for example, by collecting and transferring the heat to seasonal storage. This would improve the utilization of this urban renewable energy, even in cold climate regions.

Papers V–VII provide the answer to RQ2 by confirming that there is sufficient thermal energy under the asphalt layer to be utilized as a heat source. The conductivity of the surface layers could be improved by changing the materials.

4.3 Availability of energy from sediment and asphalt heat sources

Papers IV and VI examined the estimation of the amount of available energy from both the sediment and asphalt source. It was necessary to compare their individual performances when selecting shallow geothermal sources for optimal available energy potential.

Results of Paper IV and VI:

The novelty of Paper IV “Seabed sediment – a natural seasonal heat storage feasibility study” was its study of natural seasonal heat storage. The objective was to use a simple model to estimate the annual amount of thermal energy charged into the sediment by the Sun. The estimation was compared with the exploited energy amount.

The simplified estimation of incoming energy was calculated for a 1 m radius around the heat-collection pipe (the estimated influence area) and $\Delta T = 5$ °C (the average variation of annual sediment temperature). The calculated value for annually loaded heat energy in the Suvilahti seabed sediment system was 575 MWh. The annual extraction of seabed sediment energy was 560 MWh (Energy Vaasa 2016). Despite the heat consumption, sediment heat seemed to renew well annually.

The sediment temperature differences between the warmest and the coldest months of the year were as much as 8 °C (Fig.11). This indicates that a great amount of energy is available.

One objective of Paper VI “Utilizing asphalt heat energy in Finnish climate conditions” was to compare the available energy at a depth of 0.5 m under the asphalt layer with the energy from the same depth under the lawn field. The aim was to establish if an asphalt-covered area is an appropriate heat source in a high latitude.

The available energy amount in asphalt and lawn fields was calculated with the following dimensions and volume, shown in Fig. 17.

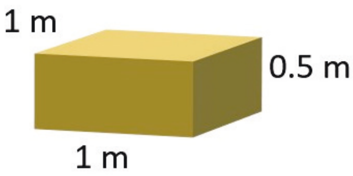

Figure 17. The dimensions and volume of asphalt- or lawn-covered layer used in calculations.

The following calculations are presented in more detail in Paper VI. A theoretical maximum for the available heat energy in the asphalt-covered layer at UVA campus area (V_{tot} = 0.5 m^3) was calculated to be 20 800 kJ ≈ 5.77 kWh when soil types are dry.

A theoretical maximum for the available heat energy in the lawn-covered layer (V_{tot} = 0.5 m^3) was calculated to be 10 400 kJ ≈ 2.88 kWh when soil is dry.

A theoretical maximum for the available heat energy in the lawn-covered layer (V_{tot} = 0.5 m^3) was calculated to be 22 100 kJ ≈ 6.15 kWh when soil is wet and the clay moisture is at 50% (the average moisture level in Finland (Ronkainen 2012)).

As an example, a new, low-energy, single family house (140 m^2, 4 people, house location on temperature zone I or II) in Finland has an average annual consumption of 11 450 kWh (31.40 kWh per day) for heating (Motiva 2019). When comparing only the energy amounts, an area of 5.4 m^2 of asphalt-covered field is equal to this average heating consumption of a single family house for one day. In the case of the lawn-covered field, an area of 10.9 m^2 is sufficient if the soil types are dry, but only 5.1 m^2 is required if the soil types are wet (see Table 4). These simplified calculations depend on the chosen values of the variables.

Table 4. A theoretical maximum for the amount of available heat energy in dry and wet soil types (kWh/0.5 m^3) and the area needed for harvesting the heat for an average daily consumption of the single family house.

	Energy/Dry soil	Harvesting area	Energy/Wet soil	Harvesting area
Asphalt	5.77 kWh	5.40 m^2	-	-
Lawn	2.88 kWh	10.90 m^2	6.15 kWh	5.10 m^2

The results from Papers IV and VI and these simplified calculations provide an answer to RQ3, showing how much thermal energy is available both from sediment and asphalt layers.

5 DISCUSSION

Sustainable energy production needs clean, renewable and domestic solutions. Sediment and asphalt heat would also offer safe local thermal energy in urban areas. This study reveals the typical features of sediment and asphalt heat and also presents areas for further research. The usability of both these renewable energy sources in a northern environment is evident.

The open-air research platform presented some challenges during the sediment temperature measurements. The well in Ketunkatu was often ice-covered in winter and early spring. The well in Liito-oravankatu was also ice-covered inside due to the water-fill from the sea. De-icing and melting delayed the measurement schedule but never prevented measurements.

In order to acquire more accurate sediment temperatures in future studies, it would be reasonable to insert the temperature measurement cable into bare sediment in Suvilahti and to compare those temperatures with the present results.

The open-air platform also caused some difficulties for the asphalt measurements. The laptop cable malfunctioned in winter due to frosty weather but full functionality was resumed after warming in the car. One previously used cable wired around the tube in the lawn field also malfunctioned from the beginning.

However, the repetition of long-term measurements on both platforms was well-managed. Good forward planning and preparation for unexpected circumstances, mainly due to the weather, were the key elements for success.

Usability of sediment heat (RQ 1) was clarified by answering the questions: Is sediment heat annually renewable energy, and how good is recovery of heat in the summer? Paper III concluded that sediment heat energy was annually renewable and recovery of heat in sediment layer during summer was found to be complete. Fang et al. (1996) have simulated sediment temperatures and noticed that open-water seasons and ice-covered seasons have different characteristics of heat flux between sediment and water. Shallow watercourses perform well in terms of gathering sediment heat.

Energy-saving ability was seen as an important aspect when considering the usability of a sediment heat based low-energy network. To develop such a network using seabed sediment heat, the depth and length of the pipeline should be sufficiently large. Correct sizing is important when utilizing this low-enthalpy geothermal energy resource. Amann et al. (2012) have showed the energy-saving ability of ground source heat systems and the importance of correct sizing.

The development of heat-collection pipes is important for effective utilization of sediment heat. The innovative Refla pipe is an example of this developmental progress. Heat pumps are another crucial part of an effective low-energy network. A centralized and jointly owned system serving a network of several households might be the best solution. There is a need for at least strict guidelines to ensure that heat pumps for households are correctly specified. This will support reliable operation of the system and avoid underestimated solutions.

Seabed sediment heat harnesses natural heat storage which is annually reloaded by the Sun. These natural heat stores should be better recognized and utilized. Local decentralized energy systems could exploit naturally generated renewable energy sources. Imported energy could be reduced or perhaps even eliminated.

Usability of asphalt heat (RQ 2) was studied by answering the questions: Is there sufficient thermal energy in the ground under the asphalt layer to be a viable heat source and is asphalt heat usable with the normal asphalt building structure (gravel, sand and clay)? Paper VI revealed that the energy under the asphalt cover is a noteworthy energy source alongside other ground heat sources because of the large usable temperature difference. In the example calculation, the annual maximum temperature at a depth of 0.5 m was 22 °C and the lowest permitted temperature chosen for the soil was 4 °C. Eicker (2014) has presented data from studies in Germany, Italy, Texas and Thailand showing that annual average ambient air temperatures correlate with the prevailing temperature at a depth of 10–15 m in soil with homogenous property. Her work is based on calculations. In this study (Paper VII), a similar result was gained at a depth of 10 m using on-site measurements in Finland. Pokorska-Silva et al. (2019) have measured the temperatures down to approximately 2.0 m from the surface in Poland. They noted that the amplitude of ground temperature decreased with depth and that the influence of air temperature also decreased with depth. The linear correlation between air temperature and ground temperature was clear.

An asphalt surface functions as an active heat collector and could therefore even replace separate solar collectors. The escape of heat during the night prevents asphalt´s use as seasonal heat storage, so its heat should be transferred to more efficient heat storage, such as a borehole (Zhou et al. 2015). Storage of daily absorbed heat by asphalt requires further study. The soil layers beneath the asphalt should be developed to act as more efficient heat transporters, but still retaining the frost insulation capability. Ho et al. (2017) have researched thermal conductivity of geomaterials, concluding that it is highly dependent on the degree of saturation and the density of the soil. These properties can be improved through compaction or replacement of soil.

The issue of energy availability from these innovative sources was investigated to answer RQ 3: How much thermal energy is available from renewable urban heat sources: sediment and asphalt? The energy available from both the seabed sediment and asphalt area proved to be sufficient. The energy potential of the sediment energy network was even higher than the amount of energy actually utilized. In a comparison with ground source heat, there is also enough heat available under the asphalt layer.

This study is the first major research of seabed sediment heat. The research showed the reliability of renewable sediment heat storage. The study platform entailed common heat collection shared by several houses, whereas heat distribution was made individually to each house. A common heat distribution center serving multiple houses, perhaps with several heat sources, would be a topic for future study. The stoniness of the sediment may restrict the implementation of a sediment heat system.

Long-term asphalt temperature measurements on the carefully planned and implemented open-air platform provided new insight about the usability of asphalt heat in northern climate conditions.

Future research should study the feasibility and implementation of asphalt heat collection coupled with storage. Utilization of asphalt heat for cooling houses or as a means of hot water priming are also interesting topics for further research. The asphalt construction structures would need some changes to reduce heat loss from the surface. Capturing and storing energy, and on the other hand, the amount of energy returned from the heat storage, are the core issues to be investigated.

6 CONCLUSIONS

Finally, pulling together all the results of Papers I–VII, the following conclusions can be drawn:

1. Sediment heat is renewable and annually fully reloaded by the Sun.
2. Seabed sediment is natural heat storage.
3. The sediment heat based low-energy system provides evident energy-saving capabilities.
4. Current sediment temperatures indicate previous weather conditions with a delay of one to two months.
5. Asphalt heat is an appropriate heat source, even in higher latitude.
6. Observed temperatures at a depth of 0.5 m under the asphalt are positive from April to December.
7. Asphalt is an urban geoenergy source which is a by-product of the built environment.
8. An asphalt layer´s positive heat flux could be further improved by lowering the temperature of the surface during daylight hours by, for example, collecting and transferring the heat to seasonal storage.
9. The usability of asphalt heat could be increased by optimizing the ground structure for better conductivity of the surface, by changing the materials or by irrigation.
10. The amounts of available energy, calculated by means of the sediment and asphalt research platforms, are suitable for utilization of these long-term low-energy sources.
11. The influence of seasons on ground temperatures dims at the depth of 10 m in the studied asphalt field.
12. The observed temperatures (4 to 12 °C) at the depth of 3 m, are suitable for using asphalt heat continuously for heating or cooling houses.

Sediment and asphalt heat can be regarded as local renewable heat energy solutions in distributed energy production.

According to the presented results and results of Mäkiranta et al. (2015), sediment heat, ground source heat and water course heat are directly usable. However, asphalt heat is worth storing due to its characteristics of daily backscattering and best availability in summer.

It would be advisable to study the possibility of a common sediment heat distribution network, working together with the common sediment heat-collection network. This combination would seem to offer potential to provide a functional, cost-effective and energy-efficient low-energy solution.

Forthcoming research is needed to define the full potential of an asphalt heat-collection and storing system.

7 SUMMARY

This thesis studied two novel shallow geothermal energy sources, namely seabed sediment and asphalt fields, as renewable urban heat sources. The aim was to clarify whether they are usable in Finnish climate conditions with four seasons. The study also included estimations of the amounts of available energy from both the sediment and asphalt sources. The dissertation is based on seven publications: four publications exploring seabed sediment heat (Papers I, II, III and IV) and three publications covering asphalt heat (Papers V, VI, VII). The experimental studies making long-term measurements were conducted using two research platforms.

The thesis introduced shallow geothermal energy and, as a part of it, urban geoenergy: specifically sediment heat and asphalt heat, which both arise in urban areas. The weather conditions in Finland were clarified. The technology for utilizing these novel heat sources was presented and shown to be available.

Two open-air research platforms and experimental methods were presented. The Suvilahti seabed sediment heat study platform was implemented in 2007. In order to study asphalt heat´s potential, the research platform at the asphalt-paved parking lot on the UVA campus site was set up by the research group in 2013–2014, together with a comparable lawn field. The validity of research and the methods were assessed to be reliable.

The results from Papers I–VII showed that both sediment heat and asphalt heat are usable in Finnish climate conditions. The energy proven to be available from these two sources showed that both can be used when considering renewable heating and cooling solutions.

Heat losses from the surface were found to be a critical point for the usability of asphalt heat. Adequate sizing of low-energy system was observed to be a crucial factor for sediment heat usability as a heat source. The possibility of a common heat distribution center is a topic that deserves more detailed investigation in any future research of sediment heat energy. In the case of heat energy from asphalt, heat collection and storing techniques in a high latitude are worthy of future study.

Altogether, twelve novel findings and conclusions were made, of which some main findings are summarized here. Seabed sediment offers abundant natural renewable thermal energy. Sediment heat is annually reloaded by the Sun, with the cooling of houses providing some assistance to the process. Asphalt heat is an appropriate urban energy source, even in higher latitudes. Temperatures at 0.5 m below the asphalt were between -4 °C and 26 °C during the whole monitoring period. The constant soil temperature was found at a depth of 10 m and it was measured as 8 °C throughout the year. Some changes in asphalt construction are proposed in order to optimize conductivity and reduce the escape of heat.

References

Aittomäki, A. (2001). Lämpöpumppulämmitys [only in Finnish]. Suomen lämpöpumppuyhdistys SULPU ry. Finland: Tampere.

Amann, J., Wilson, A., Ackerly, K. (2012). Consumer Guide to Home Energy Savings. New Society Publishers. ISBN-978-0-86571-602-5.

Andersson, O. & Gehlin, S. (2018). State of the art: Sweden. Quality management in Design and Operation of Borehole Systems. A Work document prepared within IEA ECES Annex 27. [Online] [Referred 5.12.2019] Available online: http://media.geoenergicentrum.se/2018/06/Andersson_Gehlin_2018_State-of-the-Art-report-Sweden-for-IEA-ECES-Annex-27.pdf

Banks, D. (2012). Introduction to Thermogeology: Ground Source Heating and Cooling (2nd Edition). John Wiley & Sons. ISBN- 978-0-470-67034-7.

Bertani, R. (2017). Perspectives for Geothermal Energy in Europe. USA: World Scientific. ISBN 978-1786342317.

Bertermann, D., Klug, H., Morper-Busch, L. (2015). A pan-European planning basis for estimating the very shallow geothermal energy potentials. Renewable Energy. Vol. 75. Pp. 335-347.

https://doi.org/10.1016/j.renene.2014.09.033.

Bhatia, S. C. & Gupta, R. K. (2018). Textbook of Renewable Energy. Woodhead Publishing India. ISBN-81-936446-0-3.

Bobes-Jesus, V., Pascual-Munoz, P., Castro-Fresno, D., Rodriguez-Hernandez, J. (2013). Asphalt solar collectors: A literature review. Applied Energy. 102: 962-970.

Boden, D. R. (2016). Geologic Fundamentals of Geothermal Energy. CRC Press. ISBN-1-4987-0877-3.

Bush, M. J. (2018). Climate Change Adaptation in Small Island Developing States. John Wiley & Sons, Inc.

Caesar, L., Rahmstorf, S., Robinson, A., Fuelner, G., Saba, V. (2018). Observed fingerprint of a weakening Atlantic Ocean overturning circulation. Nature. Vol.556, 191–196. 12 April 2018.

Chen, J., Wang, H., Zxu, H. (2017). Analytical approach for evaluating temperature field of thermal modified. Applied Thermal Engineering. Vol. 113: 739-748.

Climate Guide. Nykyinen ilmasto [only in Finnish]. Available online: https://ilmasto-opas.fi/fi/ilmastonmuutos/suomen-muuttuva-ilmasto/-/artikkeli/1c8d317b-5e65-4146-acda-f7171a0304e1/nykyinen-ilmasto-30-vuoden-keskiarvot.html (accessed on 7 January 2020).

Cuhac, C. (2019). Wireless Sensor Network Applications in Military, Agricultural and Energy Research. Acta Wasaensia 431. Finland: Vaasa. ISBN-978-952-476-882-5.

Duchez, A., Frajka-Williams, E., Josey, S. A., Evans, D. G., Grist, J.P, Marsh, R., McCarthy, G.D., Sinha, B., Berry, D. I, Hirschi, J.J-M. (2016) Drivers of exceptionally cold North Atlantic Ocean temperatures and their link to the 2015 European heat wave. Environmental Research Letters. Vol.11. Nr 7: 1-9.

Eicker, U. (2014). Energy Efficient Buildings with Solar and Geothermal Resources. Hoboken: Wiley. ISBN-1-118-35224-6.

EnergyVaasa. Available online: http://energyvaasa.vaasanseutu.fi/en/cases/case-renewable-energy/ (accessed on 10 October 2016)

Fang, X., Stefan, H. G. (1996). Dynamics of heat exchange between sediment and water in a lake. Water Resources Research, 32(6), pp. 1719-1727.

Finnish Meteorological Institute FMI. (2020). Available online: https://www.ilmatieteenlaitos.fi/havaintojen-lataus#!/ (accessed on 4 February 2020)

Francesco Musco & Musco, F. (2016). Counteracting Urban Heat Island Effects in a Global Climate Change Scenario. Cham: Springer International Publishing. ISBN-3-319-10424-1.

Gordon, S. (2005). Energy from the ground up [interseasonal heat transfer]," in *Power Engineer*, vol. 19, no. 4, pp. 20-23. Available online: http://ieeexplore.ieee.org/stamp/stamp.jsp?tp=&arnumber=1509816&isnumber=32330 (accessed on 29 January 2020)

Goswami, D. Y. (2015). Energy Efficiency and Renewable Energy Handbook. CRC Press.

Helsingin Sanomat. 2.6.2020. Vantaalla aletaan porata maahan kahden kilometrin syvyistä reikää. Only in Finnish. Available online: https://www.hs.fi/kaupunki/art-2000006527176.html (accessed on 25 June 2020).

Hermans, T., Nguyen, F.; Robert, T.; Revil, A. (2014). Geophysical Methods for Monitoring Temperature Changes in Shallow Low Enthalpy Geothermal Systems. Energies, 7, 5083-5118.

Ho, I.H., Dickson, M. (2017). Numerical modeling of heat production using geothermal energy for a snow-melting system. Geomechanics for Energy and the Environment. 10, 42–51.

Hoeksema, E. (2015). User Manual, HFP01 & HFP03, Heat Flux Plate/Heat Flux Sensor. Available online: https://www.hukseflux.com/uploads/product-documents/HFP01_HFP03_manual_v1721.pdf (accessed on 23 June 2020)

Huld, T., Müller, R., Gambardella, A. (2012). A new solar radiation database for estimating PV performance in Europe and Africa. Solar Energy, Vol. 86, Iss. 6, pp. 1803-1815.

ICAX ltd. (2012). Heat Storage. Interseasonal Heat Transfer. Energy World. July/August 2012. https://www.icax.co.uk/pdf/Energy_World_Interseasonal_Heat_Transfer.pdf (accesssed on 31 March 2020)

ICAX ltd. (2020). https://www.icax.co.uk/Deicing_Runways.html (accessed on 31 March 2020)

https://www.icax.co.uk/Heated_Runway_Systems.html

https://www.icax.co.uk/toddington_results.html (accessed on 30 January 2020)

Jones, C. S., Mayfield, S. P. (2016). Our energy future: Introduction to renewable energy and biofuels. Oakland, California: University of California Press. ISBN 978-0-520-27877-6.

Lieskoski, M. (2014). Private communications.

Lowrie, W. (2007). Fundamentals of Geophysics. 2. edition. United Kingdom: Cambridge University Press. ISBN-13 978-0-521-85902-8.

Lund, J.W., Boyd, T.L. (2016). Direct utilization of geothermal energy 2015 worldwide review. Geothermics, 60: 66-93.

Länsiväylä. Syvällä Otaniemen kallioperässä olevien lämpökaivojen viimeistely on valmis – seuraavana vuorossa maanpäällisten osien rakentaminen. Only in Finnish. Available online: https://www.lansivayla.fi/paikalliset/1859487 (accessed on 29 June 2020).

Majuri, P. (2016). Ground source heat pumps and environmental policy – The Finnish practitioner's point of view. Journal of Cleaner Production. Vol.139, pp. 740-749.

Mallick, R.B., Bao-Liang, C., Bhowmick, S. (2012). Harvesting heat energy from asphalt pavements: development of and comparison between numerical models and experiment. International Journal of Sustainable Engineering. Vol. 5, No. 2, June 2012, pp. 159-169.

McDaniel, A., Tinjum, J. M., Hart, D. J., Fratta, D. (2018). Dynamic Calibration for Permanent Distributed Temperature Sensing Networks, IEEE Sensors Journal, vol. 18, no. 6, pp. 2342-2352, 15 March15, 2018, doi: 10.1109/JSEN.2018.2795240.

Moharejani, A., Bakaric, J., Jeffrey-Bailey, T. (2017). The urban heat island effect, its causes and mitigation, with reference to the thermal properties of asphalt concrete. Journal of Environmental Management. Vol. 19: 522-538.

Morita, K., Tago, M. (2000). Operational Characteristics of the Gaia snow melting system in Ninohe, Iwate, Japan. GHC Bulletin, December. Pp.5-11.

Motiva Consumer Guidance. Calculator to compare the heating systems. Only in Finnish. Available online: http://lammitysvertailu.eneuvonta.fi/ (accessed on 12 January 2020).

Mäkiranta, A., Martinkauppi, J.B., Hiltunen, E., Lieskoski, M. (2015). Comparison of Different Carbon-Free near Surface Heating and Cooling Sources Usability in Low Energy Network. International Conference on Renewable Energy Research and Applications (ICRERA), proceedings, Palermo, pp. 364-368, doi: 10.1109/ICRERA.2015.7418437.

Nordell, B., Ahlström, A-K. (2007). Freezing problems in borehole heat exhangers. Thermal Energy Storage for Sustainable Energy Consumption - Fundamentals, Case Studies and Design. NATO Science Series, Series II: Mathematics, Physics and Chemistry. Vol. 234. Pp. 193-203. Ed. Paksoy, H. ISBN-978-1-4020-5288-0.

Oke, T. R. (1982). The energetic basis of the urban heat island. Quarterly Journal, Royal Meteorological Society, Vol. 108, Issue 455, pp. 1-24.

Ooms Producten. (2020). https://ooms.nl/specialismen/energie-uit-asfalt-/ (accessed on 31 March 2020).

Picon, A. (2015). Smart Cities. Wiley. ISBN 1-119-07559-9.

Pokorska-Silva, I., Kadela, M., Fedorowicz, L. (2019). Variations of Ground Temperature in Shallow Depths in the Silesian Region. IOP Conference Series: Materials Science and Engineering. 603. doi:10.1088/1757-899X/603/5/052024

Qin, Y., Hiller, J.E. (2014). Understanding pavement-surface energy balance and its implications on cool pavement development. Energy and buildings. Vol. 85: 389-399.

Quaschning, V. (2014). Understanding Renewable Energy Systems. Routledge. ISBN-1-138-78194-0.

Ronkainen, N. (2012). Properties of Finnish soil types. In Finland's Environment 2/2012; Only in Finnish; Finnish. Environment Institute: Helsinki, Finland, 2012; Available online: https://helda.helsinki.fi/handle/10138/38773 (accessed on 16 December 2019).

Rosen, M. (2017). Geothermal energy: sustainable heating and cooling using the ground. United Kingdom: John Wiley & Sons, Inc. ISBN: 978-1119180982.

Santamouris, M. (2013). Using cool pavements as a mitigation strategy to fight urban heat island –A review of the actual developments. Renewable and sustainable energy reviews. 26: 224-240.

Selker, J. S., Thévenaz, L., Huwald, H., Mallet, A., Luxemburg, W., van de Giesen, N., Stejskal, M., Zeman, J., Westhoff, M., Parlange, M. B. (2006). Distributed fiber-optic temperature sensing for hydrologic systems, Water Resources Research, Vol. 42, Issue 12. W12202. ISSN 0043-1397.

Sensornet Ltd. (2007). Oryx DTS User Manual v4. London. UK.

Sheeba, J., B., Rohini, A., K. (2014). Structural and Thermal Analysis of Asphalt Solar Collector Using Finite Element Method. Journal of Energy. Vol. 2014. Article ID 602087, 9 pages.

Song, H., Jeschke, S., Sookoor, T., Srinivasan, R. (2017). Smart Cities. Wiley. ISBN 1-119-22639-2.

Stober, I., Bucher, K. (2013). Geothermal Energy—from theoretical models to exploration and development. Springer. ISBN 978-3642133510.

Sulpu ry. (2020). Top year for heat pumps. Almost 100 000 pumps sold. Million pumps milestone was hit. Only in Finnish. Available online: https://www.sulpu.fi/uutiset (accessed on 3 February 2020).

Suomen Asuntomessut Oy (2008). Vaasa 2008. Only in Finnish. Available online: http://asuntomessut.fi/organisaatio/messuhistoria/vaasa-2008/ (accessed on 22 June 2020).

Vaasan Ekolämpö Oy. Private communications.

Van de Giesen, N.; Steele-Dunne, S.C.; Jansen, J.; Hoes, O.; Hausner, M.B.; Tyler, S.; Selker, J. (2012). Double-Ended Calibration of Fiber-Optic Raman Spectra Distributed Temperature Sensing Data. Sensors, 12, 5471-5485.

Xufeng Y., Ariaratnam, S. T., Dong, S., Zeng, C. (2018). Horizontal directional drilling: State-of-the-art review of theory and applications. Tunnelling and Underground Space Technology. Volume 72, pp. 162-173. ISSN 0886-7798.

YLE Uutiset 28.11.2014. Espoossa aletaan nostaa kaukolämpöä maasta – 120 asteista vettä kilometrien syvyydestä. Only in Finnish. Available online: https://yle.fi/uutiset/3-7657222 (accessed 29 June 2020)

YLE Uutiset 20.1.2020. Suomen ensimmäinen geolämpölaitos käynnistyi – se saattaa korvata kivihiilen ja mullistaa lämmöntuotannon: "Olen suorastaan voitonriemuinen". Only in Finnish. Available online: https://yle.fi/uutiset/3-11158359 (accessed 23 June 2020).

YLE Uutiset 27.1.2020. Suomesta Venäjälle vievän Saimaan kanavan vettä aiotaan alkaa lämmittää, jotteivät laivat jäätyisi siihen kiinni: "Ensimmäinen maailmassa". Only in Finnish. Available online: https://yle.fi/uutiset/3-11177412 (accessed 23 June 2020).

Zhou, Z.; Wang, X.; Zhang, X.; Chen, G.; Zuo, J.; Pullen, S. (2015). Effectiveness of Pavement solar Energy System—An Experimental Study. Applied Energy. 138, 1–10.

Zohuri, B. (2018). Hybrid energy systems: Driving reliable renewable sources of energy storage. Cham: Springer International Publishing. ISBN 978-3-319-70720-4.

Journal of Cleaner Production 153 (2017) 397–404

Contents lists available at ScienceDirect

Journal of Cleaner Production

journal homepage: www.elsevier.com/locate/jclepro

Renewable, carbon-free heat production from urban and rural water areas

E. Hiltunen [a], B. Martinkauppi [a,*], L. Zhu [a], A. Mäkiranta [a], M. Lieskoski [b], J. Rinta-Luoma [a]

[a] University of Vaasa, Wolffintie 34, 65200 Vaasa, Finland
[b] Geo-Pipe GP Oy, Konsterinkuja 5, 65280 Vaasa, Finland

A R T I C L E I N F O

Article history:
Received 26 November 2014
Received in revised form
26 August 2015
Accepted 10 October 2015
Available online 27 October 2015

Keywords:
Heat extraction
Renewable energy
Carbon-free
Urban energy
Sediment heat
Sediment energy system

A B S T R A C T

A new renewable and carbon-free heat energy collection system is introduced in this paper for both urban and rural water areas. Its operation principle rests on the annual renewal of heat energy at the sediment layer under a water body. Thus it is called as sediment heat energy collection system. It has some resemblance with other heat collection systems, and the most important points of these resemblances and differences are discussed in this paper. Several other aspects of sediment and water-area-related energy production are suggested by earlier studies and four of them are reviewed and compared to the suggested system. The sediment heat energy collection system has been installed 2008 for a small district to provide heating/cooling and hot service water as well. The performance analysis of the installed system includes a measure for sediment temperature and consumption of electricity, and user experiences prove the validity of the method.

1. Introduction

Urban energy is the energy which already exists in urban, built and constructed areas. People often think that energy is always imported to the cities or at least it is coming from energy production plants at the countryside. On the contrary, there is a lot of renewable energy in the urban areas where it can be collected even with small distributed systems. The main limitations of adapting to the use of renewable energy are lack of knowledge and shortage of suitable methods for energy harvest. Since the cities have wires and tubes in the ground as well as in the air, it is challengeable and restrictive to build an energy harvest system in those areas. The convenience and approval of the people living in towns is essential to take into account when wind turbines, larger solar collectors or geothermal energy is planned to be built.

In this paper it is described a new approach suitable for urban and rural renewable energy production. It is expected to overcome urban energy limitations and challenges which has been mentioned above. In this approach, the heat energy is collected from solid layers at bottoms of water bodies. These layers consist of sediments and thus the approach is called "sediment energy". The sediment energy is truly renewable energy – it is renewed annually. The main part of its heat energy is from the Sun and a very minor part is from the Earth's geothermal energy. Sediments and water bodies have also been subjected to other studies related to energy production. A review of four other sediment-related approaches has been presented in Chapter 2. The sediment energy system itself is described in detail in Chapter 3.

The sediment energy system is installed for supplying heat and service water for a very small district with 42 houses. The usability of the system has been demonstrated by measuring the sediment temperatures as well as showing the energy consumption. The results indicate that the sediment heat energy is a worthy candidate to heat houses and to produce the hot service water. Since the sediment heat energy is related to other ground source heat systems like borehole heat collection systems and pond- and lake-based ground heat systems, a discussion is provided to show their similarities and differences.

2. A review of some previous studies on sediment related energy production issues

The word "sediment" refers here to the soil existing under ooze layers located at the bottom of water bodies. Sediments are found

* Corresponding author.
E-mail addresses: birmar@uva.fi, jbirgittamartinkauppi@luukku.com (B. Martinkauppi).

http://dx.doi.org/10.1016/j.jclepro.2015.10.039

in lakes, rivers, reservoirs, bays and shallow sea, and they are in this area rich in organic matters usually derived from aquatic phytoplankton and vascular plants, including land plants and macrophytes (Woszczyk et al., 2011). The formation of sediment deposits is promoted by a high level of primary productivity, low influent rate of inorganic matters, high sedimentation rate, low water dynamics, and oxygen depletion.

Sediment compositions vary greatly among water bodies and are affected strongly by land-plant productivity, algal productivity, transport processes and climate conditions (Yang et al., 2011). Fang et al. (2014) found that the total organic carbon (TOC) concentrations of sedimentary sludge in the Lake Dianchi (China) ranged from 0.8 to 1.9%, while Woszczyk et al. (2011) discovered that the surface sediment in the Lake Sarbsko (Poland) was characterized by a TOC content between 0.3 and 18.5%, with most samples rich in TOC (>5%). The ranges of TOC and total nitrogen (TN) at 0.36–0.76% and 0.04–0.09%, respectively, were obtained during the analysis of sea bay sediments (Wang et al., 2013). The average concentrations of TOC and TN in the Yangtze River were found to be 0.79% and 0.10%, respectively (Yang et al., 2011). This variability in compositions enables different applications for sediment usage.

Brine and fresh water sediment-related energy production is a promising avenue due to their abundance. A short review is provided with four previous approaches and their aspects: sediment-based power collection using anodes and cathodes, sediment collection for burning or biogas production, gas hydrate collection from sediment and algae collection for biofuel applications.

2.1. Power collection using sediments from marine or fresh water environment

Many research instruments and vehicles need to be operated long time on sea or lakes without any outer supply current, which would make on-the-spot energy collection very useful (e.g. Wilcock and Kauffman, 1997). One solution would be the use of sediment – especially marine sediment – as a part of this kind of power collection system. For example, a collection system called sediment microbial fuel cell has been suggested and its operation is based on the oxidization of organic matter of sediment by bacteria, causing electricity formation.

As early as 2001, Reimers et al. suggested a collection of energy from marine sediment–water interface (Reimers et al., 2001). The researchers placed one electrode in marine sediment and another one in seawater in the experiments (Fig. 1). This anode–cathode system is the basic structure for the fuel cell. Reimers et al. demonstrated in their laboratory aquaria that the system was able to collect a low level power caused by microbe-based voltage gradients at marine sediments. The power obtained was on the order of 0.01 W/m^2 per geometric area of the electrode.

Tender et al. stated that the power generation is at least from two anode reactions (Tender et al., 2002). The first reaction is caused by micro-organisms close to the anode to oxidize the sedimentary organic carbon. This oxidation produces a by-product, sediment sulfide, which is then again oxidized during the second reaction. Anode materials and their processes were studied further by Lowy et al. (2006). In that study, the anodic current was demonstrated to be notable due to oxidation process of the organic matter of sediment. Micro-organisms on the anode were catalyzing the oxidation. Later Nielsen et al. suggested a chamber-based fuel cell (Nielsen et al., 2007).

Available power density is limited by the quantity of organic sediment ingredient which causes the voltage gradient via oxidation process. One inherent property of most marine sediments is, however, relatively low level content of organic ingredient. Rezaei et al. suggested increasing chitins or cellulose to the anode side to increase the power generation (Rezaei et al., 2007). The tests with substrates showed a significant improvement in the maximum power density.

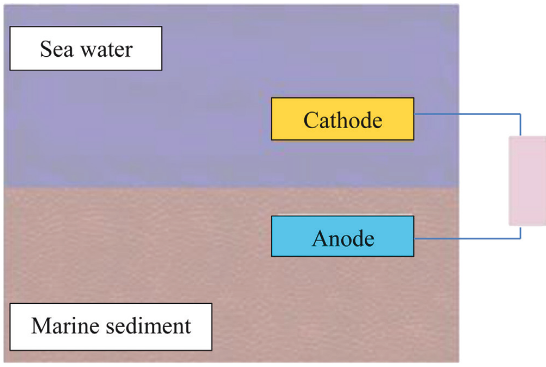

Fig. 1. Microbial fuel cell with an anode in marine sediment and a cathode in sea water.

The power collection from micro-organism is not limited to brine water environments. For example, Hong et al. made the studies in fresh water environment: physico-chemical properties of sediment organic matter were changed during electrical current production from fresh water sediments in the microbial fuel cell (Hong et al., 2010). Micro-organisms, which cause the oxidation of organic maters, are studied and analyzed e.g. in Holmes et al. (2004a,b). The study of Holmes et al. encompassed microbes from marine, salt-marsh and freshwater sediments (Holmes et al., 2004b). The sediment microbial fuel cell is still a promising and quite new approach. So far, the cell has not achieved wider usage probably due to early state of its development as well as limited available energy in sediments.

2.2. Sediment for burning or biogas production

Energy production capabilities of sediments have been tested by burning them, by using them in biogas formation, and by evaluating their content. The first phase in all cases is the collection of sediment from the bottom of a water body, for example, via a floating excavator or a suction dredger or some other means. The collection methods affect on the yield of sediment, so its selection is an important parameter by itself: the floating excavator method provides a high yield of sediment with approximately 80% water content while the suction dredger provides a small amount of dry matter (Saarela, 2012).

The sediment collection itself may cause disturbances and murky in water but its duration might be only few days (Saarela, 2012). The collection might not be suitable for some areas, for example, if it releases dangerous elements or substances from the bottom or causes inconvenience for local people. If sediments are used for burning or biogas production, more than two weeks should be allocated for drying process of the collected sediment (Saarela, 2012) as well as a suitable space for the process. Sediment quality or suitability can be evaluated in advance by measuring its total organic carbon/total nitrogen (TOC/TN) ratio, analyzing its heavy metal content or determining its available energy capacity.

The TOC/TN ratio is also an important indicator for the feasibility of sediment burning or biogas production. The ratio varies with different organic matter sources. For example, bacteria have usually approximately 2.6–4.3 for the TOC/TN ratio, phytoplankton ranges from 6.7 to 10.1 and high terrestrial plants are generally greater than 15 (Wang et al., 2013). The carbon concentration in sediment can be diminishing, due to mineralization which causes organic matter breakdown. Oxidation on the sediment surface or in the water column may obviously influence the TOC/TN ratio. It was found that the TOC/TN ratios of sediments in sea bay were 8.7–11.0 (Wang et al., 2013), lake 5.7–10.0 (Woszczyk et al., 2011) and river 6.6–14.8 (Yang et al., 2011).

Sediments can be digested alone under a high-carbon-content condition or co-digested with carbon-rich matters in the existing digesters. The ideal range of TOC/TN ratio for the anaerobic digestion of organic wastes is 20:1–30:1 (Murphy et al., 2013). As a result of a low TOC/TN ratio, sediments usually should be mixed with carbon-rich materials to efficiently produce biogas. When co-digesting marine sediments with sea wrack biomass, Marquez et al. (2013) obtained a methane yield of 94.33 mL CH_4 gVS^{-1}. A high methane yield of 380 L $kgVS^{-1}$ was achieved during the digestion of seaweed biomass mixed with lagoon sediments in the ratio 4:1 (Migliore et al., 2012).

Sediments can also be subjected to caloric value evaluation and composition analysis as in Saarela's research (Saarela, 2012). Samples from two Finnish lakes were collected from the top 6 cm of the bottom's sediment layer, due to the easy-to-reachness condition and the presumably highest organic material content. The organic material content of the samples fluctuated between 5-35% and the mineral ash content exceeded 40%. Effective caloric value of the sediment was evaluated to be 13.4 MJ/kg or 3.7 MWh/t on the basis of sediment composition. The suitability of the use of the Finnish lake sediment for burning or methane production was, however, limited by problems such as the high mineral (ash) content. The heavy metal contents of sediments did not exceed in most of the cases the limits given by statutes but this might not be the case for other lake areas.

2.3. Hydrate-containing sediments at the sea floor

Marine sediments and permafrost contains gas hydrates, also known as flammable ice. The hydrates are gas molecules with crystal structure and they can consist of, for example, methane, carbon dioxide, or hydrogen sulfide (Sloan and Koh, 2007; Speight and Speight, 2011). Their formation is caused by micro-organism decomposition of dead animals and plants, which make them abundant in many places in the sea floor.

The gas hydrate is a kind of compressed gas storage: one cubic of hydrate may comprise even 164 cubic meters of gas. The marine sediments have been estimated to have a total volume of 1.2×10^{17} m^3 of methane gas (Klauda and Sandler, 2005). Speight stated that the amount of carbon in all known fossil fuels was estimated to be only half of carbon in gas hydrates (Speight and Speight, 2011). Since the methane has energy content of 39.8 MJ/m^3 and gas hydrates existing on the seabed are abundant, the hydrate provides a huge potential energy source at least in theory.

A serious problem in the use of hydrate is the requirements for actual extraction from the sediment (see e.g. Waite et al., 2002 or Turner and Sloan, 2002). For instance, the gas hydrate needs to be at least approximately 20 bar pressure at 0 °C to stay stable on sediments of the sea floor (Stoll and Bryan, 1979). A pressure under 20 bars will cause the hydrate to be decomposed into gas and water, which can lead to a release of methane gas into the atmosphere or sea. The hydrate extraction may also destabilize the subsea landform and cause a landslide (Speight and Speight, 2011).

2.4. Biofuels production from algae blooms

Due to development in world's economy and industry, most countries are confronting worse water body eutrophication problems, which increase the rate of continuous outbreaks of blue–green blooms in those water-bodies (Zhu and Ketola, 2012; Zhu, 2014a). For example, 66% of the Chinese lakes suffer from an over eutrophication level, while 22% of the lakes sustain a severe and extreme eutrophication level (Hu et al., 2013). A feasible implementation scheme has been suggested to properly and efficiently utilize this abundant resource of algae to produce biofuels, and it has several benefits: improvement in water quality, reduction in damages of algae to aquatic ecosystem, and production of the renewable and biodegradable fuels using certain conversion technologies. Algae blooms offer an excellent occasion for the harvest of biomass, which can be re-used to manufacture various renewable and sustainable biofuels such as biodiesel, bioethanol, biogas and biohydrogen among others via thermochemical and biochemical conversion processes (Zhu, 2014a).

Microalgae biomass must be harvested and then dried before further steps in biofuel production. The most common harvest methods consist of sedimentation, filtration, flocculation, flotation and centrifugation, and the most common drying methods include spray-drying, drum-drying, freeze-drying and sun-drying. Harvest and drying are expensive process phases; their portion of costs may be even 20–30% of the total biofuel production costs, and thus optimization in these phases is actively studied for cost reduction (Zhu, 2014a).

The production process parameters are important for the yield. By increasing the temperature of process reaction from 300 °C to 500 °C, the bio-oil yield through the pyrolysis of blue–green algae blooms increased significantly from 26.66% to 54.97% (Hu et al., 2013). One of the best options for biogas production is anaerobic digestion of algae blooms, and which suitability has been verified in many publications (Zhu et al., 2014; Zhu, 2014b). For example, digestion of the sea algae blooms with the dominant species *Ulva lactuca* induced a biomethane yield of 183 L CH_4 $kgVS^{-1}$ (Allen et al., 2013). However, mono-digestion of bloom algae may be problematic, due to a low C/N ratio.

Co-digestion is a practical way to improve the anaerobic digestion performance by adding a certain amount of secondary substrates, such as grease wastes, corn straw, carbon-rich waste papers, kitchen wastes and waste activated sludge (Zhu, 2014b). Studies with different co-digestion substances have already demonstrated a good performance increment. Zhong et al. co-digested bloom algae with corn straw at a C/N ratio of 20:1, and achieved a methane yield of 234 mL CH_4 gVS^{-1} and methane productivity of 1404 mL CH_4 L^{-1} d^{-1} (Zhong et al., 2013). Miao et al. showed that co-digestion of blue algae with pig manure could produce the highest methane yield at 212.7 mL CH_4 gVS^{-1} when an inoculums/substrate ratio was set to 2 (Miao et al., 2014).

3. Suggested approach: sediment heat harvesting

Sediment heat energy utilization rests on its annual renewability. Heat energy is building up in sediment layers during a hot period (summer) when the radiation energy of the Sun is heating the water body which conducts this heat energy to the sediment layers. The conduction process is reversed during a cold period (winter): sediment layers give heat back to water. The heating effect of sediment layers is, however, ecologically significant only for small and shallow, unfrozen water bodies in near arctic or arctic regions (Tsay et al., 1992; Hondzo and Stefan, 1994; Fang and Stefan, 1996). For bigger water bodies, this heating effect has very little importance. The heat transfer from sediment has some natural limitations like ice and snow cover or stratification of water layers.

When air temperature in the near arctic regions drops below zero for a period of time, most of the water bodies will have an ice and snow cover. The ice cover slows down the cooling process by cutting off heat evaporation and thus prevents the water bodies from freezing thoroughly. The temperature of bottom water layers is typically around +4 °C in a cold period, since the water is the densest at this temperature. This water layer for its own part reduces heat conduction from the sediment. As a consequence, the mean sediment temperature is higher than the ground temperature at the corresponding depths during the first few meters. Thus, sediment heat energy system is a worthy option for heating of homes and their service water when a larger water body is near.

Here a scheme for a sediment heat harvesting system is presented and its realization as well as the evaluation of the available energy is analyzed. The sediment heat harvesting system has been implemented with measurement cables to demonstrate the eligibility of sediment energy.

3.1. Installation site

Suvilahti suburb is one of the newest local districts in the city of Vaasa in Finland. It is located at a beautiful seaside, three kilometers from downtown area. The street plan has been specially planned so that the motor traffic is as far as possible from the housing. The idea was to have a natural peace environment. Bicycle and pedestrian traffic has their specially designed roads, and public transportation provides an ecological way of motor transportation. The area has currently approximately 2500 inhabitants.

Suvilahti exhibited Vaasa Housing Fair 2008, which concentrated several themes around construction. One of Fair themes was renewable energy. The sediment energy system is one of the selected systems and it is implemented directly for real life testing. The sediment heat network is connected to 43 single-family houses. These household use the heat of the pipework via heat pumps. The pipework can also be used for cooling in a hot period (summer) via heat pump as well as via plain heat exchanger and convector exhauster.

The system is managed by a company which is owned by the City of Vaasa, the electric company of Vaasa and one private company. New customers should pay at first the joining fee and then a yearly fee related to the heated area.

The site, Suvilahti bay, was investigated in April 2006 by the Finnish Geological Survey (Valpola, 2006). The performed temperature measurements indicate that temperature profile of sediment layer has an increasing trend to the depth of approximate 3 m where a temperature of 8 °C is reached while the water–sediment interface was near 2 °C. The temperature tends to remain constant between 3 m - 6 m. The gradient change is accompanied by change in material: the upper bottom layer between 0-3 m consists of sulfidic clay gyttja while the lower layer from 3 m to 6 m is comprised of denser clay. The chemical, microbiological and bacteriological activities inside sediment clay layers may produce not more than unsubstantial amount of heat according to current knowledge.

3.2. Sediment heat harvesting pipe system

Heat collection and release is performed with a specially designed pipe structure ("flower"), which is used in a special pipe network for heat transfer. Fig. 2 displays the structure of the pipe and describes the heat collection.

On the shore side the heat collection pipes are connected to each other in a so-called heat collecting well and thus they are close to the ground (depth 0 m). The other ends in the sediment are buried in the depth of 3–4 m from the bottom of the lowest water layer. The pipe installation profile is shown in Fig. 3. The pipes were simply pushed into the sediment layer.

The pipes were installed in two groups as a fan formation (Fig. 4) with connection to a heat collection well. The current installed system consists of two collection wells. In the first well (at Ketunkatu Street) there are 14 pipes, while in the second well (at Liito-oravankatu Street) there are 12 pipes. The length of each pipe is 300 m, so the total pipework length is 7800 m.

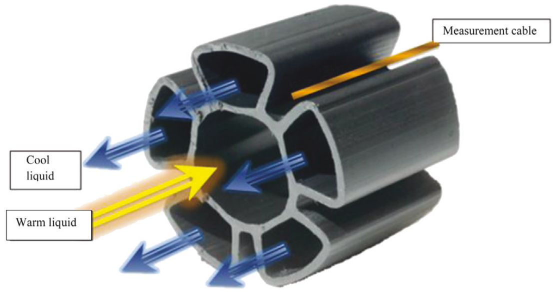

Fig. 2. A pipe structure for heat collection. Cooler heat carrier liquid flows in the outer chambers of "flower" pipe while collecting heat from the sediment and thus warming up. The warmed up heat carrier liquid returns back to the heat collection well in the middle chamber. A measurement fiber was installed along the pipe and accommodated between two outer champers (Mauri Lieskoski private communications; source of the figure: Vaasan Eko-lämpö Oy).

A special device, called heat collection well, is used to connect pipes (see Fig. 5) to the rest of the heat system. Carrier fluid from the wells traverses control point system to distribution wells. The distribution wells are used to distribute the heated fluid to individual houses. These wells are connected to the houses via pipes for coming and returning carried fluid. The system itself has in total 12 distribution wells (Fig. 6). Currently the carrier fluid is a mixture of water and ethanol whose frost resistance is −15 °C. Thus, the operation of the system is not greatly affected even under frozen condition of the sediment.

According to Aittomäki, 2001, sediments have an approximate heat extraction rate from 40 to 50 W/m or 2–3 times more than available in shallow ground for a horizontal heat collection system at Finland (Aittomäki, 2001). The theoretical available energy can be obtained by multiplying the heat extraction rate (here 40–50 W/m) with the length of the pipes (7800 m). This energy for the installed system is thus about 0.31 MW–0.39 MW or 0.31 MJ/s–0.39 MJ/s which is equal to 1.1 GJ–1.4 GJ per hour.

3.3. Fiber optic distributed sensing

Distributed temperature sensing (DTS) was selected to monitor the thermal performance of sediment heat collection. Many applications have demonstrated the usefulness of fiber optic DTS

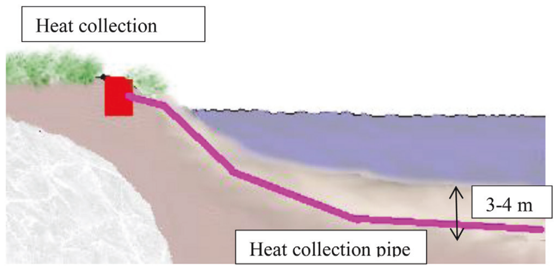

Fig. 3. A heat collection pipe is shoved into sediment at the depth of 3–4 m. The depth increases as the distance from the shore increases. The exact depth of pipes is not known e.g. due to changing conditions of the water bottom. The heat collection pipes are connected to heat collecting well.

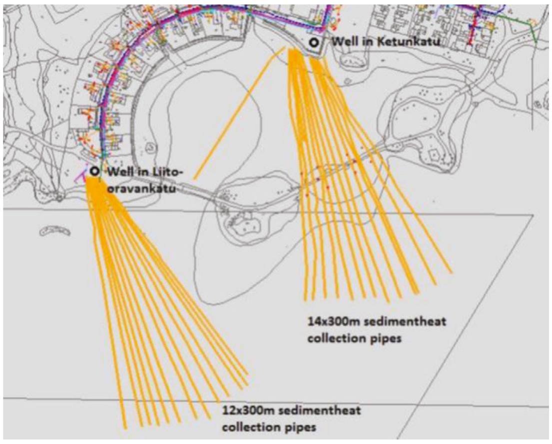

Fig. 4. The heat collection pipes were installed a fan like structure where pipes are connected to energy collection well. Current installation has two wells with 12 and 14 collection pipes. Source of Figure: Vaasan Eko-lämpö Oy.

(Selker et al., 2006; Tyler et al., 2009; Vogt et al., 2010). For example, Hurtig et al. applied DTS, especially to vertical boreholes (depth 40 m), to obtain their temperature profiles (Hurtig et al., 1994).

The operating principle of DTS is the Raman scattering of a laser pulse which is a function of temperature (Dakin et al., 1985; Kurashima et al., 1990). The laser light pulse scatters along the fiber, and the scattering depends on the prevailing temperature. One of the scattering types is Rayleigh scattering, where the frequencies of original and scattered laser light are the same. This scattering type does not provide information about the temperature. The wavelengths of the secondary maxima are shifted, and Raman scattering is used to model a particular pair of secondary maxima. A shift to the shorter wavelength is called anti-Stokes and its amplitude exhibits an exponential response to the temperature at the scattering point. Stokes shift happens to the longer wavelength and is not affected by the temperature.

A DTS control unit detects the back-scattered light with a high temporal resolution which can be fractions of a minute (Selker et al., 2006). The temperature resolution can achieve an accuracy of 0.01 °C and spatial resolution 1 m (Selker et al., 2006). The distance between the scattering position and the sensor can be calculated by dividing the time difference between pulse emitting and scattering detection by 2. The temperature of the position is determined by the ratio between Stokes and anti-Stokes signal amplitudes. The optical fiber of DTS can be also used as a sensing instrument which gives temperature profile along the interval covered by the optical fiber. This length can be even several kilometers. Thus, DTS can provide a spatial temperature profile of an area. Another option is to make a large number of separate point measurements. The spatial resolution of DTS measurements is in the order of 1 m with a further possibility to be improved it by wrapping the fiber around a pole or a tube (Selker et al., 2006).

Fig. 5. A heat collection well performed as a link between heat collection pipes and the distribution well system. The image shows the actual connections between pipes and well installed in Suvilahti.

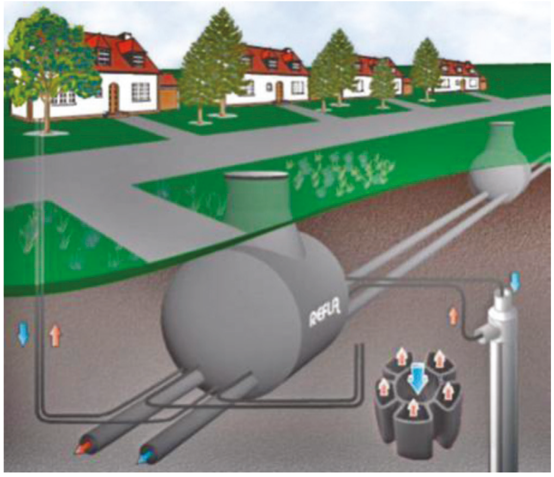

Fig. 6. The heat is delivered to houses by circulating fluid from a distribution well. A house is connected to a distribution well via an influent and efflux pipes. Source of the figure: Vaasan Eko-Lämpö Oy.

4. Experimental results

The experimental site is in Suvilahti where Vaasa Housing Fair 2008 was organized. The performance of sediment heat energy system was investigated from two different points of view. One viewpoint was to analyze the heat energy removed from the sediment layer. A way to evaluate the energy removal was to measure decrease in temperature. As we know from earlier measurements by Valpola (2006), the temperature of the sediment layer in this area stays around +8 °C during winter time. The heat energy collection should lower this temperature.

Fiber optic distributed sensing method has been demonstrated to be adequate for the temperature measurement of ground-heat-related applications and thus was selected. The measurement setup was accomplished by installing a fiber optic cable to the side of heat collection tube in two different and separate places. Insertion of the optic cables was made during the general assembly of the sediment heat energy system. The temperature measurement results for two months, August and April 2013, are shown as a function of distance from the shore in Fig. 7. This data shows that temperature of the sediment was clearly reduced. This indicates that the heat energy collection system was operated successfully.

The temperature data as shown in Fig. 7 were acquired from 50 m to 300 m distance along the optical cable. Starting point of

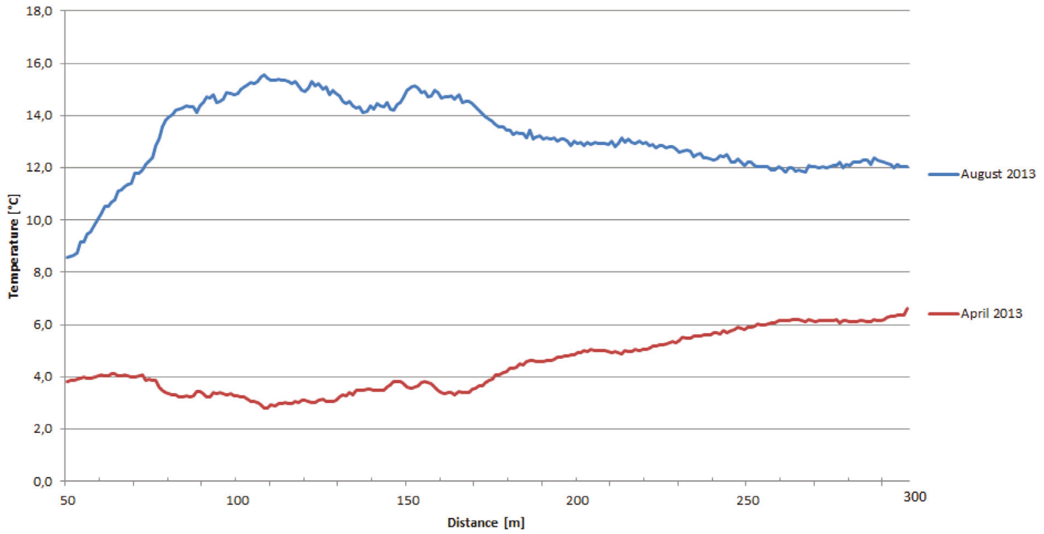

Fig. 7. The temperature decrease of the sediment caused by heat energy collection.

acquisition was selected, because the actual sediment conditions were reached in approximately 50 m distance from the shore.

The second viewpoint of performance of the sediment energy system is its operation and energy saving ability. Due to this, information related to the energy consumption of one household was collected very carefully over several years. In this household, two persons are living in the heated house of 234.5 m^2. Their heating-related energy consumption including the hot water is found to be annually 9000 kWh, all of which is supported the pumps of the sediment energy system. The total energy consumption is around 17,000 kWh and the energy consumption per square meter is 72.5 kWh/m^2. No other heating method is currently used in the household; the household does not even use the air heat pump. Energy consumption is remarkably small when compared to the average energy consumption of a half smaller house in Finland. Annual energy consumption of a new, 120 m^2 private house in Finland is typically 20,000 kWh for which heating-related energy consumption including hot water is 14,300 kWh. The average energy consumption per square meter is now more than double, 166.7 kWh/m^2. Thus, the sediment energy system provides remarkable capability to reduce the use of electricity in a carbon-free way.

5. Comparison of sediment pipe system to other ground source heat systems

In many approaches a pipe or pipework is used as a way to collect heat. These approaches include pond and lake ground heat systems, horizontal heat system and borehole heat system, all of which exhibit some similar features as the sediment heat system along with their unique properties. Table 1 shows a general comparison for the most important properties of four heat collection systems. The table indicates clearly that systems based on heat energy from the Sun are located near the surface and constructed with horizontal pipework of many collector units.

Sediment and borehole ground source heat pipelines are not very sensitive to get damaged because of their position in the ground. The only threat for horizontal GSHS is deep digging in the garden. Instead ground source heat system pipeline in the bottom of pond or lake is quite sensitive for damages at least in spring time when ice cover is breaking up. Borehole GSHS is the only system where pipes are installed vertically and the total depth of borehole is 100–300 m. Borehole GSHS utilizes geothermal energy. The heat extraction rate fluctuates in different GSHS depending on the location of installation but every system is capable in heating and cooling if the system is correctly designed for the energy demand of the target building.

5.1. Ground source heat systems GSHS for ponds and lakes

Deep ponds and lakes in higher latitude environment are very useful for ground source heat systems partly for the same reasons like the sediment heat energy system: the densest water (around +4 °C) is usually located near the bottom of the lake or pond, below thermocline zone (a special zone between warmer and cooler water) around the year. In warmer climate, water bodies offer higher temperatures to be utilized. The energy can be collected directly from water via an open-loop lake system or a closed-loop surface water system (Banks, 2012). Open-loop lake system use directly lake or pond water, while a closed-loop system uses typically antifreeze-based carrier fluid as a heat carrier fluid. The closed-loop system can be implemented with several different types of pipes. These systems are sensitive to accidental or willful damage as the pipes are more or less unprotected inside the water body.

The use of GSHS requires taking into account ecological issues, amenity issues and other issues related to the use of the pond or lake. The lake or pond needs to be deeper than 3–4 m and its heat balance must be kept in a suitable range. The open-loop lake system is additionally sensitive to debris (may cause obstruction) as well as trade-off between ice formation threat and low efficiency in cold winters. The heat extraction rate for a closed-loop system is mentioned to be 1 kW per 20 m or 43 m for high density polyethene pipe and PE coil 1 kW per 33 m (Banks, 2012).

5.2. Horizontal heat system

The horizontal heat system consists of trenches with pipes, typically at the depth of 1.2 m–2.0 m and a solution of antifreeze as

Table 1
Comparison of different ground source heat systems (GSHS).

Feature/property	GSHS ponds and lakes	Horizontal GSHS	Borehole well GSHS	Sediment GSHS
Main heat source	Solar energy	Solar energy	Geothermal energy	Solar energy
Annual renewal	Yes	Yes	No	Yes
Number of heat collector units >20	Yes	Yes	Typically not	Yes
Sensitive to damage	Yes	Not very	No	No
Main direction of pipe(s)	Horizontal	Horizontal	Vertical	Horizontal
Vertical depth of pipes	In the bottom of a water body	1.2–2 m	100–300 m	3–4 m inside the sediment layer (from the bottom of a water body)
Approximate heat extraction rate W/m	15–28 W/m	100 W/m (trench, UK)	20–92 W/m	40–50 W/m

a heat carrier fluid (Banks, 2012). Several different geometries can be employed for trench pipework installation. The efficiency of heat transfer needs to be boosted by circulating the fluid under turbulent flow region. The burial depth needs to be selected, so that diurnal fluctuations in temperature will not or have only a restricted effect on heat collection. However, the pipes should be located close enough to ground level in order to replenish the heat energy during a hot period.

The horizontal heat system needs an open space for heat collection – this is not often available in urban areas with several buildings and other pipe systems. The wetter soil improves the performance of horizontal heat system (Banks, 2012). The system is, in general, susceptible to tampering, since the pipes are buried near the surface.

The heat extraction rate of the system varies with different conditions; the literature suggests, for example, 1 kW per 10 m (Banks, 2012). Since the average temperature of soil and rock in Finland is approximately 5 °C at the depth of couple meters and the temperature of sediment can be 8–9 °C at depths of 3–5 m (Valpola, 2006; Martinkauppi, 2010), the sediment has higher heat extraction rate available for harvesting at least in theory.

5.3. Borehole wells

The borehole wells might not be suitable in all urban areas since there might be already pipes which cannot be moved or other constructions preventing drilling the well. The most commonly pipe type in a borehole is a U-tube probe. Since the heat of borehole well does renew very slowly, the vicinity of the borehole tends to be cool and a thermal drawdown cone is formed (Stober and Bucher, 2013). The extraction rate varies very much, for example, from 20 to 30 W/m for gravel (dry sand) to 65–92 W/m for quartzite (Stober and Bucher, 2013).

In the borehole wells, it is often used the so called U-pipe, in which the fluid goes down to one pipe and comes up with another pipe. Due to vertical fluid movement in the U-pipe and more horizontal movement in the Refla-pipe (sediment energy) as well as structural differences between the pipe types, the pressure drop of U-pipe is three times higher than in that of Refla-pipe (Acuña, 2013). The smaller pressure drop of Refla pipe system allows the use of a heat pump with lower-power consumption. The low-power heat pumps are generally more inexpensive to buy and use, and they consume less electricity.

6. Conclusion

Abundance of water bodies is available in many places and many approaches have been suggested for their use for energy production, heating and cooling. Some of the approaches have been suggested even for the use in urban areas, but some obstacles like space requirement of the installation, existing constructions or disturbances to inhabitants limit their usability. In this paper, we describe a novel heat collection system, where the thermal energy of sediment under a water body is utilized. It is suitable for both urban and rural water bodies, and it overcomes obstacles presented in urban areas. It provides a carbon-free and renewable method to produce heating/cooling and hot service water.

The suggested system consists of special pipes connected to heat collection wells. The distribution and removal are done via a special distribution tank, which is connected to the connection well. The physical realization of the system is done in Suvilahti suburb, a district area of City Vaasa in 2007. Its performance has been successful, and we examine it from two points of view. The first one is the system capability to extract heat from the sediment. The optical temperature measurements clearly indicate a drop in the sediment temperature from the normal temperature of 8 °C during the period of heating. Its heat extraction rate has been evaluated to be 40–50 W/m. By carefully following the energy consumption in one household, the system has been shown to reduce more than half of the electricity normally used in this type of Finnish household. The energy savings per year has reached 11,000 kWh for a household.

The sediment heat collection is not the only way to utilize sediment and water areas for energy production. Different schemas have been suggested for biogas production, biofuel production from algae, hydrate-containing sediment collection and microbial fuel cell. They consider obviously different aspects, comparing to the suggested system. However, the suggested system has some resemblance to ground heat source systems. It can be seen as a complementary of them, although there are specific differences. The most important one is the suitability for urban areas.

Acknowledgment

We thank City of Vaasa and TEKES (the Finnish Funding Agency for Innovation).

References

Acuña, J., 2013. Distributed Thermal Response Tests – New Insights on U-pipe and Coaxial Heat Exchangers in Groundwater-filled Boreholes (Doctoral thesis). Kungliga Tekniska Högskolan, Stockholm.
Aittomäki, A., 2001. Lämpöpumppulämmitys [in Finnish], Tampere: Suomen Lämpöpumppuyhdistys SULPU ry.
Allen, E., Browne, J., Hynes, S., Murphy, J.D., 2013. The potential of algae blooms to produce renewable gaseous fuel. Waste Manag. 33 (11), 2425–2433.
Banks, D., 2012. An Introduction to Thermogeology: Ground Source Heating and Cooling. Blackwell Publishing, Oxford, UK.
Dakin, J.P., Pratt, D.J., Bibby, G.W., Ross, J.N., 1985. Distributed optical fiber Raman temperature sensor using a semiconductor light source and detector. Electron. Lett. 21 (13), 569–570.
Fang, X., Stefan, H.G., 1996. Dynamics of heat exchange between sediment and water in a lake. Water Resour. Res. 32 (6), 1719–1727.
Fang, J., Wu, F., Xiong, Y., Li, F., Du, X., An, D., Wang, L., 2014. Source characterization of sedimentary organic matter using molecular and stable carbon isotopic composition of n-alkanes and fatty acids in sediment core from Lake Dianchi, China. Sci. Total Environ. 473–474, 410–421.
Holmes, D.E., Bond, D.R., Lovley, D.R., 2004. Electron transfer by *Desulfobulbus propionicus* to Fe(III) and graphite electrodes. Appl. Environ. Microbiol. 70 (2), 1234–1237.

Holmes, D.E., Bond, D.R., O'Neil, R.A., Reimers, C.E., Tender, L.R., Lovley, D.R., 2004. Microbial communities associated with electrodes harvesting electricity from a variety of aquatic sediments. Microb. Ecol. 48 (2), 178–190.

Hondzo, M., Stefan, H.G., 1994. Riverbed heat conduction prediction. Water Resour. Res. 30 (5), 1503–1513.

Hong, S.W., Kim, H.S., Chung, T.H., 2010. Alteration of sediment organic matter in sediment microbial fuel cells. Environ. Pollut. 158 (1), 185–191.

Hu, Z., Zheng, Y., Yan, F., Xiao, B., Liu, S., 2013. Bio-oil production through pyrolysis of blue-green algae blooms (BGAB): product distribution and bio-oil characterization. Energy 52, 119–125.

Hurtig, E., Grosswig, S., Jobmann, M., Kühn, K., Marschall, P., 1994. Fibre-optic temperature measurements in shallow boreholes: experimental application for fluid logging. Geothermics 23 (4), 355–364.

Klauda, J.B., Sandler, S.I., 2005. Global distribution of methane hydrate in ocean sediment. Energy Fuels 19 (2), 459–470.

Kurashima, T., Horiguchi, T., Tateda, M., 1990. Distributed-temperature sensing using stimulated Brillouin-scattering in optical silica fibers. Opt. Lett. 15 (18), 1038–1040.

Lowy, D.A., Tender, L.M., Zeikus, J.G., Park, D.H., Lovley, D.R., 2006. Harvesting energy from the marine sediment–water interface II: kinetic activity of anode materials. Biosens. Bioelectron. 21 (11), 2058–2063.

Marquez, G.P., Reichardt, W.T., Azanza, R.V., Klocke, M., Montaño, M.N., 2013. Thalassic biogas production from sea wrack biomass using different microbial seeds: cow manure, marine sediment and sea wrack-associated microflora. Bioresour. Technol. 133, 612–617.

Martinkauppi, I., 2010. Sedimenttilämpömittaukset Pohjanmaalla ja Etelä-Pohjanmaalla [in Finnish]. Available at: http://www.geoenergia.fi/pdf/I_Martinkauppi.pdf (accessed 24.11.14.).

Miao, H., Wang, S., Zhao, M., Huang, Z., Ren, H., Yan, Q., Ruan, W., 2014. Codigestion of Taihu blue algae with swine manure for biogas production. Energy Convers. Manag. 77, 643–649.

Migliore, G., Alisi, C., Sprocati, A.R., Massi, E., Ciccoli, R., Lenzi, M., Wang, A., Cremisini, C., 2012. Anaerobic digestion of macroalgal biomass and sediments sourced from the Orbetello lagoon, Italy. Biomass Bioenergy 42, 69–77.

Murphy, J.D., Thamsiriroj, T., 2013. Fundamental science and engineering of the anaerobic digestion process for biogas production. In: Wellinger, A., Murphy, J., Baxter, D. (Eds.), The Biogas Handbook: Science, Production and Applications. Woodhead Publishing, Cambridge, pp. 104–130.

Nielsen, M.E., Reimers, C.E., Stecher III, H.A., 2007. Enhanced power from chambered benthic microbial fuel cells. Environ. Sci. Technol. 41 (22), 7895–7900.

Reimers, C.E., Tender, L.M., Fertig, S., Wang, W., 2001. Harvesting energy from the marine sediment-water interface. Environ. Sci. Technol. 35 (1), 192–195.

Rezaei, F., Richard, T.L., Brennan, R.A., Logan, B.E., 2007. Substrate-enhanced microbial fuel cells for improved remote power generation from sediment-based systems. Environ. Sci. Technol. 41 (11), 4053–4058.

Saarela, A., 2012. The Extraction of Sedimentary Deposits in South Ostrobothia's Lake Region, a Presentation. http://www.seamk.fi/loader.aspx?id=9e0b762e-c4f0-4454-9b2e-4b56c17e8529 (accessed 24.11.14.).

Selker, J.S., Thévenaz, L., Huwald, H., Mallet, A., Luxemburg, W., van de Giesen, N., Stejskal, M., Zeman, J., Westhoff, M., Parlange, M.B., 2006. Distributed fiber-optic temperature sensing for hydrologic systems. Water Resour. Res. 42 (12).

Sloan Jr., E.D., Koh, C., 2007. Clathrate Hydrates of Natural Gases In: Chemical Industries, third ed., 119. CRC Press, Boca Raton.

Speight, J.G., 2011. Unconventional fuel sources. In: Speight, J.G. (Ed.), The Biofuels Handbook. Royal Society of Chemistry, Cambridge, pp. 42–75.

Stober, I., Bucher, K., 2013. Geothermal Energy from Theoretical Models to Exploration and Development. Springer, Heidelberg.

Stoll, R.D., Bryan, G.M., 1979. Physical properties of sediments containing gas hydrates. J. Geophys. Res. Solid Earth (1978–2012) 84 (B4), 1629–1634.

Tender, L.M., Reimers, C.E., Stecher III, H.A., Holmes, D.E., Bond, D.R., Lowy, D.A., Pilobello, K., Fertig, S.J., Lovley, D.R., 2002. Harnessing microbially generated power on the seafloor. Nat. Biotechnol. 20 (8), 821–825.

Tsay, T., Ruggaber, G.J., Effler, S.W., Driscoll, C.T., 1992. Thermal stratification modeling of lakes with sediment heat flux. J. Hydraul. Eng. 118 (3), 407–419.

Turner, D.J., Sloan, E.D., 2002. Hydrate phase equilibria measurements and prediction in sediments. In: Proceedings of the 4th ICGH. Yokohama, pp. 327–330.

Tyler, S.W., Selker, J.S., Hausner, M.B., Hatch, C.E., Torgersen, T., Thodal, C.E., Schladow, S.G., 2009. Environmental temperature sensing using Raman spectra DTS fiber-optic methods. Water Resour. Res. 45 (4).

Valpola, S., 2006. Sediment Temperature Measurements at Suvilahti Bay, Vaasa (mainly in Finnish; Finnish title: sedimentin lämpötilamittaukset Vaasan Suvilahden edustalla). Geological Survey of Finland, Report P31.4.054. http://arkisto.gsf.fi/p31/P31.4.053.pdf (accessed 24.11.14.).

Vogt, T., Schneider, P., Hahn-Woernle, L., Cirpka, O.A., 2010. Estimation of seepage rates in a losing stream by means of fiber-optic high-resolution vertical temperature profiling. J. Hydrol. 380 (1–2), 154–164.

Waite, W.F., deMartin, B.J., Kirby, S.H., Pinkston, J., Ruppel, C.D., 2002. Thermal conductivity measurements in porous mixtures of methane hydrate and quartz sand. Geophys. Res. Lett. 29 (24), 82-1–82-4.

Wang, Y., Liu, D., Richard, P., Li, X., 2013. A geochemical record of environmental changes in sediments from Sishili Bay, northern Yellow Sea, China: anthropogenic influence on organic matter sources and composition over the last 100 years. Mar. Pollut. Bull. 77 (1–2), 227–236.

Wilcock, W.S.D., Kauffman, P.C., 1997. Development of a seawater battery for deep-water applications. J. Power Sour. 66 (1–2), 71–75.

Woszczyk, M., Bechtel, A., Gratzer, R., Kotarba, M.J., Kokociński, M., Fiebig, J., Cieśliński, R., 2011. Composition and origin of organic matter in surface sediments of Lake Sarbsko: a highly eutrophic and shallow coastal lake (northern Poland). Org. Geochem. 42 (9), 1025–1038.

Yang, S., Tang, M., Yim, W.W.S., Zong, Y., Huang, G., Switzer, A.D., Saito, Y., 2011. Burial of organic carbon in Holocene sediments of the Zhujiang (Pearl River) and Changjiang (Yangtze River) estuaries. Mar. Chem. 123 (1–4), 1–10.

Zhong, W., Chi, L., Luo, Y., Zhang, Z., Zhang, Z., Wu, W.M., 2013. Enhanced methane production from Taihu Lake blue algae by anaerobic co-digestion with corn straw in continuous feed digesters. Bioresour. Technol. 134, 264–270.

Zhu, L., 2014. Sustainable Biodiesel Production from Microalgae Cultivated with Piggery Wastewater (Doctoral thesis). the University of Vaasa, Vaasa.

Zhu, L., 2014. The combined production of ethanol and biogas from microalgal residuals to sustain microalgal biodiesel: a theoretical evaluation. Biofuels Bioprod. Biorefin. 8 (1), 7–15.

Zhu, L., Ketola, T., 2012. Microalgae production as a biofuel feedstock: risks and challenges. Int. J. Sustain. Dev. World Ecol. 19 (3), 268–274.

Zhu, L., Hiltunen, E., Antila, E., Zhong, J., Yuan, Z., Wang, Z., 2014. Microalgal biofuels: flexible bioenergies for sustainable development. Renew. Sustain. Energy Rev. 30, 1035–1046.

Agronomy Research **14**(S1), 1191–1199, 2016

Correlation between temperatures of air, heat carrier liquid and seabed sediment in renewable low energy network

A. Mäkiranta*, J.B. Martinkauppi and E. Hiltunen

University of Vaasa, Faculty of Technology, Electrical Engineering and Energy Technology, P.O. Box 700, FI-65101 Vaasa, Finland
*Correspondence: anne.makiranta@uva.fi

Abstract. The low energy network based on renewable seabed sediment heat has been monitored for several years in Vaasa, Finland. In this study the temperatures of air, heat carrier fluid and seabed sediment are compared to each other and correlations between them are investigated. In this study data from one year 2014, was used. Correlations between these subjects clearly exist. The sizing of installed network seems to be correct; no overuse was detected.

Key words: Renewable energy, heat energy, sediment energy, carbon-free, distributed temperature sensing (DTS) method.

INTRODUCTION

The local renewable energy sources are available everywhere. The harvesting of those sources is going on worldwide in order to mitigate the global warming. The seabed sediment heat is one geothermal heat energy source which has been utilized in Vaasa, Finland since 2008. Actually this heat source is mostly generated by the sun which is common with heat sources near the soil surface. In Finland the impact of seasonal variation in air temperatures is observed to affect even in the depth of 10–15 meters from the soil surface. In Vaasa the seabed sediment heat is delivered to total of 42 households via heat collection pipes and heat pumps. This low energy network has also been used for cooling those houses in the summertime. There have been implemented temperature measurements of air, heat carrier liquid and sediment during 8 years. Mäkiranta et al. (2015) have noticed in their measurements that in the seabed sediment the temperature difference between October and the coldest month stays stable at 8 degrees.

Hiltunen et al. (2015) have investigated the dependency between air temperature and fluid temperature on the area. They observed that the heat carrier liquid achieved its maximum temperature typically after one month of the peak value of the air temperature. In this study the sediment temperature will be compared to the values of fluid and air temperature and the correlation of these three variables is analysed. The aim is to discover if the collection pipeline is sized correctly: if a high correlation between these subjects exists, then a proper interaction is likely.

MATERIALS AND METHODS

The observations of air temperature were acquired from Finnish Meteorological Institute. The heat carrier fluid temperatures were measured by one resident of the sediment heat network. The sediment heat temperatures were measured by the renewable energy research group of University of Vaasa. Temperatures of seabed sediment have been acquired by optical measurement device. The distributed temperature sensing (DTS) method observes the data with the spatial resolution of even 1 m. The optical cable (sensor) is installed along one 300 m long heat collection tube. Temperature data is collected on the shore from the distribution well. The data indicates the sediment temperatures in the 3–4 m depth, starting at the shore and extending to the distance of 300 m in the sea.

DTS method

The temperatures of the seabed sediment are measured by distributed temperature sensing (DTS) method where optical fibre functions as linear sensor. Temperatures can be measured as a continuous profile along the whole fibre not only at some points. In other words temperature measurement is distributed. Fibres can be even several kilometres long and they are typically made from doped quartz glass.

DTS-measurement device emits short optical pulses (laser light), which illuminate the glass core of an optical fibre. Different types of scattering are subjected to optical pulse while it moves along the core of fibre. One type of scattering is Raman scattering which consists of Anti-Stokes and Stokes band. Anti-Stokes band is temperature dependent, while Stokes band is not. The ratio of the Anti-Stokes and Stokes light intensities indicates the local temperature of optical fibre. The speed of optical pulse is used to evaluate the spatial position of the temperature (Ukil et al., 2012).

Measurements on the site

Seabed sediment temperature measurements were made by Oryx DTS device. The patch cord was used to calibrate the device and to secure cleanliness of the channels in the device. The rugged laptop (Fig. 1) acquired the data instantly at the measurement site. One measurement took 10 minutes which means 20 measurements totally by one measurement channel. Temperature changes are relatively slow at the seabed sediment. That is why one measurement session per month was justified and 10 minutes for data acquiring per session was observed to be long enough.

Figure 1. DTS-device was in commission at the low energy network site in Suvilahti.

The original measurement data of seabed sediment temperatures for one year period is shown in Fig. 2.

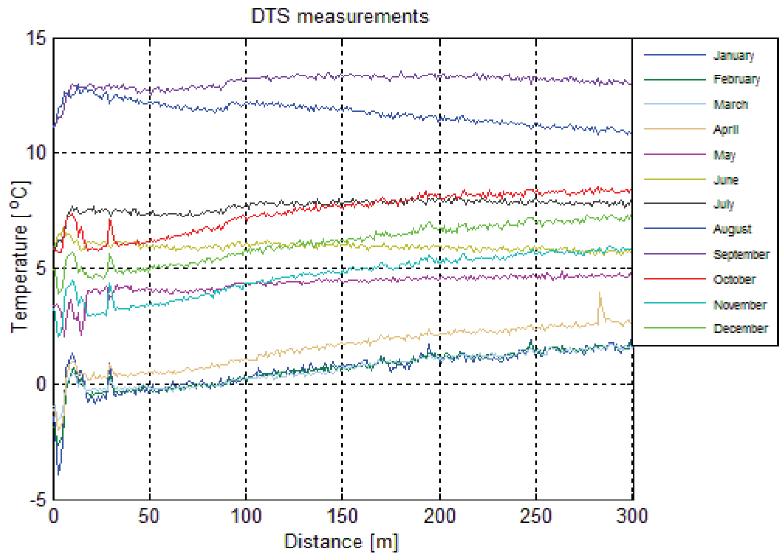

Figure 2. The original data for DTS measurements in year 2014.

Analysing method for data

First, the original data was analysed on the basis of its temperature profile. This provides a very rough estimate about the sediment temperature behaviour.

The next phase is to compare the sediment temperature to the air and heat carrier fluid temperatures. As the air and liquid temperatures are scalar, we have selected temperature data at two different points. A problem is that the temperature data is very noisy due to nature of the measurement itself, environment and other factors. This was solved using moving average-method to smooth the data. The selected window size is nine; i.e. a point value is replaced with an average of values from the point and from four other points before and after the point.

Theory and modelling

Correlations were evaluated between the following data: I air temperature and liquid temperature, II air temperature and sediment temperature and III sediment temperature and liquid temperature. The correlation was calculated using Pearson product-moment correlation coefficient and Spearman's rank correlation coefficient. A short description is provided in this article, as a more comprehensive overview is available in many statistical textbooks (e.g. Sprinthall 2012).

Pearson product-moment correlation coefficient (Pearson r) measures linear correlation or dependence between one subject's temperature data (symbol x) and another subject's temperature data (symbol y). The r –values can be between +1 and -1 where 1 is total positive correlation, -1 total negative correlation and 0 is no correlation.

The Pearson *r* is defined as

$$r_{x,y} = \frac{cov(x,y)}{\sigma_x \sigma_y} = \frac{E[(x-\mu_x)(y-\mu_y)]}{\sigma_x \sigma_y} \tag{1}$$

where *cov* indicates covariance, σ is the standard deviation, μ is mean, *E* is expectation, subindex *x* indicates the first subject's data, and subindex *y* indicates the second subject's data. The entire range of each subject's data is assumed to be normally distributed. The temperature values (Celcius degrees here) naturally belong to interval data.

The significance of Pearson *r* is tested against the null hypothesis: the correlation is due to chance. The significance is assessed using Pearson *r* table with the degree of freedom (the number of pairs of scores minus 2) (Sprinthall 2012).

Another metric used is Spearman's rank correlation coefficient (Spearman's r_s) which is a nonparametric measure. All temperature data values for each subject are converted into ordinal ranks. For each month, the absolute difference *d* between temperature ranks is calculated and squared. The Spearman's r_s is calculated using the following formula:

$$r_s = 1 - \frac{6\sum d^2}{N(N^2-1)} \tag{2}$$

where *N* is the number of pairs. It is used here to evaluate the statistical dependence between temperatures. This metric compares their relationship to a monotonic function. The values are again between +1 and -1.

RESULTS AND DISCUSSION

Correlations between the fluid temperature and sediment temperature as well as the air temperature and sediment temperature are evaluated. The sediment temperature is measured at different distances along the pipe but two different points (distances 150 m and 250 from the shore) are used for correlation calculations. A high correlation is assumed to mean that sizing of the pipeline is done correctly. The appropriate and adequate sizing is vital for improvement of renewable low energy network.

The DTS temperature profile was noticed to change depending on the month. Fig. 3 shows profiles from January to April as well as from October to December. The measured temperatures are lower near the shore than further away in the bay. These months are also the typical months when a heating is needed for the houses in Finland. Also the month November has lower temperature values than month December. This might be due to appearance of ice cover or stratification effect in bay water in December.

Fig. 4 displays the temperature profiles for the warm months from May to September. The temperature profiles exceed their highest temperature at September. The form of temperature profile is different than in Fig. 3 which contains the cold months.

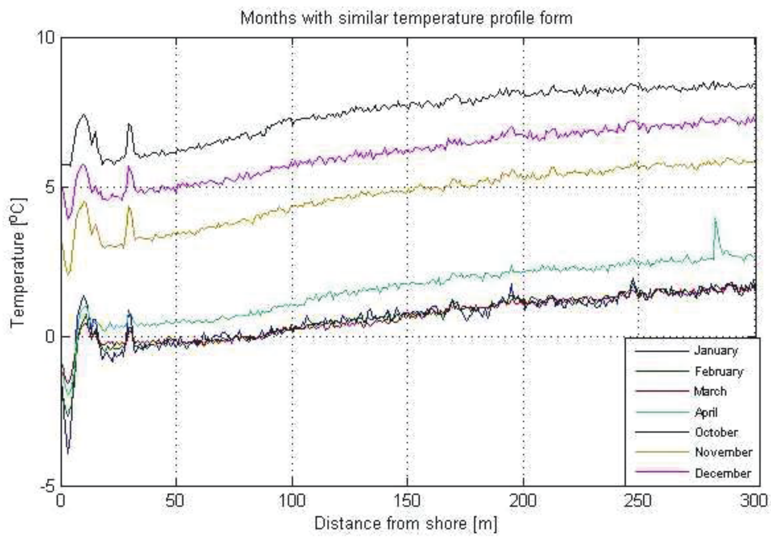

Figure 3. The temperature profiles for seven cold months in year 2014.

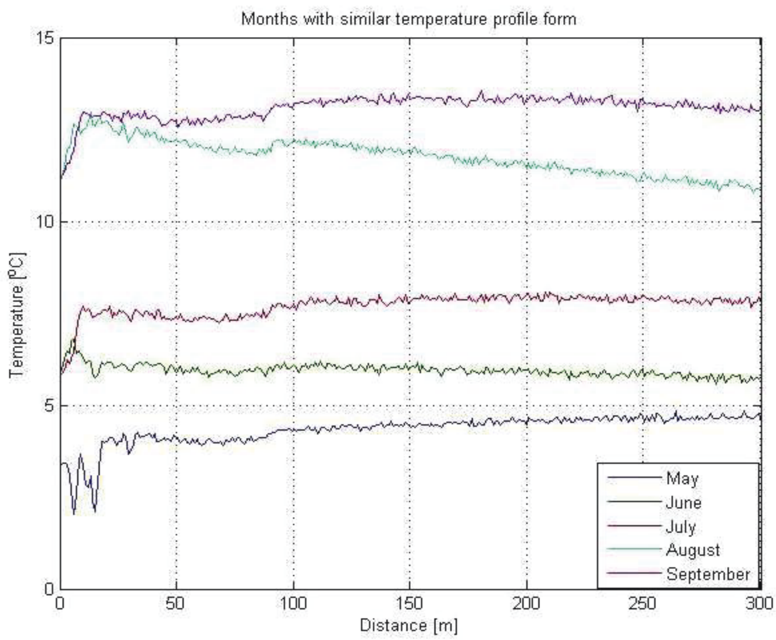

Figure 4. Temperature profiles for 5 warm months in year 2014.

The temperature profiles for year 2014 indicate that the sediment reach the maximum temperature at the late summer as well as there is a minimum temperature limit under which the current usage cannot drive.

The original data was subjected smoothing with a moving average method with window size of nine. The results for smoothing as well as selected points for correlation calculations are shown in Fig. 5. The selected analysing points were taken of the distances of 150 m and 250 m from the shore.

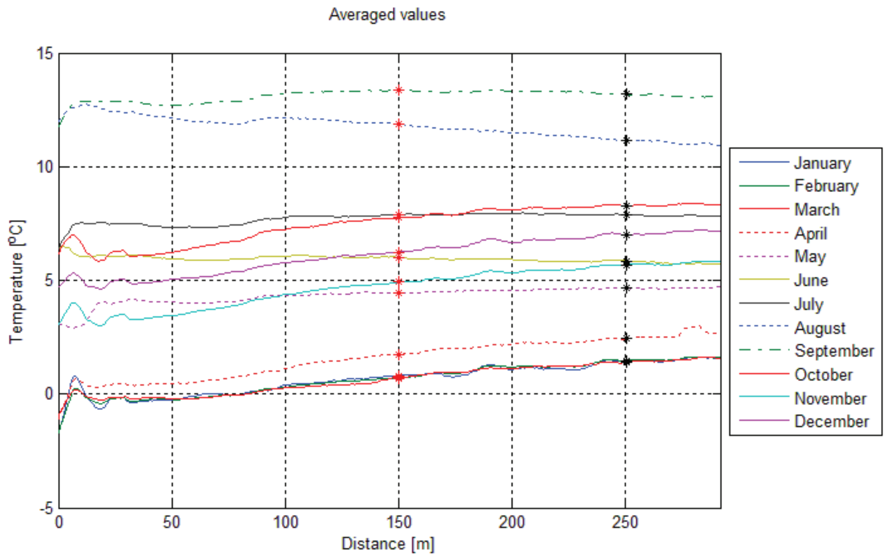

Figure 5. The averaged values are shown for each month. The selected analysing points (150 m and 250 m) are indicated with * marker.

Air, liquid and sediment temperatures were plotted as a function of time in Fig. 6. Naturally, the biggest range appears in the air temperature.

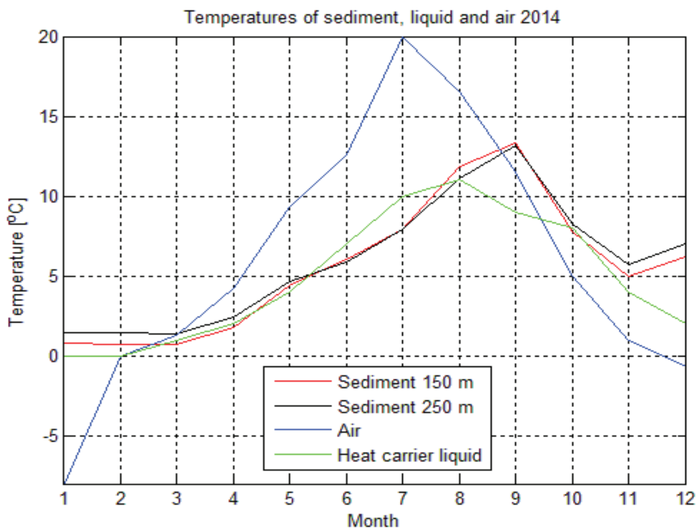

Figure 6. Temperature data from January to December 2014.

During the warmest months (June and July) the heat carrier liquid temperature exceeds the sediment temperatures. This can be understood due to the need for cooling in the houses.

Table 1 shows the correlation coefficient values calculated for different subject pairs. In the first three rows, the correlation between air data and liquid or sediment data is calculated as well as between air data and delayed or advanced liquid or sediment data. As in our earlier paper (Hiltunen et al. 2015), the highest correlation between air and liquid data occurs between liquid data is taken one month later than corresponding air data. There seems to exist also a high correlation between air temperature and temperature of sediment after one or two months.

The last two rows show the correlation between sediment data and liquid data (as well as delayed or advanced data). The correlation is high when the subjects data measured at the same time as well as when the sediment data is compared against previous months liquid data. One could interpret this so that when the liquid heats or cools sediment this affects also sediment temperature at the next months.

Table 1. Correlations

Data	Pearson coefficient	Spearman coefficient
Air temperature and liquid temperature	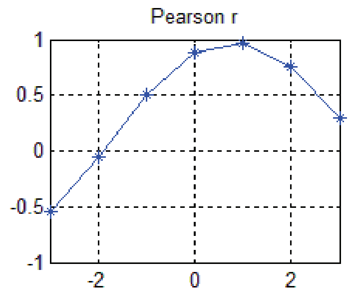	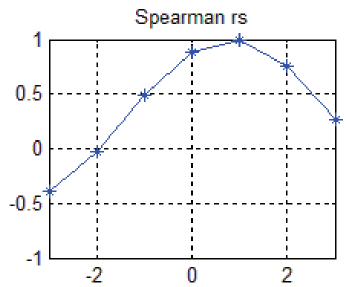
Air temperature and sediment temperature 150 m	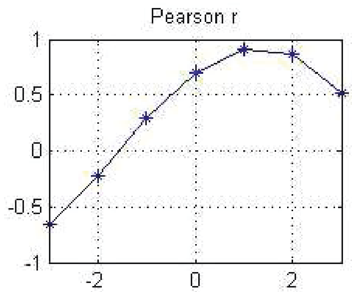	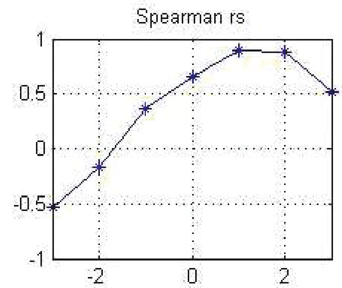
Air temperature and sediment temperature 250 m	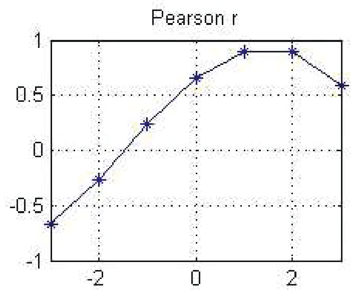	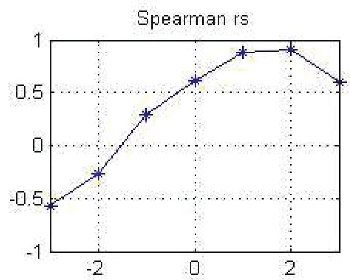

Table 1 (continued)

Sediment temperature 150 m and liquid temperature	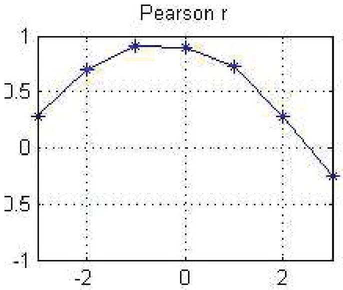	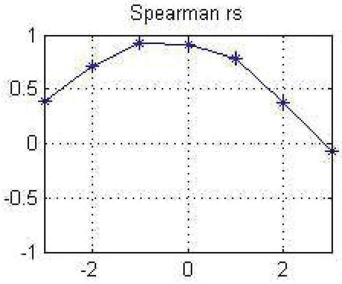
Sediment temperature 250 m and liquid temperature	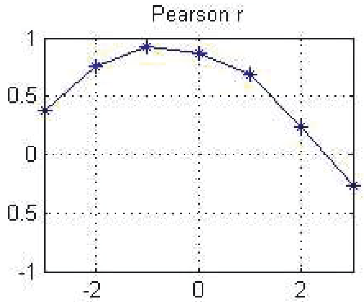	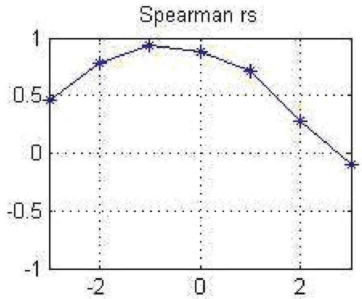

CONCLUSIONS

There was noticed high correlation between the heat carrier liquid temperature and sediment temperature. Especially, liquid temperature and sediment temperature of next month, as well as, liquid and sediment temperature of the same month are correlating strongly. This may indicate that the low energy system is really working. In winter time the sediment is getting cooler due to the usage for heating. In summer time sediment is warming due the cooling of the houses. Of course there are also other factors that are affecting to the sediment temperatures.

The sediment temperature curve (Fig. 2) seems to rise slightly to the end even in winter time. This might indicate the fact that the sizing of this site`s pipeline is played safe. In other words this network is sized bigger than would have been necessary. This is natural in pilot systems.

The high and significant correlation between air temperature and temperature of sediment after one or two months was also observed. The sediment temperature is indicating the previous weather conditions.

ACKNOWLEDGEMENTS. We thank Mr. Juhani Luopajärvi for implementing the liquid temperature measurements.

REFERENCES

Hiltunen, E., Martinkauppi, J.B., Mäkiranta, A., Rinta-Luoma, J. & Syrjälä, T. 2015. Seasonal temperature variation in heat collection liquid used in renewable, carbon-free heat production from urban and rural water areas. *Agronomy Research* **13**, 485–493.

Mäkiranta, A., Martinkauppi, J.B., Hiltunen, E. & Lieskoski, M. 2015. Seabed Sediment Heat Measurements at the House Fair Area in Vaasa. (submitted)

Sprinthall, R.C. 2012, *Basic statistical analysis*. 9th edition. Pearson. 660 pp. (in the USA).

Ukil, A., Braendle, H. & Krippner, P. 2012. Distributed Temperature Sensing: Review of Technology and Applications. *IEEE Sensors Journal* **12**, (5), 885–892.

applied sciences

MDPI

Article

Seabed Sediment as an Annually Renewable Heat Source

Anne Mäkiranta [1,*], Birgitta Martinkauppi [1], Erkki Hiltunen [1] and Mauri Lieskoski [2]

[1] School of Technology and Innovations, University of Vaasa, P.O. Box 700, FI-65101 Vaasa, Finland; birgitta.martinkauppi@uva.fi (B.M.); erkki.hiltunen@uva.fi (E.H.)
[2] Geo-Pipe GP Oy, Konsterinkuja 5, FI-65280 Vaasa, Finland; mauri.lieskoski@geopipe.fi
* Correspondence: anne.makiranta@uva.fi; Tel.: +358-29-449-8000

Received: 15 December 2017; Accepted: 9 February 2018; Published: 15 February 2018

Abstract: Thermal energy collected from the sediment layer under a water body has been suggested for use as a renewable heat source for a low energy network. A prototype system for using this sediment energy was installed in Suvilahti, Vaasa, in 2008 and is still in use. It provides a carbon-free heating and cooling solution as well as savings in energy costs for 42 houses. To be a real, renewable heat source, the thermal energy of the sediment layer needs to replenish annually. The goal of this paper is to verify the possible cooling or annual heat regeneration. The sediment temperatures were measured and analyzed in the years 2013–2015. The data were compared to the same period in 2008–2009. All measurements were taken in the same place. This paper also confirms the potential of the sediment heat, especially in the seabed sediment, using the temperature differences between the lowest and the highest values for the year. The results demonstrate that the collection of the heat energy does not cause permanent cooling of the sediment. This result was obtained by calculating the temperature difference between measurements in the warmest month and the month with the coldest temperatures. This indicates the extracted energy. The difference was found to be around 9.5 °C in 2008–2009, rising to around 11 °C for the years 2013–2014 and 2014–2015. This indicates the loaded energy. The energy utilization is sustainable: the sediment temperature has not permanently decreased despite the full use of the network for the heating and cooling of houses between 2008 and 2015.

Keywords: sediment heat; urban energy; geoenergy; low energy network; distributed temperature sensing (DTS) measurement; renewable energy

1. Introduction

The limited resources of non-renewable energy, the prevention of climate change and environmental issues like UHI (urban heat island) effect are the concerns that make the search for renewable energy sources important. One of the research topics is geothermal energy. In non-volcanic areas, geothermal energy plays a minor role compared to the radiant energy of the Sun, which has accumulated in the topmost layers of the ground. The term 'geoenergy' consists of both geothermal energy from the Earth and the radiant energy of the Sun. Geoenergy is available, for example, in ground, bedrock, watercourses, in sediment under water bodies and under asphalt and concrete surfaces. In Finland, the most exploited forms of geoenergy are ground source heat and bedrock heat.

The new renewable energy sources, such as sediment heat under water bodies and asphalt heat under the surfaces of roads and parking lots, are today attracting great interest. Sediment heat can be harvested from the sediment layers at the bottom of different watercourses. Sediment is a solid-state layer consisting of clay, mud and gyttja. There are thick sand layers on the coastline of Finland and plenty of sediment in shallow bays. According to Likens and Johnson [1], the temperature variations in overlying water and the thermal properties of the sediment affect the heat budget of the sediments.

In their study, a thermistor and a resistance bridge were used in the temperature measurements on sites in Wisconsin. Golosov and Kirillin [2] stated that the thermal effect of the sediments on the lake water temperature is observable in shallow lakes. They also noticed that in seasonally ice-covered lakes the sediment is the major heat source influencing the ecology, e.g., oxygen consumption and nutrients supply. Considering the sea bay conditions, the extraction of heat energy does not appear to be affecting the ecosystem.

In 2006, it was observed in Ostrobothnia, Finland, that at a depth of three meters under the water body of lakes the temperature of sediment reached 8 °C and remained quite stable (8–9 °C) in deeper layers.

In the same year, the interest in renewable seabed sediment heat energy arose in Vaasa in Western Finland too. The location where the heat was first noticed was in Suvilahti Bay. The elevated temperatures were verified by the Geological Survey of Finland, which performed temperature and resistance measurements at three different points on April 11. Following this discovery, the temperatures of sediment were researched as point measurements in many waterways in Ostrobothnia and, according to private communications with the Geological Survey of Finland, it was noticed that there was potential for heat energy at the bottom of lakes and also the sea.

Due to previous results, which confirmed the discovery of the promising heat resource, two years later, the low energy network for seabed sediment was introduced in the Vaasa House Fair area of Suvilahti. The Vaasa House Fair area was situated close to the seashore and sediment in the area was found to consist of sulfide clay mud. The long-term average air temperature in Vaasa is −5.7 °C in winter and 14.9 °C in summer [3].

In our previous papers we have found out that the calculated annual loaded seabed sediment heat energy of 7800 m heat collection pipeline is 575 MWh. Meanwhile the annual extraction of energy in such low energy network is 560 MWh [4].

The goal of the present study is to verify the adequacy of this heat resource for continuous heating of houses. The paper will identify the potential of sediment heat, especially in seabed sediment, using the temperature differences between the lowest and the highest values. Measurements of sediment temperatures were taken in a residential area that utilizes the sediment heat-based low energy network. One focus is to ascertain whether the usage of the low energy network has caused permanent temperature changes in the sediment. At the same time, it is essential to annually investigate the principle of the heat loading and unloading: for how many months are the temperatures increasing each year and for how many months are they decreasing each year? One of the major issues in the utilization of sediment energy is the availability and sustainability of heat energy.

2. Thermal Interaction between Water and Sediment

The use of sediment thermal energy for heating is based on the annual recharge of the thermal energy in sediments. This recharging is mainly caused by an interaction between water and sediment. Of course, water and sediment interact in many ways. Here, the focus is on the thermal interaction when water is either brine or fresh water. The main feature affecting the thermal energy of sediments is the temperature of the overlaying body of water when there is no tide. Birge et al. [5] carried out one of the first studies of this feature as early as 1927 at Lake Mendota where the heat exchange of mud was measured at different water depths but with sediments within the thickness of five meters. Birge et al. noted a variation in the migration rate of the heat. They showed that the annual oscillation at the sediment temperature attenuates as a function of increasing depth. In a study conducted at Indian River on the Atlantic Coast of Florida in the 1980s, Smith [6] also reported results that show that the water column and underlying sediments have an active exchange of heat.

Many publications indicate that the heat exchange between the water body and the lake sediments cannot be ignored, especially when a lake is shallow or has an ice cover for some period of the year [7–10]. The role of sediment in transferring the stored heat back to the water body during winter has been investigated in the arctic lakes, for example by Welch and Bergmann [9]. According to

Bengtsson [11], the heat flow from the sediments happened during the whole of winter but the convective mixing was very slow.

The sediment heat flux is a signification parameter when simulating the stratification conditions in shallow lakes but not in deeper lakes [10]. A study of dynamic heat exchange in the sediment-water interface of a lake indicates the same conclusion: Fang and Stefan [12] noted that the sediment heat fluxes are a very important factor in shallow lakes. The lake sediments provide seasonal heat storage and thermal inertia to water columns. The direction of the heat flux has both seasonal and daily variations. Seasonal variation causes heat transfer from water to sediment in the summer and from sediment to water in the winter.

Brewer [13] studied shallow lakes with depths approximately between 0.5–1.0 m and 1.8–2.7 m in the Barrow area of Alaska. He stated that during the ice-free period, the water in the lake can be considered to be in an isothermal state with a maximum recorded temperature of 12 °C. Following the icing of the lake surface, the heat radiation through the ice can quickly warm the water, even from approximately 0 °C to 2 °C, as long as the ice is not covered by snow. The snow on the ice causes the cooling of the water and then the bottom sediments start to warm the water. Warming depends on the distance from the shore and the depth of the water body.

A great deal of heat energy is available in urban areas. Buildings and surface materials, such as concrete and asphalt pavements, absorb and store sunlight effectively; together, the built environment, people, vehicles and lack of flora are the reasons for the extra heat [14]. This phenomenon, referred to as the urban heat island (UHI) effect, is largely noticed in big cities. The air in an urban area is warmer than that in the nearby rural area. The difference may even be several degrees [15]. In Turku, Finland, the average UHI intensity has been measured as 1.9 °C and the periodic difference between temperatures in the city center and surrounding areas have risen up to 10 °C [16]. The UHI effect also has an influence on ground and water temperatures. There are many different kinds of water courses, bottom sediment and heat beneath urban areas and these can be utilized as low energy sources for buildings. In their research, Canbing, Jincheng and Yijia concluded that the urban heat island effect feeds itself [17]. Thus, the best energy-saving potential can be reached by mitigating the UHI effect. Santamouris [18] also sees the use of energy supply systems that utilize renewable energy sources for buildings, as one solution in the battle against urban warming.

3. Materials and Methods

The House Fair was arranged in Suvilahti, Vaasa in the summer of 2008. The themes of the Fair were homes for everyone and ecology. The energy solutions for the area were based on renewable energy. The heating and cooling energy for 42 detached houses was delivered from the seabed sediment. This energy was mainly produced by the Sun. The combined heat and power plant, which utilizes the biogas of the landfill, was also built in the area. The combined heat and power (CHP) station produced electricity to the heat pumps of the low energy network. The House Fair Area of Vaasa and its unique low energy network were thoroughly described by Hiltunen et al. [19].

The temperatures of the seabed sediment can be measured from two places on the shore. Immediately after the assembling process in 2008, the temperatures were measured once a month for a period of 13 months using the optical cables of the distributed temperature sensing method (DTS). The measurements were carried out by the Geological Survey of Finland with the help of Agilent N4386A and had a temperature accuracy of ±0.17 °C. In 2013–2015, the University of Vaasa recorded the sediment temperature measurements. The measurements were taken once a month with the help of the Sensornet Oryx DTS device. The temperature accuracy of the DTS device was ±0.5 °C. The sediment temperatures were measured by utilizing the same methods as those noted earlier. The results were obtained from a distance of 0–300 m, starting from the shore. The spatial resolution of the measurements was 1 m. The final sediment temperatures were acquired as an average of eight temperatures measured on the same day during a period of around ten minutes.

The optical cables for temperature measurements were installed at the same time as the assembly process of the collector pipes. The position of an optical cable (yellow line) is shown in Figure 1a.

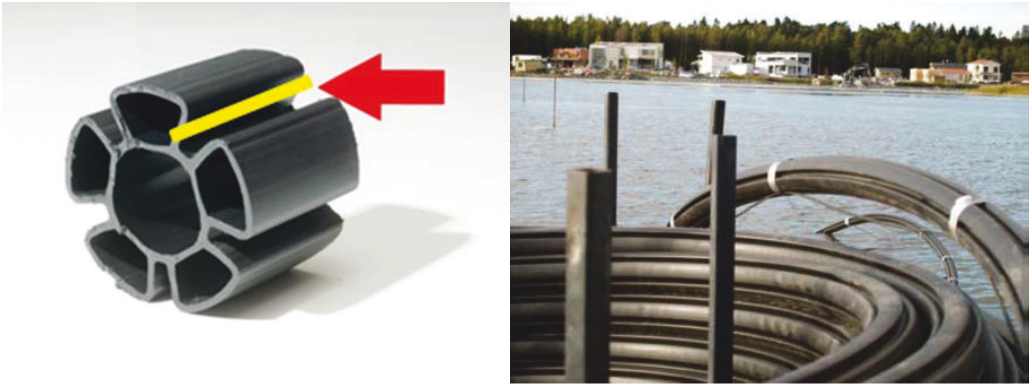

(**a**) (**b**)

Figure 1. (**a**) Profile of the heat collector pipe and the location of an optical cable; (**b**) The assembling of heat collection pipes.

The present study is concerned with the temperatures measured in Liito-oravankatu in the Suvilahti suburb during six-month periods in 2013–2014 and 2014–2015. The temperatures for those periods were compared with results from the corresponding months in 2008–2009 to illustrate the cooling period in the sediment layer. The measurements were taken in the same place in each period of 2008–2009, 2013–2014 and 2014–2015. In addition to these results, the warming of the sediment layer is also presented for the respective years.

Data are also available for the temperatures of the heat carrier fluid measured by a resident of one single-family house in the low energy network area in Suvilahti. Using an Ouman thermistor, the resident monitored the temperatures of incoming geothermal fluid for periods from September 2008 to February 2009, from September 2013 to January 2014 and from September 2014 to February 2015. The accuracy of the measurement device was ± 1.0 °C. The measurements of the heat carrier fluid were made in the engineering and utility service room inside the house. The data give the temperature of the heat carrier fluid after its journey from sediment, through the collection pipes to the distribution pipeline and then, finally, into the house. These data have been published and are analyzed in this study. Hiltunen and Mäkiranta et al. [20,21] noted that there is a clear correlation between the temperatures of air, heat carrier fluid and sediment, which is one of the prerequisites for the renewability of sediment heat.

4. Results

According to the initial measurement period in 2008–2009, the cooling of the sediment took place until February 2009, when the lowest temperatures were measured. Sediment temperatures were very close together in December and January. The sediment temperatures for a six-month period in 2008–2009 are shown in Figure 2 (Huusko, A; Martinkauppi, I. Geological Survey of Finland. Personal communication, 2009). This was the first season in which the houses were heated using the low energy network. The sediment temperatures were presented from a distance of 50 to 300 m from the shore. This distance was chosen because 0–50 m is relatively close to the shore and, therefore, flora (reeds, etc.) might affect the temperatures.

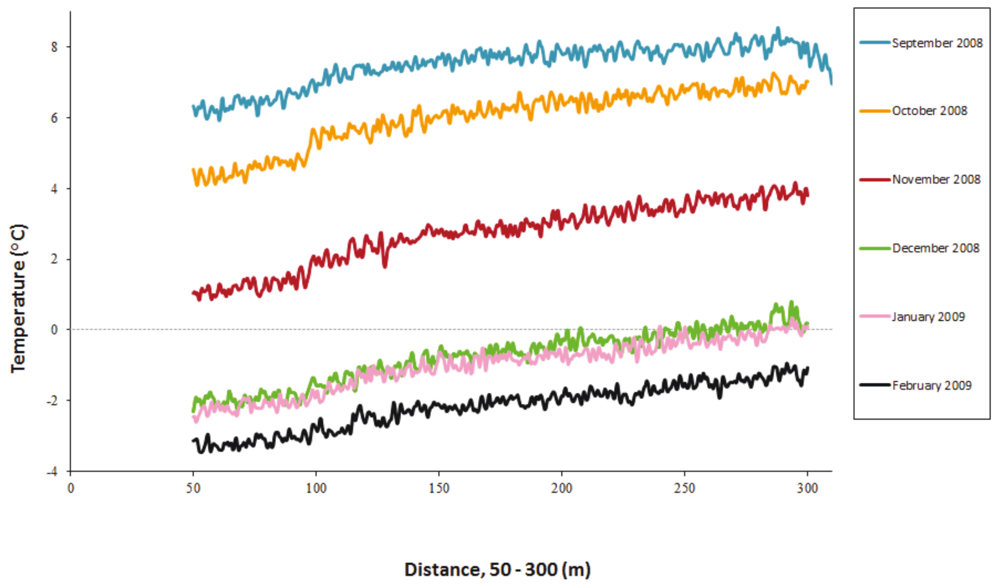

Figure 2. Seabed sediment temperatures measured from September 2008 to February 2009 in Liito-oravankatu.

The mean air temperature in Ostrobothnia in the year 2008 was over 5.0 °C and in the year 2009, it was 4.0–5.0 °C [22]. The monthly mean air temperature in Vaasa is shown in Table 1 (Pirinen, P. Finnish Meteorological Institute. Personal Communication, 2017). The heating season began in October, which can be observed as a decrease in sediment temperatures in November 2008. Further, the mean air temperatures were already dropping when the winter season arrived. A high and significant correlation has been observed between the air temperature and the temperature of sediment after one or two months [21]. The value of the maximum sediment temperature per month (Table 1) was calculated as an average of temperatures at a distance of 280–300 m from the shore (Huusko, A; Martinkauppi, I. Geological Survey of Finland. Personal communication, 2009).

Table 1. The monthly mean air temperatures (t_{ka_air}) and the monthly maximum sediment temperatures (t_{max_sed}) and the geothermal fluid temperatures (t_{ka_fluid}) in Vaasa during the measurement period in 2008–2009.

Year	Month	t_{ka_air} [°C]	t_{max_sed} [°C]	t_{ka_fluid} [°C]
		Air	**Sediment**	**Geothermal Fluid**
2008	September	9.3	8.1	-
	October	6.7	7.0	-
	November	1.8	3.9	4.0
	December	0.2	0.4	2.0
2009	January	−3.6	0	0.0
	February	−6.1	−1.2	0.0

The temperatures of the geothermal fluid were measured for the period November 2008 to February 2009 in one house connected to the low energy network. The relationship between the temperatures of the air, sediment and geothermal fluid from September 2008 to February 2009 are shown in Figure 3. In December, the geothermal fluid was measured as slightly warmer than the sediment, which can be explained by the different measurement locations.

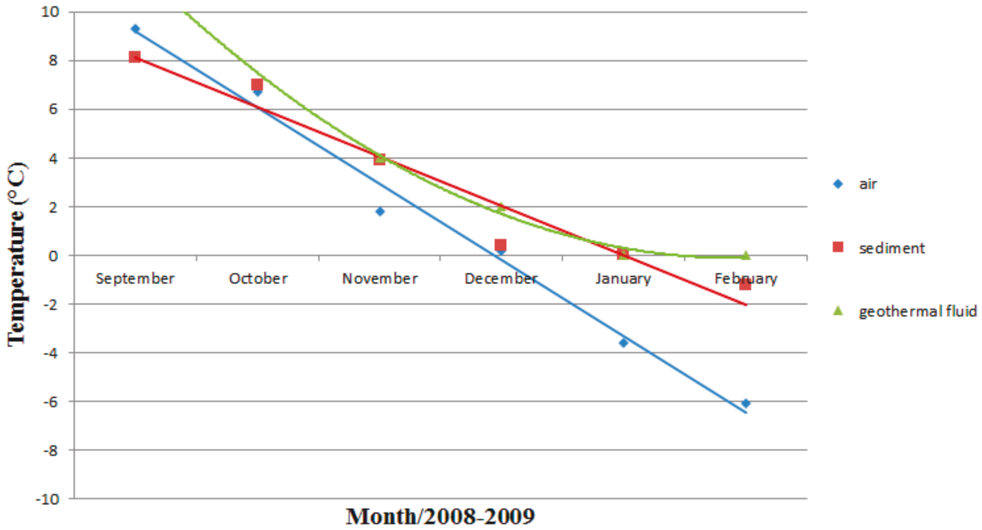

Figure 3. The relationship between the air, sediment and geothermal fluid temperatures in the low energy network of Suvilahti, Vaasa, 2008–2009. The lines are drawn to visualize and approximate relationship between measurements points.

The loading of sediment heat is shown in Figure 4. The temperatures of the sediment increased between March and August up to 11–12 °C. By May, the ambient air had warmed up and the snow and ice had melted. The water was becoming warmer and the heat in the sediment layer was also increasing. Another great difference in sediment temperatures occurred between June and July. This indicates the end of the house-heating season. The heat loading in the sediment layer starts from the shore and goes to the end of the pipe, which can be observed as a constant curve without any slope in July and August.

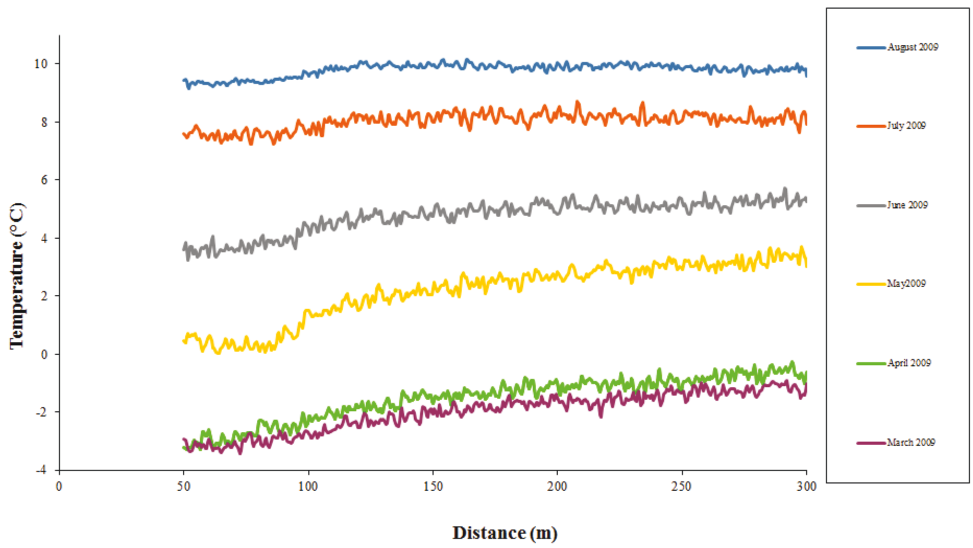

Figure 4. Seabed sediment temperatures measured from March 2009 to August 2009 in Liito-oravankatu. The Sun is obviously loading the heat to the seabed sediment.

In the follow-up study of 2013–2014, the sediment temperature cooled down until January 2014 (Figure 5). The heating of houses began in October, which can be seen in the great sediment temperature difference between October and November.

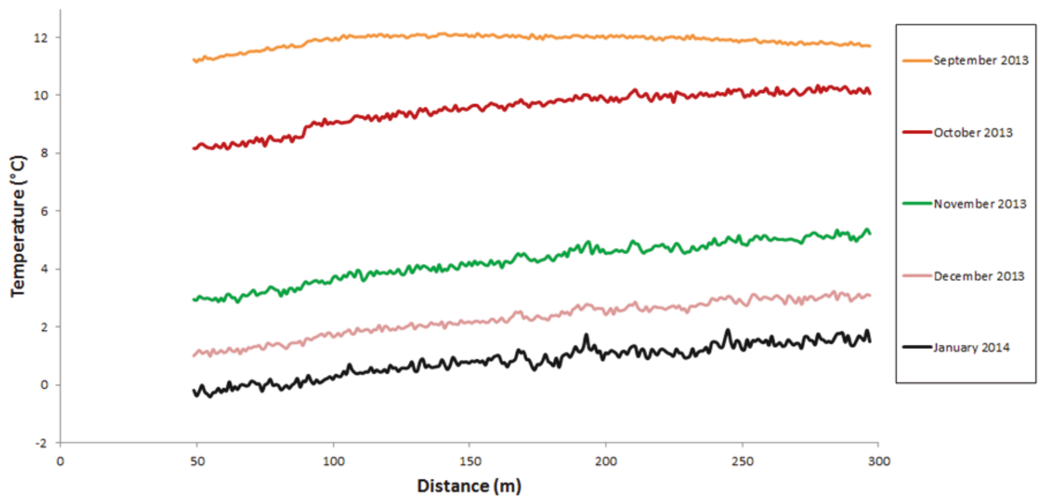

Figure 5. Seabed sediment temperatures measured from September 2013 to January 2014 in Liito-oravankatu.

The mean air temperature in Ostrobothnia, Finland in 2013 was 5–6 °C [22]. The monthly mean air temperatures in Vaasa for a five-month period in 2013–2014 are presented in Table 2 (Pirinen, P. Finnish Meteorological Institute. Personal Communication, 2017). During the measurement period of 2013–2014, it can be noticed that, on average, the sediment temperatures were higher than the air temperatures in every month except September, when they were almost equal.

Table 2. The monthly mean air temperature (t_{ka_air}), the maximum sediment temperatures (t_{max_sed}) and the geothermal fluid temperatures (t_{ka_fluid}) in Vaasa in the measurement period 2013–2014.

Year	Month	t_{ka_air} [°C]	t_{max_sed} [°C]	t_{ka_fluid} [°C]
		Air	**Sediment**	**Geothermal Fluid**
2013	September	11.9	11.7	10.0
	October	6.3	10.2	7.0
	November	2.6	5.2	5.0
	December	0.8	3.1	2.0
2014	January	−8.0	1.6	0.0

The relationship between the temperatures of the air, sediment and geothermal fluid in the period September 2013 to January 2014 are shown in Figure 6. The temperatures of the geothermal fluid were cooler than the sediment temperatures for the whole measurement period of 2013–2014.

The warming of the sediment layer from spring to late summer 2014 is shown in Figure 7. The temperatures of the sediment were increasing by up to 14 °C from March to August. The greatest difference in sediment temperatures is between April and May. The heat loading in the sediment layer takes place along the whole area from the shore to the distance of 300 m, which can be observed as a constant curve without any slope in July and August. The difference in temperatures in July and August is about 3.5 °C. The effect of the Sun is obvious.

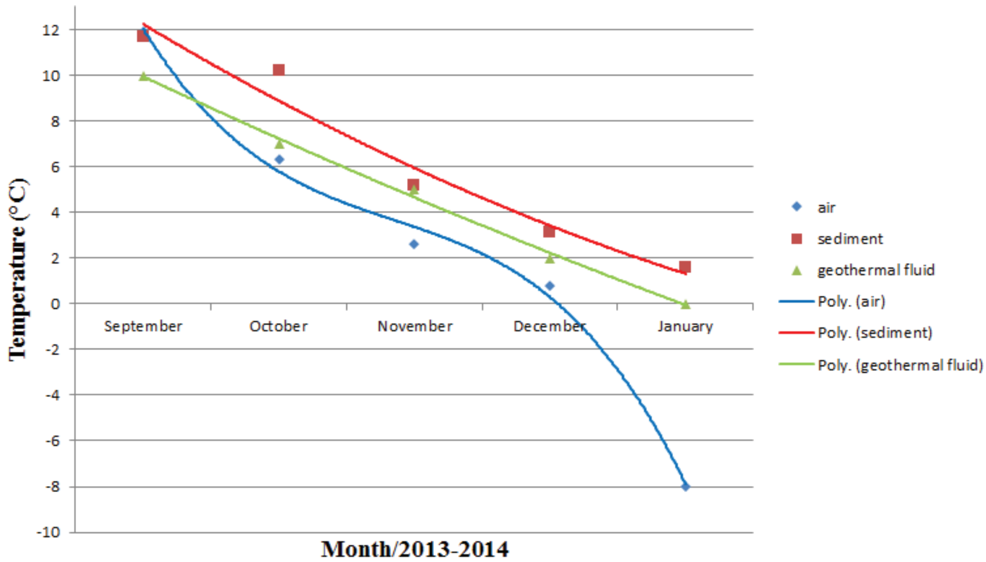

Figure 6. Temperatures of air, sediment and geothermal fluid in measurement period 2013–2014.

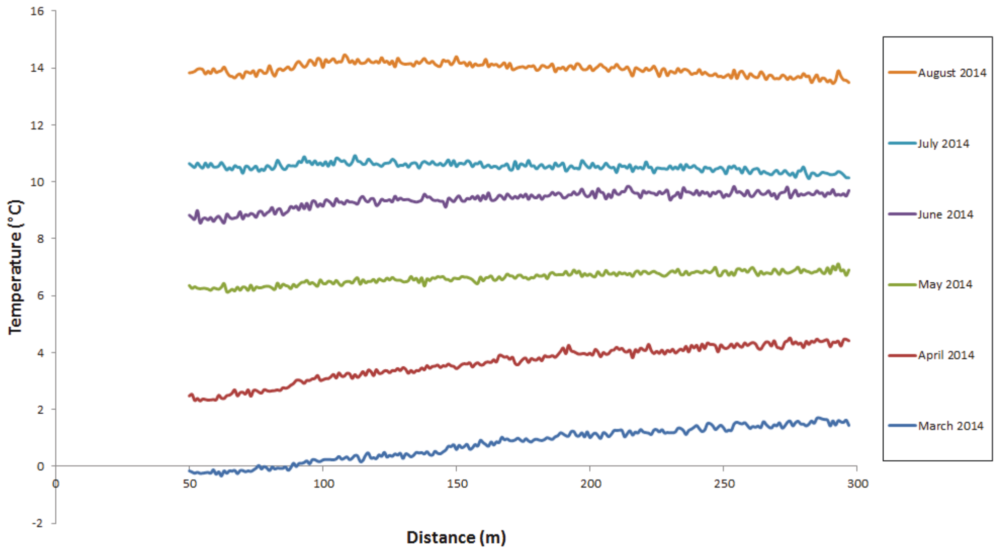

Figure 7. Seabed sediment temperatures measured from March 2014 to August 2014 in Liito-oravankatu. Temperatures increase after the winter months.

In the final follow-up study, 2014–2015, the sediment was cooling down until February 2015 (Figure 8). The great gap between the temperatures measured in September and October is due to the start of the house-heating season. Exceptionally, the sediment in December was warmer than in November. The autumn of 2014 was unusual in terms of sea water and air temperatures [22]. Energy consumption was minor in November and the heat was gathering close to the collection pipe.

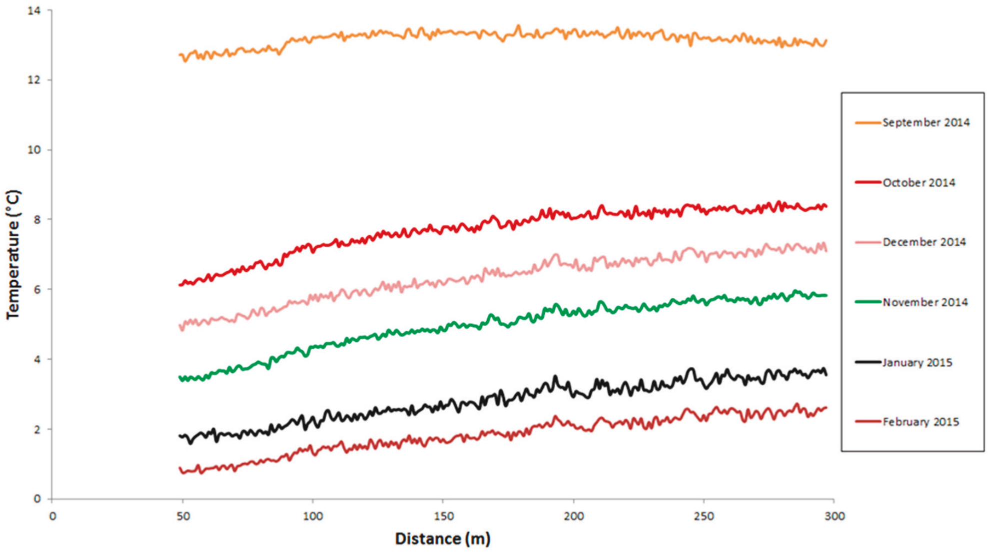

Figure 8. Seabed sediment temperatures measured from September 2014 to February 2015 in Liito-oravankatu.

The mean air temperature in Ostrobothnia, Finland in 2014 was 6.1 °C and in 2015 it was 6.4 °C (Pirinen, P. Finnish Meteorological Institute. Personal Communication, 2017). The monthly mean air temperatures in Vaasa in a six-month period in 2014–2015 are presented in Table 3. In the measurement period 2014–2015, it can be seen that, on average, in every month, the sediment temperatures were higher than the air temperatures. Further, the sediment temperatures were higher than the geothermal fluid temperatures for the whole period.

Table 3. The monthly mean air temperature (t_{ka_air}), the maximum sediment temperatures (t_{max_sed}) and the geothermal fluid temperatures (t_{ka_fluid}) in Vaasa in the measurement period 2014–2015.

Year	Month	t_{ka_air} [°C]	t_{max_sed} [°C]	t_{ka_fluid} [°C]
		Air	**Sediment**	**Geothermal Fluid**
2014	September	11.5	13.1	9.0
	October	5.0	8.4	8.0
	November	1.0	5.9	4.0
	December	−0.7	7.2	2.0
2015	January	−3.1	3.6	0.0
	February	−0.2	2.5	0.0

The relationship between the temperatures of the air, sediment and geothermal fluid in the period September 2014 to February 2015 are shown in Figure 9. The sediment was warmer than the air during the whole period. The geothermal fluid temperatures were cooler than the sediment temperatures for the whole measurement period of 2014–2015, as expected.

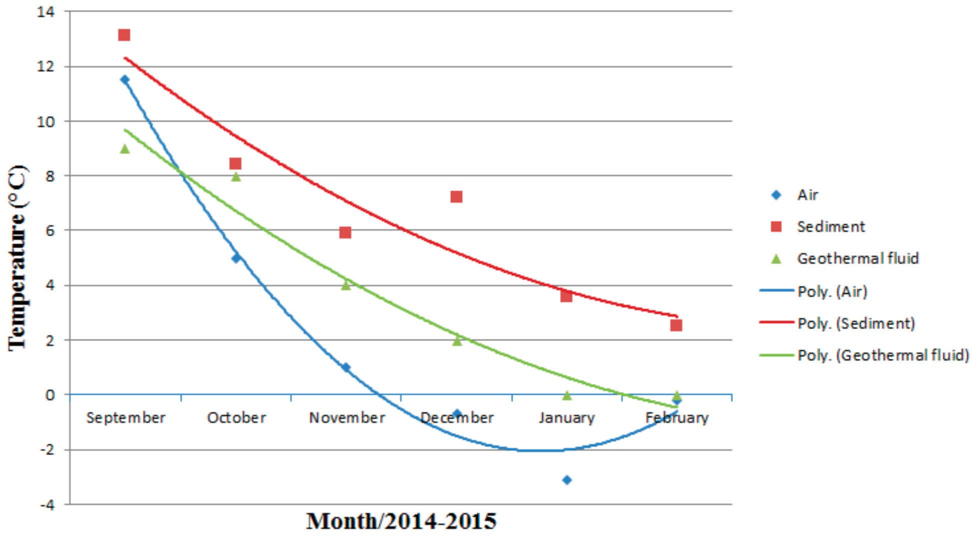

Figure 9. Temperatures of the air, sediment and geothermal fluid in the measurement period 2014–2015.

The warming of the sediment layer from spring to late summer 2015 is shown in Figure 10. The temperatures of sediment were increasing from March to August, by up to 12 °C. The greatest difference in the sediment temperatures was between April and May and the sediment had clearly warmed up by July.

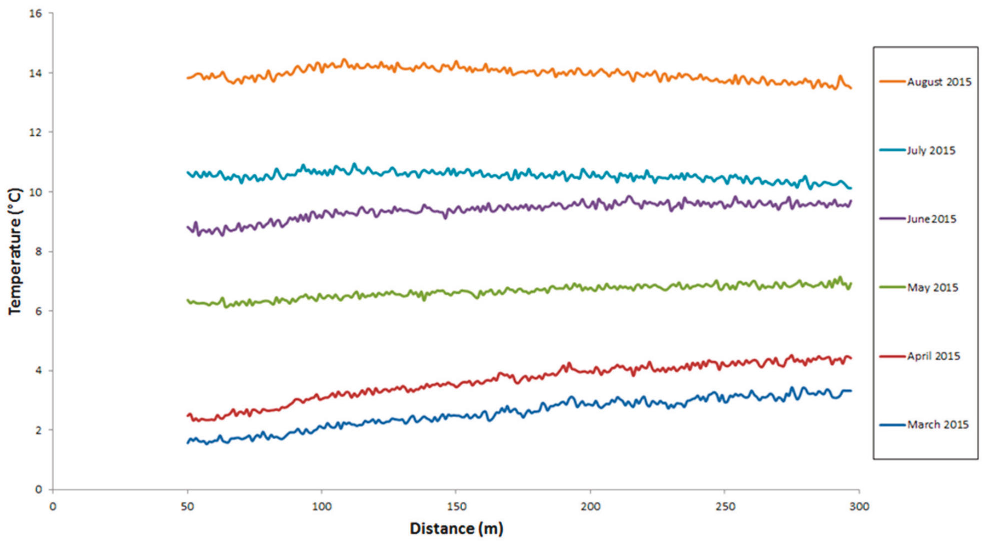

Figure 10. Seabed sediment temperatures measured from March 2015 to August 2015 in Liito-oravankatu. Heat loading is observed as increased temperatures in the sediment layer.

In 2008–2009, the average difference between the sediment temperature in September (the month with the highest temperature value) and February (the month with the coldest sediment temperature) was 9.7 °C. In 2013–2014, the average difference between the sediment temperature in September and that of the month with the lowest sediment temperature, i.e., January, was 11.1 °C. In 2014–2015, the difference between the temperature in September and the lowest temperature values in February was 11.2 °C. Thus, the absolute decrease in temperature was essentially the same in both periods (Figure 11).

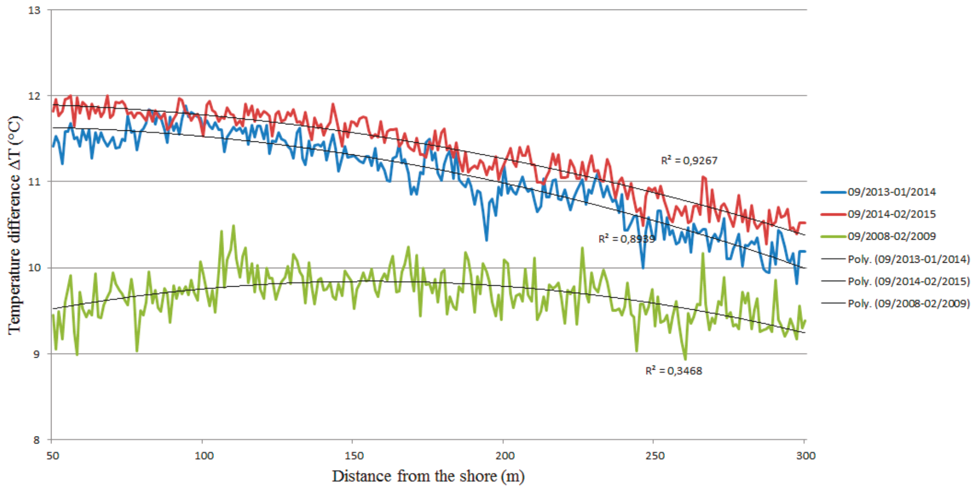

Figure 11. The between-month difference in sediment temperatures for the months with the highest and the lowest temperature values in the periods 2008–2009, 2013-2014 and 2014-2015. The polynomials of second degree are drawn as trend lines.

In the years 2013–2014 and 2014–2015 the difference in temperatures was higher nearer to the shore and decreased smoothly, being around 1.5 °C lower at the distance of 300 m than at the distance of 50 m from the shore.

5. Discussion

Different models of interaction between water and sediment has been studied e.g., in North-Western Russia and Germany, [2] and in United States [10,23]. The measured data for all the periods—2008–2009, 2013–2014 and 2014–2015—show the cooling of sediment during the autumn and winter seasons. The difference in sediment temperatures between a month with the highest temperature value and a month with the lowest temperature value in each period varied from 9.7 to 11.2 °C. The level of the temperatures was about 4 °C lower in the early stage of the new low energy network (2008–2009) than it was five years later. In the first measurement period, 2008–2009, measurements were taken with a device that was different to that used in the follow-up measurement period of 2013–2015. It is also true that because of heating and the drying of the constructions, the houses needed more energy during the first heating season than they did in later years. This has had a decreasing influence on the temperatures of the sediment.

There is a roughly 2 °C difference between the temperatures measured near the shore and those measured at a distance of 300 m from the shore. This difference may reflect the depth of the water layer over the sediment. The farther from the shore the measurement is taken, the thicker the water layer and the warmer the sediment. Accurate data about the depth of the water layer are not available for the Suvilahti area. On the other hand, the position of the cable is estimated to be 3–4 m under the seabed but the exact position of the cable at the different distances from the shore cannot be measured.

In the measurement period 2008–2009, the heat carrier fluid temperature was higher than the highest sediment temperature each month in that period. This is explained by the accuracy of the Ouman fluid temperature meter, which was ±1 degree. The result is intelligible if the limit of error is taken into account. The other factor that may have had an effect on the comparability of the fluid and sediment temperatures is that the measurements of the heat carrier fluid were made in the engineering and utility service room inside a house, whereas the sediment temperature measurements were taken next to the collection well on the shore. It may also be possible that the surroundings of the collection pipe in the seabed sediment were frozen and that ice cover may have acted as an insulator for the heat carrier fluid.

The validity of the sediment temperature data is somewhat questionable because of the location of the temperature measurement cable, i.e., connected to the side of the operating heat collection pipe that contains the heat carrier fluid. On the other hand, the influence of the fluid can be expected to be quite small. In future studies, to gain more accurate sediment temperatures, it would be good to attach the temperature measurement cable to bare sediment in the same location and to compare those temperatures with the current results.

The possible flow of groundwater should be known when estimating the heat capacity of a particular area of the sediment. These data are missing for Suvilahti.

Ice and snow cover have an effect on the temperatures of water, which, according to Birge et al. [6] interacts with the sediment. There are no data available about the thickness of the ice or the depth of snow cover in Suvilahti. The stationary stage of sediment temperatures can be observed in a particular section of every study period and this reflects the impact of ice and snow cover. The heat transfer occurs farther from the pipeline and a stationary stage prevails close to the pipeline.

6. Conclusions

These follow-up sediment temperature measurements show that sediment has reloaded perfectly every year. Despite the usage of the energy, the temperature rate of the sediment did not essentially decrease during the five-year period in the Vaasa Housing Fair area. The start of the heating season can be clearly observed.

Consideration of the between-month difference in sediment temperatures for the month with the highest temperature and the month with the lowest temperature value for all measurement periods shows that the usage of the low energy network has not permanently changed temperatures in the sediment. The temperatures vary annually and the influence of the radiant energy of the Sun can be noted. The accumulation of heat can be seen in the sediment temperatures in autumn as the highest values of the year.

There is a drop of several degrees in the temperatures of October The first heating month harvests the energy from areas close to the heat collection pipe. The sea has yet no covering of ice. The air temperature has an influence on the water and, due to heat conduction, also on the sediment temperatures. All this appears as a notable decrease in the sediment temperature in November and continues until the stationary stage has been achieved in February–March 2009, January–March 2014 and January–March 2015.

This research indicates that the sediment heat is a potential energy source. In future development of these systems the depth of the pipeline should be known and kept in at least 3 m downwards from the sea bottom.

Acknowledgments: We would like to express our thanks to Juhani Luopajärvi (heat carrier fluid measurements) and the Geological Survey of Finland in Kokkola. This work was supported by the City of Vaasa and the University of Vaasa.

Author Contributions: Anne Mäkiranta and Erkki Hiltunen conceived and designed the experiments; Anne Mäkiranta performed the experiments, analyzed the data and wrote the paper; Birgitta Martinkauppi contributed to the theory; Mauri Lieskoski contributed to the materials.

Conflicts of Interest: The authors declare no conflict of interest. The founding sponsors had no role in the design of the study; in the collection, analyses, or interpretation of data; in the writing of the manuscript and in the decision to publish the results.

References

1. Likens, G.E.; Johnson, N.M. Measurement and analysis of the annual heat budget for the sediments in two Wisconsin lakes. *Limnol. Oceanogr.* **1969**, *14*, 115–135. [CrossRef]
2. Golosov, S.; Kirillin, G. A parameterized model of heat storage by lake sediments. *Environ. Model. Softw.* **2010**, *25*, 793–801. [CrossRef]
3. Finnish Meteorological Institute. Available online: http://ilmatieteenlaitos.fi/tilastoja-vuodesta-1961 (accessed on 12 October 2017). (In Finnish)
4. Mäkiranta, A.; Martinkauppi, J.B.; Hiltunen, E. Seabed sediment—A natural seasonal heat storage feasibility study. *Agron. Res.* **2017**, *15*, 1101–1106.
5. Birge, E.A.; Juday, C.; March, H.W. The temperature of the bottom deposits of Lake Mendota; a chapter in the heat exchanges of the lake. *Trans. Wis. Acad. Sci.* **1927**, *XXIII*, 187–231.
6. Smith, N.P. Observations and simulations of water-sediment heat exchange in a shallow coastal lagoon. *Estuaries* **2002**, *25*, 483–487. [CrossRef]
7. Gu, R.; Stefan, H.G. Year-round temperature simulation of cold climate lakes. *Cold Reg. Sci. Technol.* **1990**, *18*, 147–160. [CrossRef]
8. Hondzo, M.; Ellis, C.; Stefan, H. Vertical diffusion in small stratified lake: Data and error analysis. *J. Hydraul. Eng.* **1991**, *117*, 1352–1369. [CrossRef]
9. Welch, H.E.; Bergmann, M.A. Water circulation in small arctic lakes in winter. *Can. J. Fish. Aquat. Sci.* **1985**, *42*, 506–520. [CrossRef]
10. Tsay, T.; Ruggaber, G.J.; Effler, S.W.; Driscoll, C.T. Thermal stratification modeling of lakes with sediment heat flux. *J. Hydraul. Eng.* **1992**, *118*, 407–419. [CrossRef]
11. Bengtsson, L. Mixing in ice-covered lakes. *Hydrobiologia* **1996**, *322*, 91–97. [CrossRef]
12. Fang, X.; Stefan, H.G. Dynamics of heat exchange between sediment and water in a lake. *Water Resour. Res.* **1996**, *32*, 1719–1727. [CrossRef]
13. Brewer, M.C. The thermal regime of an arctic lake. *Am. Geophys. Union Trans.* **1958**, *39*, 278–284. [CrossRef]
14. Allen, A.; Dejan, M.; Sikora, P. Shallow gravel aquifers and the urban 'heat island' effect: A source of low enthalpy geothermal energy. *Geothermics* **2003**, *32*, 569–578. [CrossRef]
15. Zhu, K.; Blum, P.; Ferguson, G.; Balke, K.; Bayer, P. The geothermal potential of urban heat islands. *Environ. Res. Lett.* **2010**, *5*, 1–6. [CrossRef]
16. Suomi, J. Characteristics of Urban Heat Island (UHI) in a High-Latitude Coastal City—A Case Study of Turku. SW Finland. Ph.D. Thesis, Department of Geography and Geology, University of Turku, Turku, Finland, 2014. Available online: http://urn.fi/URN:ISBN:978-951-29-5912-9 (accessed on 21 November 2017).
17. Li, C.; Shang, J.; Cao, Y. Discussion on energy-saving taking urban heat island effect into account. In Proceedings of the IEEE International Conference on Power System Technology (POWERCON), Hangzhou, China, 24–28 October 2010; pp. 1–3.
18. Santamouris, M. *Solar Thermal Technologies for Buildings—The State of the Art*; Cromwell Press: Trowbridge, UK, 2003, ISBN 1-902916-47-6.
19. Hiltunen, E.; Martinkauppi, B.; Zhu, L.; Mäkiranta, A.; Lieskoski, M.; Rinta-Luoma, J. Renewable, carbon-free heat production from urban and rural water areas. *J. Clean. Prod.* **2017**, *153*, 397–404. [CrossRef]
20. Hiltunen, E.; Martinkauppi, J.B.; Mäkiranta, A.; Rinta-Luoma, J.; Syrjälä, T. Seasonal temperature variation in heat collection liquid used in renewable, carbon-free heat production from urban and rural water areas. *Agron. Res.* **2015**, *13*, 485–493.
21. Mäkiranta, A.; Martinkauppi, J.B.; Hiltunen, E. Correlation between temperatures of air, heat carrier liquid and seabed sediment in renewable low energy network. *Agron. Res.* **2016**, *14*, 1191–1199.
22. Finnish Meteorological Institute. Available online: http://ilmatieteenlaitos.fi/jaatalvi-2014-2015 (accessed on 11 December 2017). (In Finnish)
23. Fang, X.; Stefan, H.G. Temperature variability in lake sediments. *Water Resour. Res.* **1998**, *34*, 717–729. [CrossRef]

Agronomy Research **15**(S1), 1101–1106, 2017

Seabed sediment – a natural seasonal heat storage feasibility study

A. Mäkiranta*, B. Martinkauppi and E. Hiltunen

University of Vaasa, Faculty of Technology, Electrical Engineering and Energy Technology, P.O. Box 700, FI-65101 Vaasa, Finland
*Correspondence: anne.makiranta@uva.fi

Abstract. The new discovery among renewable energy resources, seabed sediment, has been utilised as a heat source for 42 houses in Vaasa since 2008. Sediment heat is annually loaded by the Sun. In this study the amount of annually charged energy is estimated. The difference of sediment temperatures between the coldest and the warmest month during the year is a key value in the approximation of the loaded energy. Sediment temperatures are measured once per month via optical cable by distributed temperature sensing (DTS) method. The monitoring period is three years, 2014–2016. The estimation of incoming energy (575 MWh) versus known exploited energy (560 MWh) is reasonable. Despite of the extraction this seasonal heat storage in the seabed of the Baltic Sea seems to reload well annually.

Key words: renewable energy, sediment heat, distributed temperature sensing, heat storage.

INTRODUCTION

Renewable, Sun-based energies are often available when the need of energies is low. Especially in the Northern countries, the demand of heat is greater in wintertime but a lot of renewable heat is available in summertime. Due to the seasonal nature of the solar energy, its utilisation requires storing. Water tanks, bedrock batteries and aquifers are the most used applications as heat storages. Old flooded mines have also been studied as potential heat storages (Watzlaf et al., 2006; Martinkauppi & Hiltunen, 2015). There are also natural seasonal heat storages like seabed sediment. The natural seasonal storing guarantees that the heat is available in winter time when the heating season is going on. The advantages of natural storage are also automatical annual function, fewer infrastructure constructions and thus less CO_2 emissions.The aim of this study is to estimate the amount of reloaded energy. This will help to estimate how much energy is exploited without detrimental effects.

Local renewable energy sources are available almost everywhere on Earth. The seabed sediment heat is one geothermal heat energy source which has been utilized in Vaasa, Finland since 2008. Actually the heat of this source is mainly coming from the Sun which is a common feature of natural heat sources in the upper crust. In Finland, the seasonal variation in air temperatures is observed to correlate even to the depth of 10–15 meters from the soil surface (Mäkiranta et al., 2016a).

Geological Survey of Finland made a geological analysis of the sediment in Suvilahti area in 2006. They also measured the sediment temperatures in house fair area in 2008–2009 (Martinkauppi, 2013). Valpola (2007) discovered that the annual air temperature variation is observed only to the depth of 3 m in the seabed sediment in Vaasa area. Instead in the ground that variation is observed even to the depth of 10–15 m. The Research group of Renewable Energies from University of Vaasa continued temperature measurements in 2013 in the same site, Suvilahti suburb.

Hiltunen et al. (2015) and Mäkiranta et al. (2016b) have investigated the dependency between the air temperature, the sediment heat collection fluid (water ethanol mixture) temperature and the sediment temperature on the residential area which is utilizing the seabed sediment as a heat source. They observed that there is a clear correlation between the heat carrier liquid temperature and the sediment temperature of the next month and the temperatures of the same month as well. The conclusions of that study were that there is heat energy sufficiently available for all the houses included in the low energy network, the collection pipeline is sized correctly.

In this study, the annual recovery of the sediment heat is examined. The annually loaded energy is estimated by means of the seasonal temperature variation in sediment when the composition of sediment is known to be wet clay.

MATERIALS AND METHODS

Seabed sediment has been utilised since 2008 as a heat source in the residential area in Vaasa next to the Gulf of Bothnia in the Baltic Sea. This low energy network is used for heating and cooling houses throughout the year. The main heating season starts on October continuing to May. During the summer season cooling is used occasionally. Instead the loading occurs from April to October. The sediment temperature measurements have been executed there starting from the year 2013 by the Renewable Energy Research group of University of Vaasa. The used measurement method is distributed temperature sensing (DTS) method and the device is a product of Sensornet, Oryx DTS. The method and more detailed description of measurements are presented by Mäkiranta et al. (2016c).

Figure 1. The measurement site is located in Ketunkatu street. A box including optical fibers with connectors is placed in the distribution well.

There is assembled an optical cable along one heat collection pipe in Ketunkatu street (Fig.1). In measurement session the laser pulse travels along the optical glass fiber inside the cable. So the cable functions as a thermal profile sensor transferring temperature data with spatial resolution of 1 meter. The cable is 300 meters long and it is diagonally drilled to the depth of 3–4 meters, see Fig. 2. During the drilling action there was noticed some rocks and the direction of drilling had to be changed. Because of this variety in the composition of sediment layer the depth position of cable may vary from the supposed one.

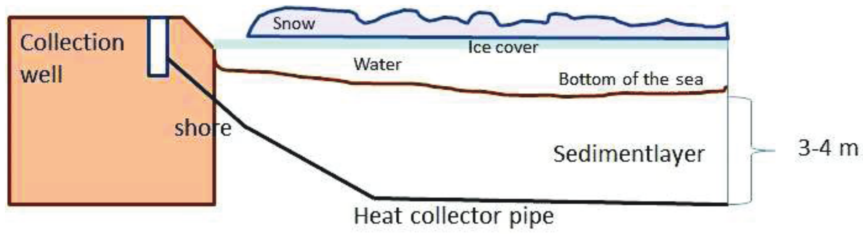

Figure 2. The conjectural position of the collection pipe and measurement cable along it in the seabed sediment is visualized in this graphical presentation. (not in scale).

The measurements were made once per month throughout the years. To discover the annual reloading of sediment heat the temperature difference between the warmest and the coldest month of the year were calculated. Year 2013 was measured only partly, thus the first year for observing the reloading of the seabed sediment heat was 2014. The highest sediment temperatures were observed in October 2014, 2015 and 2016. Instead the time of the coldest month varied being February in 2014 and March in 2015 and 2016. The temperature difference curves are shown in Fig. 3. The *x*-axis shows the length and the distance of the cable from the shore. The zero point is on the shore in the well and the sediment layer occurs after about 5 meters distance from the well. The first hundred meter is partly covered by reeds and there is located a pedestrian route with a bridge, too. They may have an effect on temperatures. Therefore, the starting point for calculating the differences was decided to be at 100 meter distance from the shore. The sediment temperature differences are presented 100–300 meters distance from the shore in years 2014–2016 in Fig. 3.

According to the Finnish Meteorological Institute (2017) the annual average air temperature in Finland during the year 2016 was the warmest compared to the long term average in 1981–2010. Sediment temperatures in 2016 were indicating the warming too. Based on the previous research by Mäkiranta et al. (2016b) the sediment temperature correlates strongly with the air temperature of two previous months.

The amount of annually loaded energy in the sediment layer is estimated with help of the facts that how much energy is bound to close range around the collection pipe while the annual temperature variation in sediment is known. The calculated energy is compared to the experimental extraction of energy which is known to be 560 MWh per year in the low energy network (Energy Vaasa, 2016).

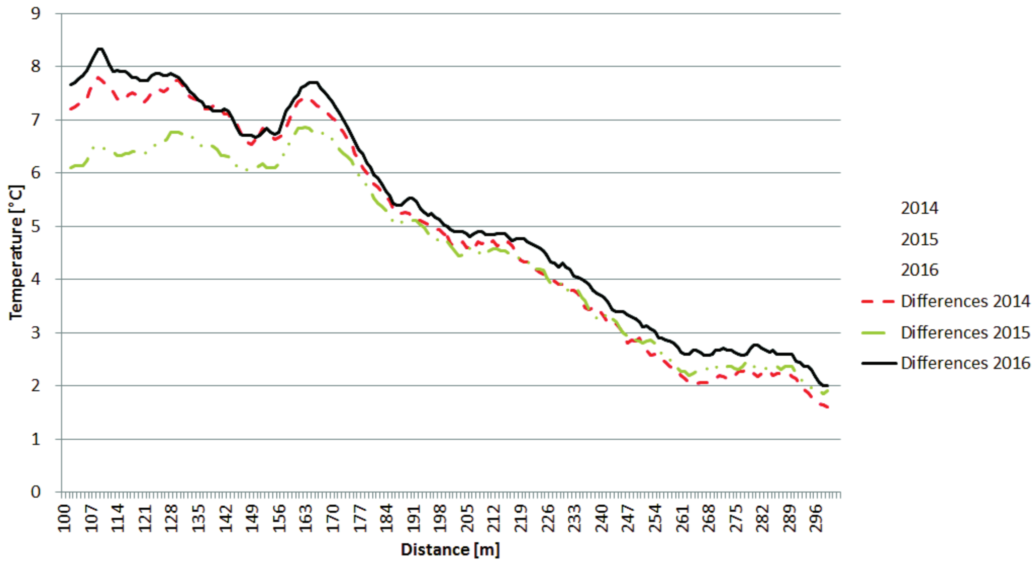

Figure 3. Temperature differences between the warmest and the coldest months during three annual loading periods in 2014, 2015 and 2016 as a function of length and distance of the cable from the shore. (Note: data is smoothed in Excel with the following option: moving averages with period 3, as the original data is very noisy).

The estimation of loaded and later extracted energy by the Sun is calculated as follows. First, the volume

$$V = \pi r^2 h \tag{1}$$

The volume of heat collection pipeline (26 pipes, h = 300 m, Ø = 84 mm) in the sediment is 43 m³ calculated with Eq. 1. The volume of seabed sediment around the pipeline with a radius of 2 m is 98.0 10^3 m³. The mass of the volume is calculated using the basic formula (Eq. 2):

$$m = \rho \cdot V \tag{2}$$

The calculation gives the value of mass as 172 10^6 kg when density of wet clay ρ = 1,760 kg m^{-3} is used. The heat energy is:

$$Q = cm\Delta T \tag{3}$$

The quantity of heat energy Q in the seabed sediment for heat collection is calculated with help of Eq. (3), when the average variation of annual sediment temperature (ΔT) is 5 °C and specific heat capacity of wet clay c =2.4 kJ kg^{-1} °C. By using these consumptions the quantity of heat energy is counted to be 2,070 10^6 kJ which is equal to 575 MWh.

RESULTS AND DISCUSSION

The absolute temperatures at the distances of 100–170 m are variating from 3–14 °C. This reveals that the depth of the heat collection pipe is not more than 3 m. The annual air temperature variation is clearly affecting to the sediment temperatures. Instead the effect of air temperature is not noticed in winter months measured sediment temperatures. The ice cover and snow form an isolating layer against the effect of the air temperature.

The absolute temperatures at the distances of 180–230 m variate from 5–12 °C and at the distances 240–300 m about 6–10 °C throughout the year. According to these last values (h = 300 m - 240 m = 60 m and ΔT = 10 °C – 6 °C = 4 °C), the heat energy Q = 92 MWh is available in the sediment layer.

The temperature difference (ΔT) between the warmest and the coolest month remain almost at the same level year after year. The variation is only between 0–2 °C and the difference curve follows the same shape every year. After 180 m distance the variation in the temperature differences is about 0.5 °C. This may indicate the fact that the sediment heat collection pipe is located deeper in the sediment layer at the distance of 180–300 m than closer to the shore. Thus the air temperature has not such a great impact on the sediment temperature.

The annual variation of the sediment temperature indicates the fact that the heat energy is truly naturally loaded to the seabed sediment despite of the usage for heating houses in the residential area.

The estimation of incoming energy compared to known exploited energy is reasonable when the estimated influence area`s radius is 1°m around the heat collection pipe and ΔT = 5 °C. The annual extraction of energy is 560°MWh and the calculated value for annually loaded heat energy is 575°MWh. Despite of the extraction the sediment heat seems to reload well annually.

CONCLUSIONS

Sediment temperature measurements were made once per month for three years period by using distributed temperature sensing (DTS) method. With help of the temperature differences of coldest and warmest month the annual reloading of heat was calculated and verified. The stage of annual charging may vary due to the average air temperature level of the year but still the variation is only 0–2 °C. Regardless of the heat extraction the annual reloading of sediment heat seems to be complete and even in the long run no cooling is expected.

This study shows that nature formulates seasonal storages to the watercourse sediment layers. The renewable heat will stay there waiting for the utilization.

ACKNOWLEDGEMENTS. We thank for Geological Survey of Finland for sharing the data and knowledge of seabed sediment in Vaasa area.

REFERENCES

EnergyVaasa. Available on the Internet (last access on 10.10.2016): < http://energyvaasa.vaasanseutu.fi/en/cases/case-renewable-energy/>

Finnish Meteorological Institute FMI (2017). Available on the Internet (last access on 28.3.2017): < http://ilmatieteenlaitos.fi/tiedote/291348664>. Only in Finnish.

Hiltunen, E., Martinkauppi, J.B., Mäkiranta, A., Rinta-Luoma, J. & Syrjälä, T. 2015. Seasonal temperature variation in heat collection liquid used in renewable, carbon-free heat production from urban and rural water areas. *Agronomy Research* **13**, 485–493.

Martinkauppi, B & Hiltunen, E. 2015. *Water heat battery-preliminary survey* (Vesilämpöakku-esiselvitys). EAKR-project. Final report. 18 p. Only in Finnish.

Martinkauppi, Ilkka. 2013 Private communications.

Mäkiranta, A., Martinkauppi, B. & Hiltunen, E. 2016a. Seasonal temperature variations under lawn and asphalt fields: *Proceedings of the11th Conference on Sustainable Development of Energy, Water and Environment Systems,* SDEWES2016.0281, 1–6.

Mäkiranta, A., Martinkauppi, J.B. & Hiltunen, E. 2016b. Correlation between temperatures of air, heat carrier liquid and seabed sediment in renewable low energy network. *Agronomy Research* **14**, 1191–1199.

Mäkiranta, A., Martinkauppi, B. & Hiltunen, E. 2016c. Design of Asphalt Heat Measurement in Nordic Country. *Proceedings of the11th Conference on Sustainable Development of Energy, Water and Environment Systems*, SDEWES2016.0580, 1–7.

Valpola, Samu. 2007. Unpublished results.

Watzlaf, G. & Ackman, T.E. 2006. Underground Mine Water for Heating and Cooling using Geothermal Heat Pump Systems. *Mine Water and the Environment* **25**, 1–14.

SDEWES2016.0580 Design of Asphalt Heat Measurement in NOrdic Country

A. Mäkiranta*, B. Martinkauppi, E. Hiltunen

University of Vaasa, Finland(*anne.makiranta@uva.fi)

Abstract

There are a plenty of urban geoenergy available in the built environment. One of the geoenergy forms is asphalt heat. The black asphalt is an effective solar energy absorber and it is abundant in towns and cities. This energy is suitable for many heating applications: e.g. in England, asphalt pavement is used as a heat collector during summer time and this stored heat is used in floor heating system in houses or as in Netherlands, the asphalt heat from roads is used for the warming of public buildings [1,2]. In Northern countries it is debatable if the asphalt heat is appropriate for utilisation at all. Is there heat enough despite of the frozen season in winter?

This study presents the design of asphalt heat measurement field which is implemented in Vaasa, Finland. The installation includes several hundreds of meters optical fibre buried to the soil, connection box with fibre splices, wells for water level measurements, heat flux plate and pyranometer. There are also a lawn covered similar measurement field next to the asphalt field. The distance of measurement fields is about 200 m which guarantees similar solar and other weather conditions. The unique temperature measurement fields were planned and implemented next to the University of Vaasa.

The ground temperatures under the asphalt and lawn layer can be measured even to the depth of 10 m. The measurement field consist of two wells with the depth of 10 m and one well of 5 m depth. In those wells the spatial resolution for temperature measurements is 1 m. Near the surface it would be significant to monitor the temperatures more precisely. That's why there are implemented two three meters deep holes where the optical fibre has been wired around the tube. Then the spatial resolution is even 2-3 cm.

The measurements are made by using DTS (distributed temperature sensing) method which is based on the optical light scattering. Optical cables have been installed permanently in both measurement fields. Heat flux plate is measuring the heat flow by W/m^2.

The presented design unique but it is appropriate to apply in any Northern country.

0580-1

Design of Asphalt Heat Measurement in Nordic Country

Anne Mäkiranta*, Birgitta Martinkauppi and Erkki Hiltunen
Faculty of Technology
University of Vaasa, Vaasa, Finland
e–mail: anne.makiranta@uva.fi

ABSTRACT

This study presents the design of asphalt heat measurement field. The installation includes several hundreds of meters optical fibre buried to the soil, connection box with fibre splices, wells for water level measurements, heat flux plate and pyranometer. There are also a lawn covered similar measurement field next to the asphalt field. The distance of measurement fields is about 200 m which guarantees similar solar and other weather conditions. The unique temperature measurement fields were planned and implemented next to the University of Vaasa.
The implementation process was successful. Only one cable in lawn field is malfunctioning but still there is a possibility to measure in both fields.
The presented design is unique but it is appropriate to apply in any Northern country.

KEYWORDS

asphalt heat, renewable energy, solar energy, distributed temperature sensing

INTRODUCTION

There is a plenty of urban geoenergy available in the built environment. One of the geoenergy forms is asphalt heat. The black asphalt is an effective solar energy absorber and it is abundant in towns and cities. This energy is suitable for many heating applications. In the United Kingdom asphalt pavement is used as a heat collector during summer time and this stored heat is used in floor heating system in houses. In Netherlands, the asphalt heat from roads is used for warming of public buildings [1,2]. In Nordic countries it is debatable if the asphalt heat is appropriate for utilisation at all. Is there heat enough despite of the frozen season in winter? To answer that question the study field for asphalt heat measurements was made.

This study presents the design of asphalt heat measurement field which is implemented in Vaasa, 63°06'N 021°37'E, Finland. The installation includes several hundreds of meters optical fibre buried to the soil, connection box with fibre splices, wells for water level measurements, heat flux plate and pyranometer. The optical fibre functions as a linear sensor to acquire the soil temperatures under asphalt cover even to the depth of 10 m. Heat flux plate indicates the heat flow and pyranometer is detecting the solar radiation. There is also a lawn covered similar measurement field next to the asphalt field. The distance of measurement fields is about 200 m which guarantees similar solar and other weather conditions. The unique temperature measurement fields were planned and implemented next to the University of Vaasa.

* Corresponding author

0580-2

The effect of seasonal variation in the air temperature on the soil temperature is noticed to prevail in approximately 10-15 m depth in Finland. That is why in the configuration of measurement field the deepest temperature measurement point was settled to the depth of 10 m.

MATERIALS AND METHODS

Implementation of measurement fields

The measurement fields with asphalt and lawn cover consist of two wells with the depth of 10 m and one well of 5 m depth. In those wells the spatial resolution for the temperature measurements is 1 m. Near the surface it would be significant to monitor the temperatures more precisely. That's why there are implemented two 3 m deep holes where the optical fibre has been wired around the tube (Figure 1). Then the spatial resolution is even 2-3 cm. These special installations have been implemented in both fields.

Figure 1. The tubes to measure the soil temperatures.

Temperature measurements are made by using the DTS (distributed temperature sensing) method which is based on the optical light scattering. Optical multimode glass fibres cables (Brugg: BRUSens Temperature 4xMMF and Optical Cable Corporation: Laser Ultra-Fox Breakout 4xMM) have been installed permanently in both measurement fields. Cables function as linear sensors both under the asphalt and lawn covered field.

The aim is to investigate if there are some differences in the temperatures due to the upmost layer on the top surface. The measurements are made at the same time both in asphalt and lawn field. The design of asphalt heat measurement field is presented in Fig. xx. The total length of optical cable is 550 m. About 70 m of that is for calibration and 480 m is buried to the soil. Actually in the installation stage there were four cables which were spliced together afterwards (total 550 m). There are four fibers inside the cable, but only one of those is used in temperature measurements. This fiber is spliced of four different pieces together. Thickness of the asphalt layer is approximately 7-10 cm, gravel and sand layer is approximately 60 cm thick and clay lies under those layers (Fig. 2).

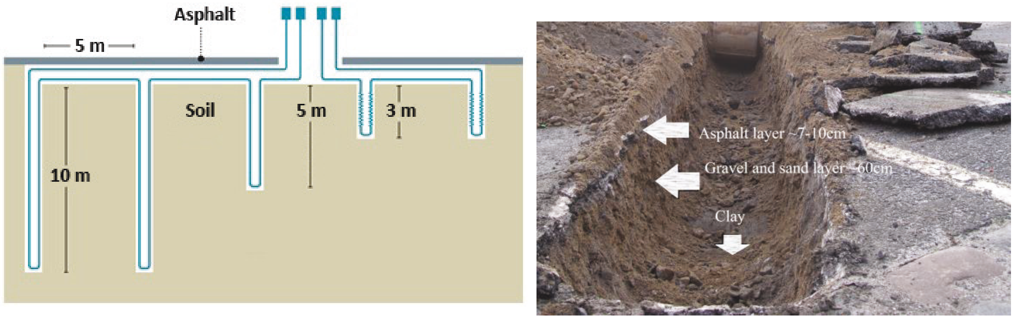

Figure 2. The configuration of measurement cables and structure and thickness of layers beneath the asphalt.

The layout of the measurement field in the parking lot (Fig. 3) visualises the positions of measurement wells. The cable is installed to the wells which are located at minimum distance of 5 m of each other. There is a possibility to measure the water level in two wells. The layout of the measurement field in the lawn covered area is similar compared to the asphalt field.

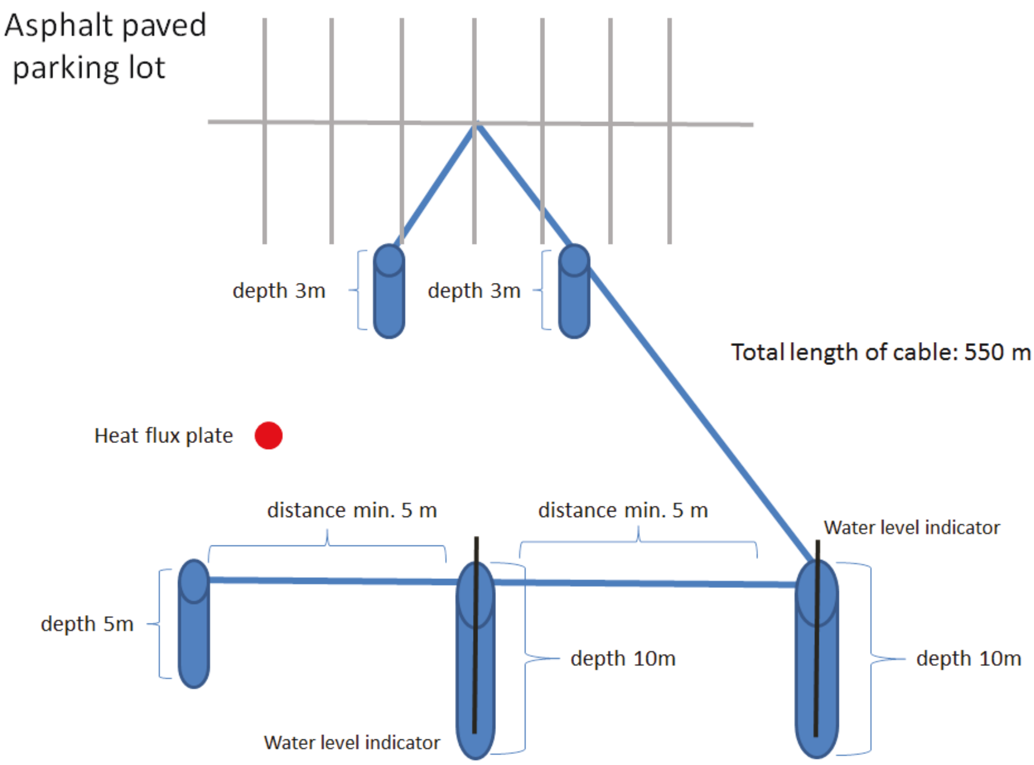

Figure 3. Measurement field layout in asphalt paved parking lot.

The implementation of the measurement fields took three working days. First the measurement wells had to be drilled (Fig. 4) and the connection channels between the wells dug (Fig. 5).

0580-4

Figure 4. Drilling of measurement wells in the parking lot and lawn field was done in the late Autumn 2013.

Figure 5. Excavator was necessary in establishing the measurement field.

After the cable installation was done the wells and the channels had to be covered at the both measurement fields. The parking lot`s asphalt pavement was fixed and grass seeds were sowed to get the lawn field appropriate (Fig 6).

Figure 6. The implementation of cables and the completed measurement fields.

Measurement devices and methods

<u>*Pyranometer and heat flux plate*</u> Hukselux LP02-TR pyranometer is located on the roof of the University`s library (next to the measurement fields) to gain the daily data of solar radiation (Fig. 7 a)). Hukseflux HFP01 heat flux plate is installed only to the asphalt field (Fig. 7 b)) right under the asphalt cover to measure the heat flux through the asphalt layer. Measurements after every 10 minutes are recorded.

a) b)

Figure 7. a) A pyranometer is measuring the solar radiation. b) A heat flux plate was assembled under the asphalt cover.

The pyranometer and the heat flux plate indicates the solar radiation in W/m^2 . The accuracy of both devices is dependent on many factors e.g. calibration, weather and soil conditions. In a perfect environment, the initial calibration accuracy of the heat flux sensor is estimated to be ±3 %. The data acquired by the pyranometer help to estimate how much solar energy is coming to the surface and the heat flux plate is indicating how much energy is transferring to the different layers beneath.

DTS method

The distributed temperature sensing (DTS) method is based on the optical light scattering. The DTS device emits short laser pulses to the optical fibre and a part of that light scatters back. The device records the Stokes and Anti-Stokes bands of Raman scattering and calculates the temperatures. The Anti-Stokes band is sensitive for temperature. The location of certain temperature is determined with help of the time of flight of the optical pulse. Sensornet Oryx SR DTS device (Fig. 8) was acquired for these temperature measurements. The maximum range for Oryx SR is 5.3 km and temperature accuracy is ± 0.5°C.

0580-6

The measurement is made as a single way measurement where the cable connector is installed to channel 1 and laser pulse travels through the whole cable and backscattered light is detected and acquired by the DTS device. Another end of the cable is installed to channel 2 and another single way measurement can be made vice versa from the end of the cable to the beginning.

Interpreting of measurement data requires the knowledge of cable configuration in the field. The exact locations and depths must have been written down in the installation stage. Otherwise it would be impossible to construe the data correctly.

Figure 8. Splice box with connectors in the asphalt field and DTS device, laptop, calibration coil and battery.

Every measurement is calibrated. Two PT100 sensors are attached to isolated cable coil (Fig. 8). The coil consists of 20 m of measurement cable. The coil temperature is acquired by cable (linear sensor) and two PT100 point sensors. The isolation guarantees the stable temperature in the whole coil.

RESULTS AND CONCLUSIONS

The measurement fields were implemented successfully. Only one cable in 3 m deep holes in the lawn field was malfunctioning. Despite of that the same configuration works correctly in the asphalt field. Obviously the cable which has been wired around the tube has too much tension, either mechanical or some stone is pushing the fibre. Instead cable in deeper wells is working properly also in the lawn field. Altogether there is a possibility to make measurements in the both fields and compare the results with each other. The monitoring of temperatures has been going on since April 2014. Temperatures are measured once per month except in summertime they are performed twice a month. Temperature data is given as a function of cable length (Fig. 9). To interpret the data the location of cables have to be known.

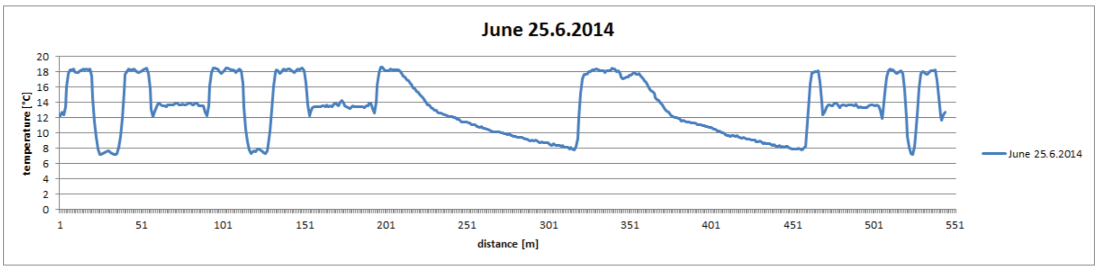

0580-7

Figure 9. Example of temperature data in asphalt field.

The data from longer measurement period (2014-2016) in asphalt and lawn field will be analysed and reported in near future.

The presented design is unique and it is appropriate to be applied in any Northern country. While making the plans for implementation it is important to notice if there are some cables or pipelines under the asphalt already. It is also recommended to apply brand new or at least unused cable in wired 3 m deep special installations. Ensure that the splice box is big enough.

The asphalt pavements are great heat collectors in urban environment. In the future studies it would be good to test different kinds of soil layer structures in practice to maximize the heat collection, taking into account the frost isolating properties.

REFERENCES

1. ICAX. Available on the Internet. (last access in 11.6.2016) <URL: http://www.icax.co.uk/asphalt_solar_collector.html>.
2. Gordon, S., Energy from the ground up [interseasonal heat transfer], in *Power Engineer* , vol.19, no.4, pp.20-23, Aug.-Sept. 2005.

energies

Article

Utilizing Asphalt Heat Energy in Finnish Climate Conditions

Anne Mäkiranta * and Erkki Hiltunen

School of Technology and Innovations, University of Vaasa, 65101 Vaasa, Finland; erkki.hiltunen@univaasa.fi
* Correspondence: anne.makiranta@univaasa.fi; Tel.: +358-29-449-8000

Received: 2 May 2019; Accepted: 24 May 2019; Published: 1 June 2019

Abstract: Geothermal energy is a form of renewable energy, which offers carbon-free solutions for heating and cooling spaces. This study evaluates the use of renewable asphalt heat energy in frozen ground conditions. Asphalt heat energy can be harnessed using a low-energy network, heat collection pipes and heat pumps. This study measured temperatures under the asphalt layer during a three-year period between 2014 and 2017. Measurements were made using a distributed temperature sensing method based on light scattering. Temperatures taken at four different depths under the asphalt (0.5 m, 1.0 m, 3.0 m and 10 m) are presented here. These temperatures are compared with that detected at the depth at which the temperature remains constant all year round. The temperature difference curve between 0.5 m depth and the constant soil temperature depth indicates that from April to October the soil at 0.5 m depth is warming and the temperature difference is positive, even as much as 18 °C. Instead, at the 3.0 m depth, the difference curve is smoother and it varies only from −5 to +5 °C. It is positive from June to November. The surface layer (0 m–1.0 m) is suitable for harvesting heat that can be stored in a deeper (1.5 m–3.0 m) purpose-built storage or in a bedrock heat battery. The calculated heat capacities indicate that asphalt energy, because of high temperatures, is a noteworthy renewable energy source.

Keywords: urban energy; geoenergy; low-energy network; distributed temperature sensing (DTS) measurement

1. Introduction

It is commonly accepted that climate change and global warming are serious issues that can be addressed by reducing greenhouse gas (GHG) emissions. According to Shrestha et al. [1], technological innovations and research to develop new solutions are essential to limit global warming. This is particularly true in developing countries, where there is still much to do. In Finland geothermal energy systems have been a popular heat source for new single family-houses in recent years. Heat pump systems most commonly use the bedrock, the ground and the air as a heat source. Even old houses and summer cottages are increasingly equipped with an air-to-air heat pump. Finns bought 76,000 heat pumps in 2018 [2]. People are prepared to invest in renewable sources, driven by the desire to cut their electricity and heating bills. At the same time, households are becoming more self-sufficient in heat energy. The Finnish government released its new national energy and climate strategy report in November 2016. According to that report, Finland will abandon the burning of coal for energy by 2030. Moreover, the aim is for at least 38% of the energy used by then to come from renewables. These targets mean that new approaches are needed in Finland to develop cost-effective applications with consumer-friendly prices for carbon-free energy systems. Studies of yearly savings and the payback period are made by Mallick et al. [3]. Geothermal energy, or more specifically the radiant energy emitted by the sun and stored in the upper layers of the earth, is a renewable energy source with a great potential in Finland.

There is a large amount of heat energy available in urban areas due to the proliferation of buildings, people, vehicles, concrete, asphalt and a lack of flora [4]. The air of an urban area is even several degrees warmer than in an adjacent rural area [5]. This urban heat island (UHI) effect is well-known, especially in the world's big cities. The same phenomenon is found even in northern latitudes: the average yearly UHI intensity measured in the city of Turku, Finland, was 1.9 °C, compared with the rural area [6]. Not only is it apparent that there is much heat energy available in an urban area, but there is also a great demand for energy in the same area. It would be logical to use the energy near its birthplace.

Asphalt pavements, such as roads, car parks and pedestrian areas, are most prevalent in cities. They gather solar heat, and in doing so they bind a significant quantity of energy. Part of that energy conducts to underlying layers of asphalt. According to Qinwu & Mansour [7], the specific heat of asphalt concrete is 920 J/kg °C, measured as an average of several mixtures. Asphalt heat energy has already been utilized, for instance in England, where commercial solutions also exist [8]. The usual exploitation method entails a pipe network within an asphalt pavement or concrete slabs. The tubes are typically metallic, such as steel, aluminum or copper, but polymers like polyethylene or polyvinyle chloride (PVC) are also used. Pascual-Munoz et al. [9] have presented and tested a highly porous asphalt layer. This acts as a solar heat collector, removing the need for the tubes. It has excellent thermal efficiency, but needs further research to increase the flow rate. Different asphalt mixtures have also been studied by Dawson et al. [10]. The simulation of the thermal properties of asphalt pavements has been presented by Wang et al. [11].

The storage of heat is an important issue when considering the seasonal characteristics of asphalt energy. Borehole thermal energy storage (BTES) is a thick underground array of many shallow boreholes (35 m–120 m). For example, in the Drake Landing Solar Community, Canada, the BTES consists of 144 boreholes [12]. In Tianjin, China, Zhou et al. [13] have implemented an experimental asphalt-covered 12 m × 8 m field including heat-harvesting pipes and one vertical 120 m-deep heat storage. Heat collection was carried out during the summer 24 h per day, and that heat was used to warm the asphalt surface to prevent freezing for 24 h a day in winter. The heat harvesting in summer reduced the asphalt surface temperature and eliminated rutting [14]. Heat release during winter reduced the time that the asphalt pavement was frozen by 32%. The biggest BTES in Finland is located in the Sipoo logistics center, where there are 157 boreholes in a 310 m × 270 m area, with most of the boreholes being under the building [15].

The Finnish climate conditions are very hard when compared to China, Tianjin [13], but there is no permafrost like in Siberia. Here, the ground is frozen during the winter, even to a depth of 1.5 m [16]: hence, this study's main objective is to assess if asphalt heat energy is at all viable in Finland.

The ground temperature remains relatively constant throughout the year beyond a certain depth because the seasonal variation of air temperature has no effect that far beneath the surface. For instance, in Cyprus this constant temperature is reached at a depth of 5.0 m [17]. In Finland, that depth is about 15 m [18]. According to Florides et al. [17] there are three main factors affecting the temperature distribution in the ground. First, there is the structure and physical properties of the ground. Second, there is the cover material on the ground surface (e.g., lawn, asphalt, etc.). The third factor is the climate conditions (air temperature, wind, solar radiation, air humidity and rainfall), because these have an influence on the ground temperature in the subsurface. It is primarily geothermal energy that influences the ground temperature below the depth at which the temperature is constant throughout the year.

Martinkauppi et al. [19] used a laboratory set-up to establish that different layers under the asphalt pavement stored the heat. A sample of asphalt pavement was heated with a bulb. After the heating ceased, the asphalt layer cooled down to the ambient temperature relatively rapidly, but the lowest layer, sand, stored some of the heat energy. That study indicated that different layers (asphalt, gravel, sand) had different thermal conductivities. During the heating period, the upper layer influenced the thermal behavior of what was below it, but its influence was not observed during the cooling.

The aim of this paper is to study ground temperatures below an asphalt-covered surface. Specifically, it focuses on temperatures at depths of 0.5 m to 3.0 m beneath the surface, because this is the portion of the ground most relevant to heat utilization in a low-energy network. These depths are also interesting in terms of seasonal heat energy storage. In this study, the depth of 0.5 m is found to retain appropriate temperature levels of up to 26 °C and to have positive temperature values for at least nine months per year. This layer is suitable for assembling heat collection pipes. This study shows that temperatures remain over 4 °C over the whole year at a depth of 3.0 m. That is why this layer might be suitable for seasonal heat storage, even in northern locations like Finland. Additionally, 3 m is still relatively shallow in civil engineering terms, so the installation of pipework at this depth is not onerous. The study also evaluates the temperature and the depth of constant soil temperature (CST) at the test site. Temperatures at different depths are compared with the CST. The temperatures under a lawn-covered field at a depth of 0.5 m are also presented as an example of a typical ground source heat potential under a non-asphalt field.

2. Materials and Methods

The measurement field for monitoring temperatures beneath the asphalt layer (five holes) and a similar lawn-covered field (five holes) was planned and installed by the research group for renewable energy in the University of Vaasa. The site for the measurement field was found at the University of Vaasa's seaside campus area in the parking lot near the Gulf of Bothnia. In late autumn 2013, five holes were drilled through the asphalt-paved surface. Two holes went to a depth of 10 m, one to a depth of 5.0 m and two to a depth of 3.0 m (Figure 1). The temperature monitoring in the 10 m- and 5 m-holes was at a 1 m spatial resolution. However, it was possible to use a much smaller resolution in the 3.0 m-deep holes. The optical fiber inside the cable functions as a linear sensor. The cables were installed in the drilled holes. A more precise description of the measurement fields is written by Mäkiranta et al. [20,21]. The completed asphalt energy measurement field was finished with a new asphalt pavement and lawn field with grass seeds (Figure 2) in spring 2014.

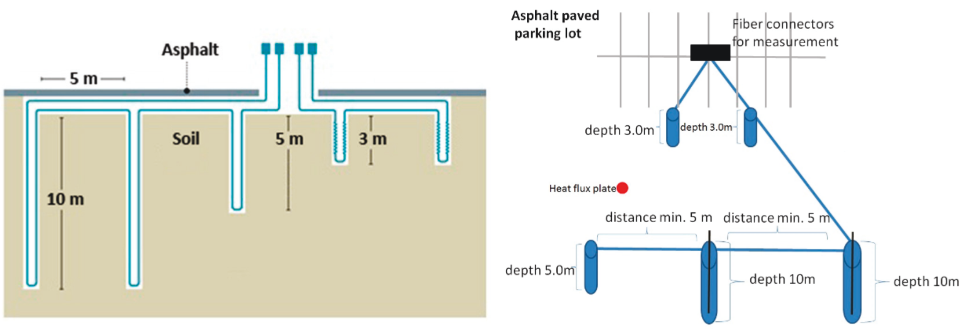

Figure 1. The measurement arrangements of the cables (**left**) and the geometrical positions of the holes (**right**) in the asphalt field. The same kind of independent measurement configuration was installed under the lawn.

The monthly mean air temperature data have been measured at the nearest weather station (less than 3 km) of the Finnish Meteorological Institute (see Table 1).

The distance between the asphalt and lawn measurement fields is no more than about 200 m, which ensures that the solar and other weather conditions are similar.

The temperature monitoring beneath the asphalt cover was made by using the distributed temperature sensing (DTS) method. This method entails an optical fiber inside an armored cable in each hole. The optical fiber functions as a linear sensor, and the DTS measurement device (Sensornet Oryx) observes the temperatures along the fiber. Short pulses of laser light are emitted by the DTS measurement device to illuminate the glass core of the optical fiber. Part of the incident light pulse is backscattered while it moves along the core of fiber. The intensity of these backscattered bands is acquired by the DTS measurement device. The device estimates the temperatures based on the temperature dependent part of the scattering, Raman scattering [22]. The temperature accuracy of the Oryx device is ±0.5 °C. The optical fibers in the 3 m-deep holes were spiral-wrapped around a measurement pipe, improving the resolution in these shallow holes to 0.03 m. Spiral-wrapping was not used in the 10 m- and 5 m-holes, so their spatial resolution was 1 m.

Figure 2. The measurement field receives asphalt pavement after drilling and digging.

During the three-year measurement period of 2014–2017, the temperatures were monitored at several depths, from a 0.2 m up to a 10 m depth. The most interesting layer, in terms of the asphalt heat collection, was observed to be at 0.5 m. The layer for optimal seasonal storage was found to be at 3.0 m. The temperatures at an intermediate depth of 1.5 m are also presented for comparative purposes and to verify the suitability of the two other layers.

The measurements were made once per month, except in July and August when they were made at two-week intervals (Table 2). The long intervals between the measurements were possible because temperature changes in the soil were relatively slow. Each measurement action lasted 10 min, during which the DTS device made two measurements per minute per channel. The total temperature data consist of 20 measurements per channel. Figures 3–8 graph the average temperatures of eight measurements on each measurement date. The measurement field includes two 3.0 m-deep holes.

In respect to the lawn-covered field, this study only includes data from the period of April 2014–December 2015. Problems with splice connections caused a temporary interruption in the measurements on that field.

3. Results

Figures 3, 5 and 6 show the temperature data taken at depths of 0.5 m, 1.5 m and 3.0 m in the two 3.0 m-deep holes in the asphalt field. For a comparison, the temperatures at the depth of 0.5 m in the lawn-covered field are presented in Figure 4. Figure 3 represents the monthly mean air temperatures measured during April 2014–March 2017 [17]. In each of the three years of the monitoring period, either July or August was the warmest month, and either January or February was the coldest.

Figure 3. The temperature at a 0.5 m depth under the asphalt layer in two different holes, and the average air temperature of the month [23].

Table 1. The monthly mean air temperatures [°C] measured during April 2014–March 2017 at the weather station of the Finnish Meteorological Institute [23].

	Jan.	Feb.	Mar.	Apr.	May.	Jun.	Jul.	Aug.	Sep.	Oct.	Nov.	Dec.
2014				4.2	9.3	12.6	20.0	16.5	11.5	5.0	1.0	−0.7
2015	−3.1	−0.2	0.1	4.0	8.4	12.1	15.2	16.5	12.1	5.9	3.9	1.2
2016	−9.7	−2.3	0.1	3.3	11.0	14.0	17.2	14.6	11.9	4.0	−1.1	−0.5
2017	−2.3	−3.9	−0.3									

The timetable of the measurements is converted into the number of days between two measurement actions. The cumulative time *t* [day] since the beginning of the measurements is also presented (Table 2).

The temperatures measured at 0.5 m depth under the asphalt layer show a seasonal variation from −3.9 °C to 26.0 °C (Figure 3). The graph shows that the soil was frozen each year from January to as late in the year as March. A temperature increase of ten degrees can be seen during a one-and-a-half-month period right at the beginning of the study, from April to May 2014. Finland had especially warm weather in July 2014, which can be seen as a temperature peak under the asphalt pavement throughout that month. In contrast, 2015's summer was cooler, and the warming of the soil was slower. In that year, the highest soil temperature (19.7 °C) at a depth of 0.5 m under the asphalt layer was not measured until the end of August. In 2016, the highest value, 19.4 °C, was measured at the beginning of August.

The data from both measurement holes are almost identical throughout the whole period of 2014–2017 for both the asphalt-covered (Figure 3) and lawn-covered areas (Figure 4).

The temperatures at 0.5 m under the lawn-covered field (Figure 4) were lower in the summer than in the asphalt-covered area. (Figure 3): summer 2014: 20 °C -> 26 °C, summer 2015: 16 °C -> 20 °C. With the exception of the temperature values in Figures 3 and 4, the curves have only small differences in the shape of the temperature maximum.

The temperature graph at the depth of 1.5 m (Figure 5) under the asphalt layer demonstrates that the seasonal temperature variation was about 13–14 °C. The lowest temperatures were monitored from January to April, when they varied from 2.4 °C to 4.8 °C. The highest temperatures were in August of each year. At this intermediate depth of 1.5 m, the temperatures were quite low during winter and at the beginning of spring. Once again, the data from both measurement holes are almost identical throughout the whole period of 2014–2017.

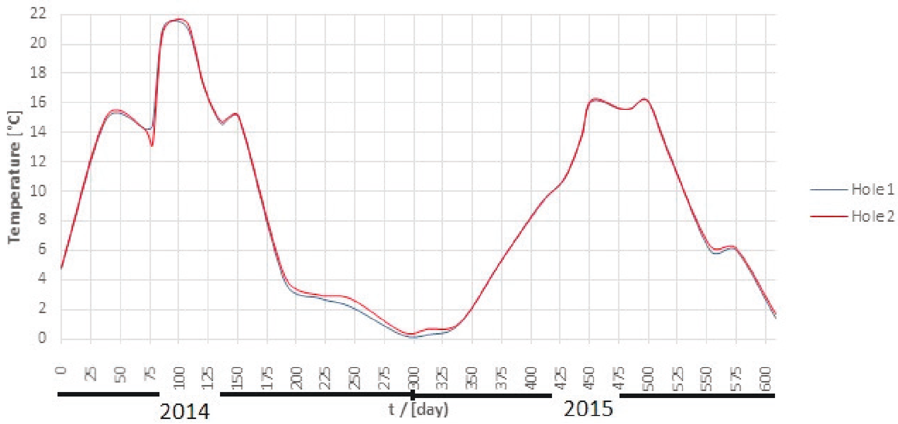

Figure 4. The temperatures in the soil at a 0.5 m depth under the lawn cover.

Table 2. The timetable for the measurements, between April 2014 and March 2017; the number of days between two measurements (Δ*t*), and the time *t* [day] since the beginning of the measurements (used as the *x*-axis in Figures 3–6).

Year	Date	Δ*t*	*t* [Day]	Year	Date	Δ*t*	*t* [Day]
2014	16 April	0	0	**2015**	27 August	14	500
	23 May	39	39		14 September	18	518
	25 June	33	72		19 October	35	553
	1 July	6	78		10 November	22	575
	10 July	9	87		14 December	34	609
	30 July	20	107	**2016**	22 January	39	648
	14 August	15	122		23 February	32	680
	29 August	15	137		24 March	31	711
	12 September	14	151		22 April	29	740
	22 October	40	191		30 May	38	778
	19 November	28	219		22 June	23	801
	17 December	28	247		7 July	15	816
2015	30 January	44	291		20 July	13	829
	20 February	21	312		5 August	16	845
	20 March	28	340		18 August	13	858
	24 April	35	375		13 September	26	884
	28 May	34	409		14 October	31	915
	17 June	20	429		16 November	33	948
	1 July	14	443		16 December	30	978
	10 July	9	452	**2017**	18 January	33	1011
	3 August	24	476		15 February	28	1039
	13 August	10	486		16 March	29	1068

Figure 6 indicates the temperatures at a depth of 3.0 m under the asphalt layer during the three-year period. The temperatures vary from 2.9 °C (April) to 13.1 °C (August and September). The seasonal variation of about 8–10 °C is smaller than at the two shallower depths, and this soil layer has no frost. There is some variation between the two holes' temperature data, particularly in the period of

2015–2017. The distance between the holes is only about 4.5 m, but the soil moisture and sand content may vary at a depth of 3.0 m. The heat capacity of the soil material at these two measurement points is apparently different.

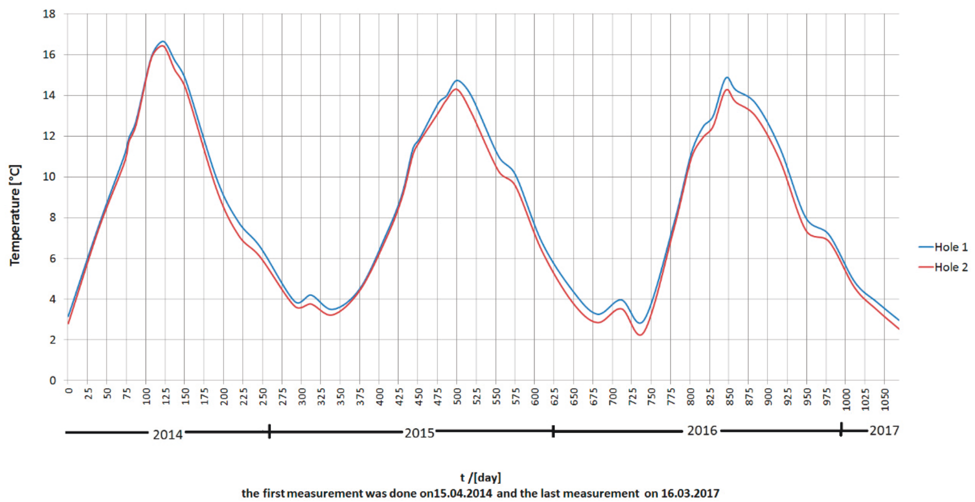

Figure 5. The temperatures in the soil at a 1.5 m depth under the asphalt layer.

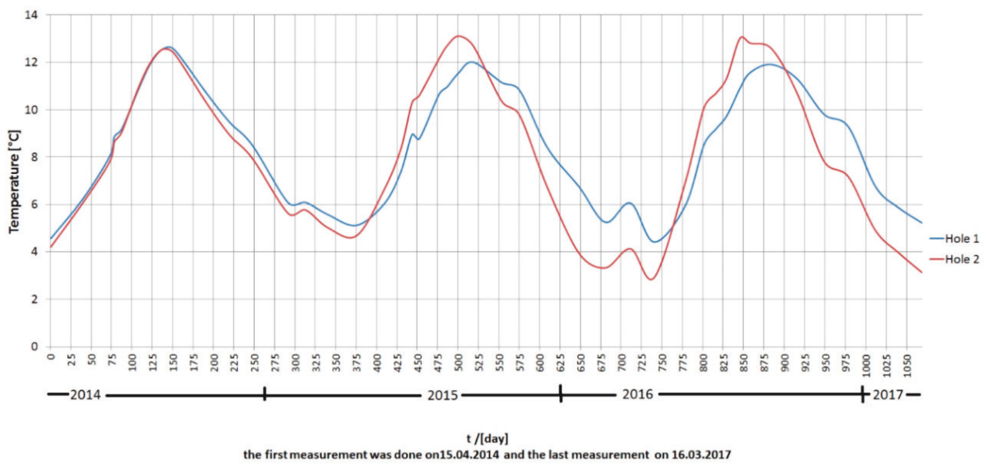

Figure 6. Temperatures in the soil at a 3.0 m depth under the asphalt layer.

Temperature Variation in Different Layers and the Constant Soil Temperature (CST) Layer

The seasonal variation in the soil temperature diminishes as the depth increases until a point is reached where the seasonal variation of the air temperature has no effect on the soil temperature (Figure 7). That depth was observed to be 10 m in this study. The temperature at this point was measured at a constant of 8 ± 1 °C throughout the year.

This stabilization of the temperature to 8 °C at a depth of 10 m, regardless of the season, was also noticed in the periods of April 2015–March 2016 and April 2016–March 2017. Figure 7 shows that from May to September the upper layers were warmer than the deeper layers; and from October to April the upper layers were cooler than the deeper layers. The heat transfer occurred from beneath, toward the asphalt layer.

The difference curves in Figure 8 indicate the seasonal variation of the temperatures compared to the CST in different depths under the asphalt throughout the three-year study. It also shows the differences in the heat conduction speed between the studied layers. For example, it can be seen that the maximum temperature difference at 1.5 m occurred more than two weeks later than at 0.5 m. The variation in the temperature differences smoothen from the surface to the deeper layers. At a 0.5 m depth, the difference varies by even 30 °C, while at a 3.0 m depth the variation is less than 10 °C.

An estimation of the amount of heat energy E [kJ or kWh] in a 50 cm-thick soil layer including the asphalt cover (total volume 1 m·1 m·0.5 m = 0.5 m^3), can be calculated

$$E = m\,c\,\Delta T,\; m = \rho \cdot V \quad (1)$$

where E is the stored energy in the soil layer, m is the mass of the soil layer, c is the specific heat capacity (Table 3) and ΔT is the temperature difference of the two compared stages, ρ is the density of the soil layer (Table 3) and V is the volume of the soil layer.

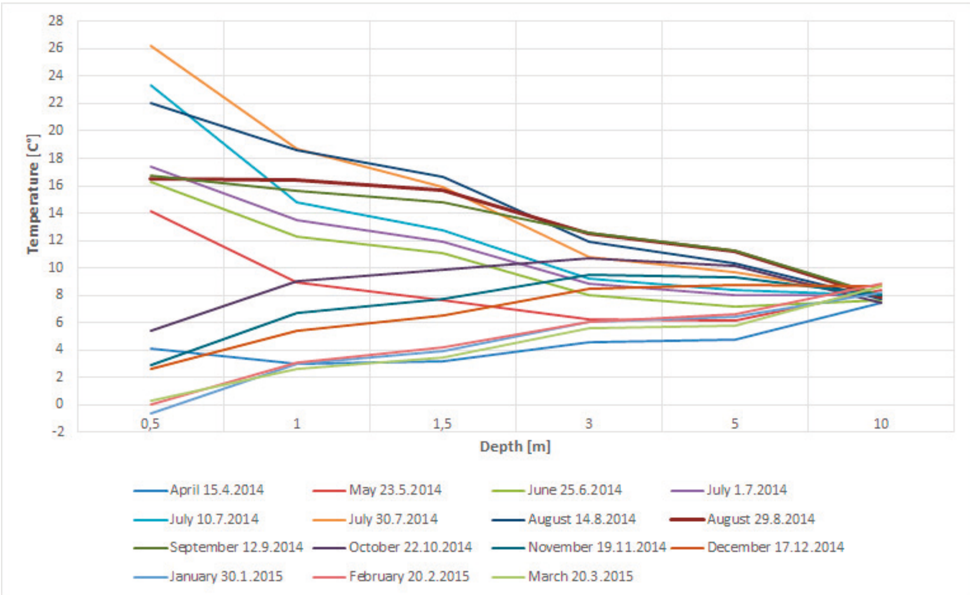

Figure 7. The temperatures in different layers from 0.5 m to 10 m are monitored at one hole. The temperatures vary between 7.4 °C and 8.8 °C at a depth of 10 m.

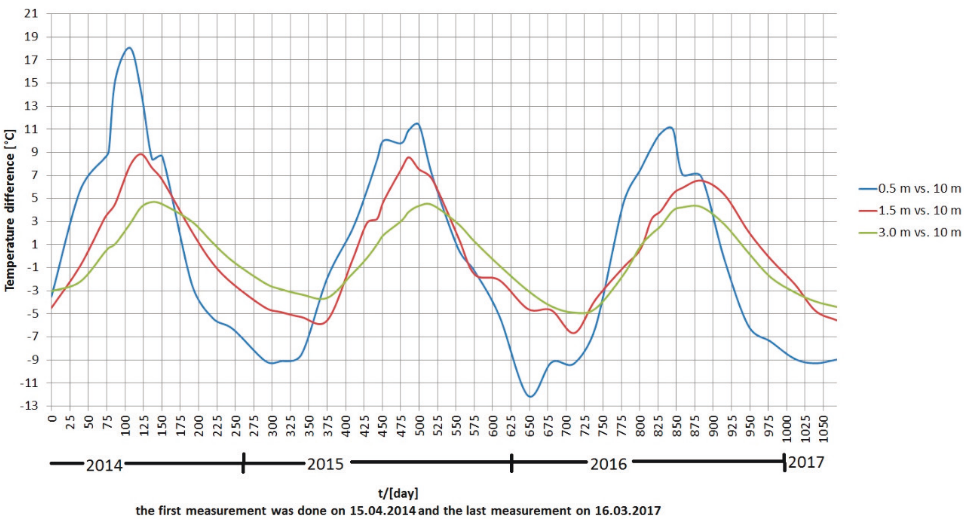

Figure 8. The difference curves compared with each other at 0.5 m, 1.5 m and 3.0 m.

Table 3. Some physical properties of the soil in the literature [7,24–26].

Soil Type	Specific Heat Capacity [kJ/kg·°C]	Density [kg/m^3]
Asphalt	0.92	2400
Gravel	1.50 (dry)	1680 (dry)
Sand	0.84 (dry, 20 °C)	2660

Thickness of the asphalt layer: 0.07 m; $V = 0.07$ m^3; $m_a = 168$ kg.

Thickness of the gravel (1/3) and sand layer (2/3) is 0.43 m; $V_{g+s} = 0.43$ m^3; $V_g = 0.14$ m^3; $V_s. = 0.29$; $m_g = 235$ kg; $m_s = 771$ kg.

A theoretical maximum for the available heat energy amount in the asphalt-covered layer ($V_{tot} = 0.5$ m^3) is 20,785 kJ ≈ 5.77 kWh when soil types are dry and $\Delta T = 18$ °C (the annual maximum temperature of the depth is 22 °C and the lowest permitted temperature chosen for the soil is 4 °C).

The estimation of the heat energy amount (heat capacity) in the 50 cm thick soil layer including the lawn cover (total volume 1 m ×·1 m·× 0.5 m = 0.5 m^3; soil properties (Table 4)):

$$E = m\,c\,\Delta T,\; m = \rho \cdot V$$

Thickness of the soil layer: 0.1 m; $V_s. = 0.1$ m^3; $m_s = 160$ kg.

Thickness of the clay layer is 0.4 m; $V_c = 0.4$ m^3; $m_{c,dry} = 640$; $m_{c,wet} = 704$ kg.

Table 4. Some physical properties of the soil. [25,27].

Specific Heat Capacity [kJ/kg·°C]	Density [kg/m^3]
Soil 0.80 (dry) 1.48 (wet)	1600 (rammed)
Clay 0.88 (10% moisture) 1.76 (50% moisture)	1600 (dry) 1760 (wet)

A theoretical maximum for the available heat energy amount in the lawn-covered layer ($V_{tot} = 0.5$ m^3) is 10,368 kJ ≈ 2.88 kWh when soil is dry and $\Delta T = 15$ °C (the annual maximum temperature of the depth is 19 °C and the lowest permitted temperature chosen for the soil is 4 °C). A theoretical maximum for the available heat energy amount in the lawn-covered layer ($V_{tot} = 0.5$ m^3) is 22,138 kJ ≈ 6.15 kWh when soil is wet and the clay moisture is at 50% (average moisture ratio in Finland [28]).

A new, low-energy, single family house (140 m^2, 4 persons) in Finland consumes 12,400 kWh annually for heating on average. This equates to 33.90 kWh per day [28].

To cover this average heating demand for a single family house for one day, an area of 5.9 m^2 is needed in the asphalt-covered field. In the case of the lawn-covered field, an area of 11.8 m^2 is needed if the soil types are dry, but only 5.5 m^2 is sufficient if the soil types are wet. These calculations depend on the chosen values of the variables.

4. Discussion and Conclusions

The temperatures at a depth of 0.5 m (Figure 3) under the asphalt layer are very promising for heat collection from May until as late in the year as September. The temperatures at that depth are 10–14 °C in May, rising to 26 °C in July and then falling back to 15–16 °C in September. This five-month period from late spring to autumn can be utilized to collect heat. However, due to a low heating demand in summer, even in Finland, it is desirable that heat collected during that period can be stored. A purpose-designed storage deeper under the asphalt, or a bedrock heat battery, could act as a seasonal thermal energy storage (STES). It would be loaded by the asphalt energy during the summer and then the heat would be exploited at cooler times of the year. This asphalt heat energy would be suitable for hybrid energy systems. Asphalt heat can be used to cut off the peak loads of heat energy consumption during winter. Similarly, solar and wind energy are intermittent energy forms that require supplementary elements in order to produce a functional hybrid energy system.

The DTS measurement method was found to be reliable and accurate. There were two measurement holes with similar installations, and both sites gave very similar results without any interruptions (see Figures 2–4).

At a depth of 1.5 m, the temperature falls below 3 °C. During a hard and snowless winter, this layer is frozen, at least in northern Finland. In contrast, 3 m below the asphalt layer the ground remains unfrozen year-round. The temperatures there range from 4 to 12 °C, which is eminently suitable for using asphalt heat continuously for heating or cooling houses. A low-energy system using asphalt energy as the heat source should comprise vertically installed heat-collection pipes and a heat pump. The heat carrier fluid in the pipeline gathers the heat energy, which is mainly emitted by the sun, absorbed by the asphalt and conducted through the soil.

Because of the large usable temperature difference, asphalt energy under the asphalt cover is a noteworthy energy source alongside other ground heat sources. Future research should also investigate the potential and implementation of heat storage to complement asphalt energy. Such a study should evaluate the properties of the asphalt layer and sand layer in capturing and storing energy, and, crucially, the amount of energy returned from the heat storage. In the future, asphalt pavements could act as passive solar collectors in urban areas.

Author Contributions: A.M.; investigation, original draft preparation, writing—review and editing, data curation; E.H.; supervision, funding acquisition, resources, writing—review and editing.

Funding: This research received external funding from Groove program of TEKES (Business Finland).

Acknowledgments: We would like to express thanks to the University of Vaasa for convenient research platform for these new kinds of measurements and the supervising group from the industry.

Conflicts of Interest: The authors declare no conflict of interest.

References

1. Shrestha, S.; Babel, M.S.; Pandey, V.P. *Climate Change and Water Resources*; CRC Press: Boca Raton, FL, USA, 2014; pp. 69–80.
2. The Finnish Heat Pump Association (SULPU). Available online: https://www.sulpu.fi/documents/184029/0/SULPU%20Press%20release%201.2019_en%20with%20picture%20.pdf (accessed on 28 January 2019).
3. Mallick, R.; Carelli, J.; Albano, L.; Bhowmick, S.; Veeraragavan, A. Evaluation of the potential of harvesting heat energy from asphalt pavements. *Int. J. Sustain. Eng.* **2011**, *2011. 4*, 164–171. [CrossRef]
4. Allen, A.; Dejan, M.; Sikora, P. Shallow gravel aquifers and the urban 'heat island' effect: a source of low enthalpy geothermal energy. *Geothermics* **2003**, *32*, 569–578. [CrossRef]
5. Zhu, K.; Blum, P.; Ferguson, G.; Balke, K.-D.; Bayer, P. The Geothermal potential of urban heat islands. *Environ. Res. Lett.* **2010**, *5*, 1–6. [CrossRef]
6. Suomi, J. Characteristics of Urban Heat Island (UHI) in a High-Latitude Coastal City—A Case Study of Turku. SW Finland. Annales Universitatis Turkuensis A II: Biologica. Geographica. Geologica. 2014. Available online: http://urn.fi/URN:ISBN:978-951-29-5912-9 (accessed on 28 January 2019).
7. Xu, Q.; Solaimanian, M. Modeling temperature distribution and thermal property of asphalt concrete for laboratory testing applications. *Constr. Build. Mater.* **2010**, *24*, 487–497. [CrossRef]
8. ICAX ltd. Asphalt Solar Collector. Available online: https://www.icax.co.uk/asphalt_solar_collector.html (accessed on 22 May 2019).
9. Pascual-Munoz, P.; Castro-Fresno, d.; Serrano-Bravo, P.; Alonso-Estebanez, A. Thermal and hydraulic analysis of multilayered asphalt pavements as active solar collectors. *Appl. Energy* **2013**, *111*, 324–332. [CrossRef]
10. Dawson, A.R.; Dehdezi, P.K.; Hall, M.R.; Wang, J.; Isola, R. Enhancing thermal properties of asphalt materials for heat storage and transfer applications. *Road Mater. Pavement Des.* **2012**, *13*, 784–803. [CrossRef]
11. Wang, H.; Wu, S.; Chen, M.; Zhang, Y. Numerical simulation on the thermal response of heat-conducting asphalt pavements. *Phys. Scr.* **2010**, *2010*. [CrossRef]

12. Mesquita, L.; McClenahan, D.; Thornton, J.; Carriere, J.; Wong, B. Drake Landing Solar Community: 10 years of operation. ISES Solar World Congress 2017. *IEA SHC International Conference on Solar Heating and Cooling for Buildings and Industry*. Available online: http://proceedings.ises.org (accessed on 10 April 2019). [CrossRef]
13. Zhou, Z.; Wang, X.; Zhang, X.; Chen, G.; Zuo, J.; Pullen, S. Effectiveness of pavement-solar energy system—An experimental study. *Appl. Energy* **2015**, *138*, 1–10. [CrossRef]
14. Mallick, R.B.; Chen, B.-L.; Bhowmick, S. Harvesting energy from asphalt pavements and reducing the heat island effect. *Int. J. Sustain. Eng.* **2009**, *2*, 214–228. [CrossRef]
15. Korhonen, K.; Leppäharju, N.; Hakala, P.; Arola, T. Simulated temperature evolution of large BTES—Case study from Finland. In Proceedings of the IGSHPA Research Conference 2018, Stockholm, Sweden, 18–20 September 2018; pp. 482–490.
16. Finnish Environment Institute. Depth of ground frost. Available online: URL:http://wwwi3.ymparisto.fi/i3/paasivu/ENG/Routa/Routa.htm (accessed on 28 January 2019).
17. Florides, G.; Kalogirou, S. Ground heat exchangers—A review of systems, models and applications. *Renew. Energy* **2007**, *32*, 2461–2478. [CrossRef]
18. Leppäharju, N. *Kalliolämmön hyödyntämiseen vaikuttavat geofysikaaliset ja geologiset tekijät. Pro Gradu tutkielma*; University of Oulu: Oulu, Finland, 2008; Available only in Finnish.
19. Martinkauppi, J.B.; Mäkiranta, A.; Kiijärvi, J.; Hiltunen, E. Thermal Behavior of an Asphalt Pavement in the Laboratory and in the Parking lot. *Sci. World J.* **2015**, *2015*, 7. [CrossRef] [PubMed]
20. Mäkiranta, A.; Martinkauppi, B.; Hiltunen, E. Design of Asphalt Heat Measurement in Nordic Country. In Proceedings of the SDEWES2016, Lisbon, Portugal, 4–9 September 2016. ISSN (printed) 1847-7178.
21. Mäkiranta, A.; Martinkauppi, B.; Hiltunen, E. Thermal profiles under an asphalt and lawn covered fields. In Proceedings of the SDEWES2017, Dubrovnik, Croatia, 4–8 October 2017. ISSN (printed) 1847-7178.
22. Abhisek, U.; Braendle, H.; Krippner, P. Distributed Temperature Sensing: Review of Technology and Applications. *IEEE Sens. J.* **2012**, *12*, 885–892.
23. Finnish Meteorological Institute FMI. *Monthly average air temperature data 2014–2017*; Finnish Meteorological Institute FMI: Klemettilä, Vaasa, Finland.; Available online: https://ilmatieteenlaitos.fi/havaintojen-lataus#!/ (accessed on 28 January 2019).
24. Valtanen, E. *Handbook of Math and Physics. Matematiikan ja fysiikan käsikirja. (in Finnish) 2.painos*; Genesis-kirjat Oy: Jyväskylä, Finland, 2007; ISBN 978-952-9867-28-8.
25. Engineering toolbox. Densities and heat capacities of materials. Available online: https://www.engineeringtoolbox.com (accessed on 12 February 2019).
26. Blocon, A.B. *EED Earth Energy Designer—Vertical Borehole Design Program for PC*; BLOCON SWEDEN: Lund, Sweden, 2018.
27. Ronkainen, N. Properties of Finnish soil types. In *Finland's Environment 2/2012*; Only in Finnish; Finnish Environment Institute: Helsinki, Finland, 2012; Available online: https://helda.helsinki.fi/handle/10138/38773 (accessed on 10 April 2019).
28. Motiva Consumer Guidance. Calculator to compare the heating systems. Only in Finnish. Available online: http://lammitysvertailu.eneuvonta.fi/ (accessed on 12 February 2019).

energies

MDPI

Article

Temperature Measurements on a Solar and Low Enthalpy Geothermal Open-Air Asphalt Surface Platform in a Cold Climate Region

Caner Çuhac, Anne Mäkiranta *, Petri Välisuo, Erkki Hiltunen and Mohammed Elmusrati

School of Technology and Innovations, University of Vaasa, P.O. Box 700, FI-65101 Vaasa, Finland; canercuhac@gmail.com (C.Ç.); petri.valisuo@uva.fi (P.V.); erkki.hiltunen@uva.fi (E.H.); mohammed.elmusrati@uva.fi (M.E.)

* Correspondence: anne.makiranta@univaasa.fi; Tel.:+358-29-449-8302

Received: 10 December 2019; Accepted: 18 February 2020; Published: 21 February 2020

check for updates

Abstract: Solar heat, already captured by vast asphalt fields in urban areas, is potentially a huge energy resource. The vertical soil temperature profile, i.e., low enthalpy geothermal energy, reveals how efficiently the irradiation is absorbed or radiated back to the atmosphere. Measured solar irradiation, heat flux on the asphalt surface and temperature distribution over a range of depths describe the thermal energy from an asphalt surface down to 10 m depth. In this study, those variables were studied by long-term measurements in an open-air platform in Finland. To compensate the nighttime heat loss, the accumulated heat on the surface should be harvested during the sunny daytime periods. A cumulative heat flux over one year from asphalt to the ground was 70% of the cumulative solar irradiance measured during the same period. However, due to the nighttime heat losses, the net heat flux during 5 day period was only 18% of the irradiance in spring, and was negative during autumn, when the soil was cooling. These preliminary results indicate that certain adaptive heat transfer and storage mechanisms are needed to minimize the loss and turn the asphalt layer into an efficient solar heat collector connected with a seasonal storage system.

Keywords: asphalt solar collector; heat flux; distributed temperature sensing; low enthalpy geothermal energy; renewable energy; soil temperature profile

1. Introduction

Today's society is obliged to search for new low carbon energy resources to fight against global climate change. In cold-climate regions, fossil fuels are often used for heating. Solar energy, which is one of the most important inexhaustible sustainable energy resources, can be harvested using heat collectors or solar panels. Solar heat is renewable, and therefore, can potentially reduce dependency on fossil fuels. On the other hand, collecting of solar energy from the asphalt layer during the hottest season also saves the asphalt from large temperature changes, which can cause structural damage like rutting or hardening [1,2].

Surface temperature changes caused by solar irradiation degrade exponentially with a time constant of a few hours due to the thermal energy flowing back into the atmosphere. The accumulation of the daily gains or losses in terms of solar energy leads to small temperature increases in the deeper layers of the soil, creating long-term warming or cooling of the soil [3,4]. A diurnal and/or seasonal storage is necessary for a solar heating system in a cold climate region. Majorowicz et al. [5] and Loomans et al. [6] have expressed an application of an asphalt collector for summer and winter conditions. They have also studied the thermal energy potential of an asphalt collector and what the critical parameters are.

Some simple storage systems operate without heat pumps; only solar collectors and panels are connected with seasonal thermal energy storage [7]. Solar heat collectors, together with heat pumps and seasonal thermal energy storage systems, are frequently used in heating real estate, industrial buildings, and greenhouses [8,9]. Drake Landing Solar Community in Canada has experience in the harvesting and storing of solar energy [10,11]. In Drake Landing, 52 detached houses are heated using 2293 m^2 of flat plate solar collectors. The storage volume used for seasonal storage consisted of 144 boreholes, each being the depth of 35 m. The temperature of the borehole thermal energy storage system (BTES) reached above 65 °C in summer after three years of operation, and the temperature dropped nearly at 40 °C during the winter [10,12]. Experimental measurements and a Comsol simulation model of thermal energy from solar collectors in the ground were studied also by Haq and Hiltunen [13]. The theories and models used by Haq and Hiltunen can later be used to optimize the parameters of the asphalt heat collection and seasonal storage system.

The focus and novelty of this research was to study the thermal energy absorption of asphalt surface and soil layers beneath an asphalt layer in a cold climate region. The goal was reached by benchmarking and analyzing the solar irradiance and the absorption rates of the asphalt surface around the clock in different seasons. The vertical temperature distribution in the soil was studied for possible solar and low enthalpy geothermal energy harvesting applications in future.

The laboratory experiments, carried out before this study, indicated that dark asphalt is efficient in absorbing solar irradiance and conducting thermal energy to the soil [14]. Ho et al. [15] has modeled an asphalt paved area with most important parameters and variables by Comsol finite element simulation. In Finland, logistic centers are interested in snow melting systems. In this research, the thermal behavior of commonly used asphalt paved soil structures, e.g., parking spaces, is studied in high latitudes above 63° N at University of Vaasa campus site (see Figure 1), which is farther north than the previous research projects cited above. The monthly mean air temperatures and heating degree days in Vaasa during the study period are declared in Table 1.

Figure 1. Location of measurement site marked by red circle, Vaasa, Finland [16].

Table 1. The monthly mean air temperatures [°C] measured during April 2014–December 2015 at the weather station of the Finnish Meteorological Institute [17] and the heating degree days (HDD) in Vaasa [18].

	Jan.	Feb.	Mar.	Apr.	May	Jun.	Jul.	Aug.	Sep.	Oct.	Nov.	Dec.	HDD
2014				4.2	9.3	12.6	20	16.5	11.5	5	1	−0.7	3926
2015	−3.1	−0.2	0.1	4	8.4	12.1	15.2	16.5	12.1	5.9	3.9	1.2	3546
2016	−9.7	−2.3	0.1	3.3	11	14	17.2	14.6	11.9	4	−1.1	−0.5	4124

The modeling of the thermophysical properties of pavement materials on the evolution of temperature depth profiles in different climatic regions has been refereed by Hall et al. [19].

2. Materials and Methods

According to Strzelczyk et al. [20] it is important to know the thermal parameters of the surroundings, the weather, and the solar radiation properties in a given location in order to design and improve energy systems. The shallow geothermal energy originates mainly from sun. The measurements in this study were obtained by three main sources: (1) a pyranometer, (2) a heat flux plate, and (3) a distributed temperature sensing (DTS) system. These three independent methods complement each other, giving on a reliable picture of the different layers. The pyranometer measured solar irradiance, the heat flux plate measured the heat flux through the asphalt layer, and the DTS described the temperature distribution down to several meters' depth.

2.1. Pyranometer Measurements

In this research solar irradiance is measured by using a Hukseflux LP02-TR (Hukseflux Inc., Delft, The Netherlands) pyranometer [21] which was placed on the roof of the neighbour building. In this position it was under the open sky without shadows. The measured values were sampled using a DataTaker—data logger (Thermo Fisher Scientific Australia Pty Ltd.,Melbourne, Australia) in 10 s time intervals. The data was logged with a timestamp and stored for analysis. The calibration accuracy of the pyranometer is less than 1.8%.

2.2. Heat Flux Measurements on the Asphalt Surface

The heat flux plate together with pyranometer can be used to study the efficiency of an asphalt layer as a heat collector. Heat flux data were collected using a Hukseflux heat flux plate HFP01-15 (Hukseflux Inc, The Netherlands) [22] buried 5 cm below the asphalt surface at the data collection site (see Figures 2 and 3). This sensor plate generates a small analog output voltage proportional to the net heat flux passing through it. The heat flux towards the ground is interpreted as positive and the heat flux from the ground to the surface is interpreted as negative. The aim of taking the heat flux measurements is to quantify the net energy from solar radiation absorbed by the asphalt during the day and the amount of thermal energy released back to the atmosphere during the night. These energy flows depend on multiple factors, such as irradiance, air temperature, the weather, current soil temperature, the thermal properties of the medium, thermal conductivity, and heat capacity [23]. The accuracy of calibration is ±3%.

A data collection system was developed for reading, transferring, and storing the ground heat flux plate data. This system consisted of an analog-to-digital converter (ADC) and a wireless sensor platform, a wireless gateway, and an embedded PC (see Figure 4). The analog voltage provided by the sensor was digitized by an ADC and the wireless sensor platform sampled the value every 10 s and sent the values to the wireless gateway platform located inside the building. The wireless gateway was connected to the embedded PC, which stored the data on the hard drive. During the data collection period, the measurement devices faced cold temperatures, as low as −30 °C, and continued to operate.

Figure 2. Installation of heat flux plate "Hukseflux" before asphalt pavement.

Figure 3. Heat flux data collection site, "Hukseflux," under the plank.

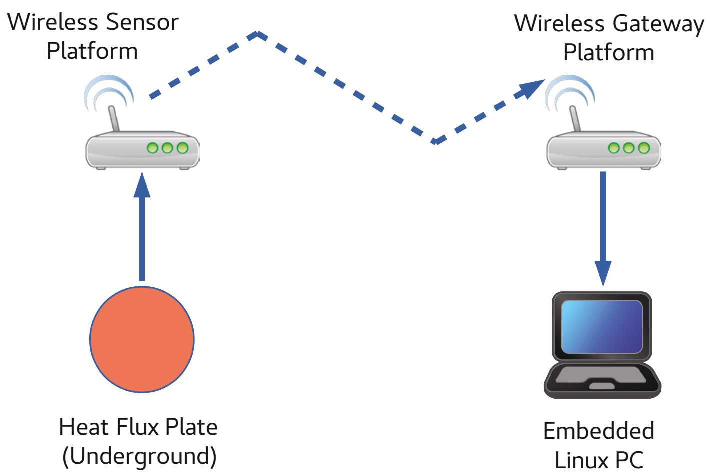

Figure 4. Network structure for wireless data collection of the heat flux sensor.

The collected data were analyzed using the mathematical computing software MATLAB (Version 9.2., The MathWorks Inc., Natick, Massachusetts, USA) to extract information about the net flux of the heat depending on the meteorological conditions of the season and the time of day. Statistical computations were used to make the estimations of the future heat transfers.

2.3. Underground Temperature Measurements

The distributed temperature sensing (DTS) method was used to measure the temperatures in soil layers under the asphalt pavement. This method was chosen because it is known to be usable in cold climate regions [24] and is successfully used in monitoring of boreholes too. The boreholes can be open-holes or sealed wells, as in this study, and the installation can be permanent [25–27]. This method is based on optical light scattering in fiber [28]. Short pulses of laser light are sent to the optical fiber by the DTS measurement device. Part of the incident light pulse is scattered by elastic scattering while it moves along the core of the fiber. The properties of the scattered light are acquired by the DTS measurement device, which then estimates the temperature based on the temperature dependent part of elastic scattering [29,30]. An optical fiber, therefore, can be used as a linear sensor. In this study, the temperatures were observed with 1 m spatial resolution.

A measurement fiber was installed into the vertical boreholes drilled under the asphalt (more exactly described by Mäkiranta et al. [4]). The aim was to measure soil temperatures from the depth of 50 cm down to 10 m at the same time. Temperatures under the asphalt layer were acquired by a DTS device (Oryx DTS, Sensornet Ltd, Hertfordshire, UK) once or twice per month, depending on the season. These measurements were made on site using special instruments in addition to the meteorological data. The accuracy of the DTS device is $+/-0.5\,^{\circ}$C.

The structure of an asphalt-paved parking lot is shown in Figure 5. The thickness of the asphalt layer is between 7 and 10 cm, the gravel and sand layer is about 60 cm thick , and the clay layer lies beneath those. The physical properties of soil is listed in Table 2.

Figure 5. Soil layers under the asphalt in the measurement field at the University of Vaasa campus area.

Table 2. Some physical properties of the soil in the literature [31–35].

Soil Type	Specific Heat Capacity [kJ/kg·°C]	Density [kg/m^3]
Asphalt	0.92	2400
Gravel	1.50 (dry)	1680 (dry)
Sand	0.84 (dry, 20 °C)	2660
Clay	0.88 (10% moisture) 1.76 (50% moisture)	1600 (dry) 1760 (wet)

3. Results

3.1. Analyzing Pyranometer and Heat Flux Data

The ratio of the incoming solar irradiance leading to a heat flux under the asphalt can be used as a measure of the efficiency of the asphalt layer as a heat collector. The daily average absorption ratio, σ, for the given day was calculated by integrating the solar irradiance, E_e (radiant exposure [H] = Wh/m^2) and heat flux, ϕ, over a 24 h period, as follows:

$$\sigma = \frac{(1/T)\int_{t\in T}\phi(t)\mathrm{d}t}{(1/T)\int_{t\in T}E_e(t)\mathrm{d}t} = \frac{\overline{\phi}}{\overline{E_e}} \tag{1}$$

This formula applied for the 23th of April gives the following result:

$$\sigma = \frac{14\ \mathrm{Wh/m^2}}{230\ \mathrm{Wh/m^2}} = 5.9\%, \tag{2}$$

As expected, the soil warms up in April, which is spring time in the northern hemisphere. The net heat flux is rather small due to high negative flux during the night. Liquid circulation assisted by pumps could be utilized for optimizing the heat transfer to the soil. Heat loss can also be reduced by many other technical means, such as by selecting optimal materials in different soil layers, or by using an insulating cover during the night. The full potential of the asphalt layer can be estimated by calculating the absorption ratio in an optimal case where the nighttime heat loss is totally eliminated by accumulating only the positive heat flux. The absorption ratio of this optimal case, σ_p, is:

$$\sigma_p = \frac{139\ \mathrm{Wh/m^2}}{230\ \mathrm{Wh/m^2}} = 60\%, \tag{3}$$

Although the average heat flux was 139 Wh/m^2 during the daytime, which is 60% of the daytime solar irradiance, the absorption rate for the entire day was only 14 Wh/m^2, which is only 5.9% of the solar irradiance. This reduction was caused by the heat loss that occurred during the nighttime; see Figure 6.

3.2. Relation between the Cumulative Heat Flux and Soil Temperature

The soil temperature, T, is directly proportional to the heat, Q, stored in the soil since $Q = c\,m\,\Delta T$, where m is the mass of the volume unit of soil [m] = kg/m^3 and [c] = [kJ/kg·°C] is the specific heat capacity of soil. Since the heat, Q, is an integral of heat flux, ϕ, in time t and the surface S, the following equation, showing the dependency between soil temperature and heat flux, is obtainable:

$$\int_0^t \oint_S \vec{\phi}\cdot d\vec{s}\,dt = c\,m\,\Delta T, \tag{4}$$

where ϕ is the heat flux into the unit of soil volume surrounded by the closed surface, S, during time dt.

The pyranometer and the heat flux plate data were used for estimating the absorption efficiency of the asphalt layer. Changes in the underground temperatures were acquired using the DTS measurement method, and they are proportional to the integral sum of the net heat flux.

As an example of daily data analysis, Figure 6 represents the measured solar irradiance and heat flux on the 23rd of April.

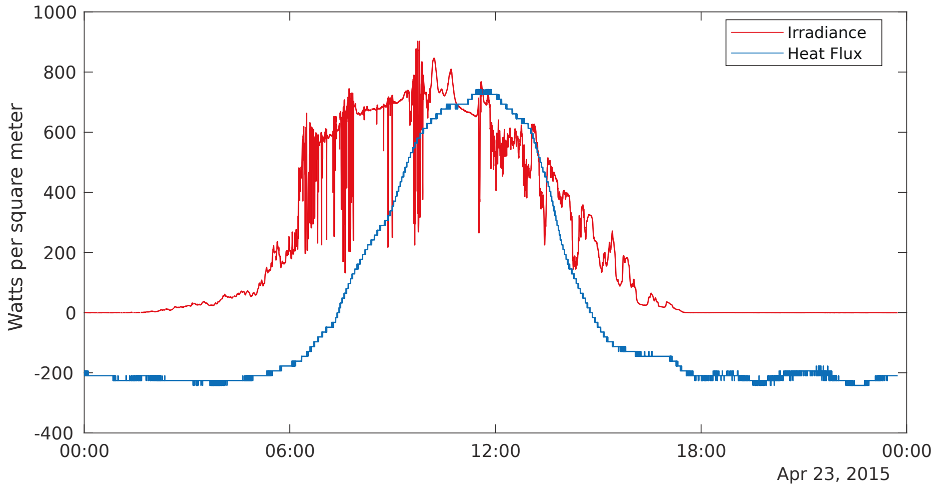

Figure 6. Solar irradiance, $E_e(t)$[W/m^2] (pyranometer) and heat flux, $\overline{\phi}$ [W/m^2] (heat flux plate), as a function of time (h) for the 23rd of April 2015.

The solar irradiance measured by the pyranometer is always positive since it represents the solar energy received as watts per square meter. The data shown in Figure 6 spans from 00:00 until 23:59. The sunlight on the 23rd of April 2015 started at 3:30 due to the northern latitude of Finland and lasted until 17:00, having a peak of 900 W/m^2 at 11:00. The data were sampled every 10 s and included relatively large and fast fluctuations due to cloud shadows and reflections.

Figure 6 also represents the net heat flux, ϕ, through the asphalt surface for the same day. Heat flux can have negative values when the thermal energy is dissipated back onto the surface from the ground. The figure shows that the solar irradiance induces a positive heat flux towards the ground, whereas the heat flux becomes negative when the irradiance is close to zero. The solar irradiance must be greater than the heat loss to achieve positive heat flux. The heat loss depends on the soil temperature, air temperature, and the weather conditions. The heat loss is relatively small in spring when the soil is still cool and relatively high in autumn when the soil is warm. Although the peak heat flux was 700 W/m^2, the average heat flux $\overline{\phi}$ for the given day was only 14 W/m^2. The average heat loss was approximately 130 Wh/m^2.

Figures 7–10 illustrate the instantaneous balances during 5 day periods of heat flux (average net heat flow and average positive heat flow are measured with heat flux plate, including diffuse irradiance) and irradiance (direct solar irradiance measured by pyranometer) in four different seasons. The data shown in the figures are summarized in Table 3. Heat flux value for autumn is negative because the soil is still warm but is cooling down continuously. In winter, the positive heat flux is small, depending more on the air temperature than negligible irradiance, and losses are small due to the annual soil temperature minimum and the insulating snow cover. The soil starts warming quickly during spring when the irradiance is increasing but the soil temperature is still low, keeping losses small. Solar irradiance is greatest during the summer, but the net heat flux is not very strong because the soil is already warm and the losses are also high.

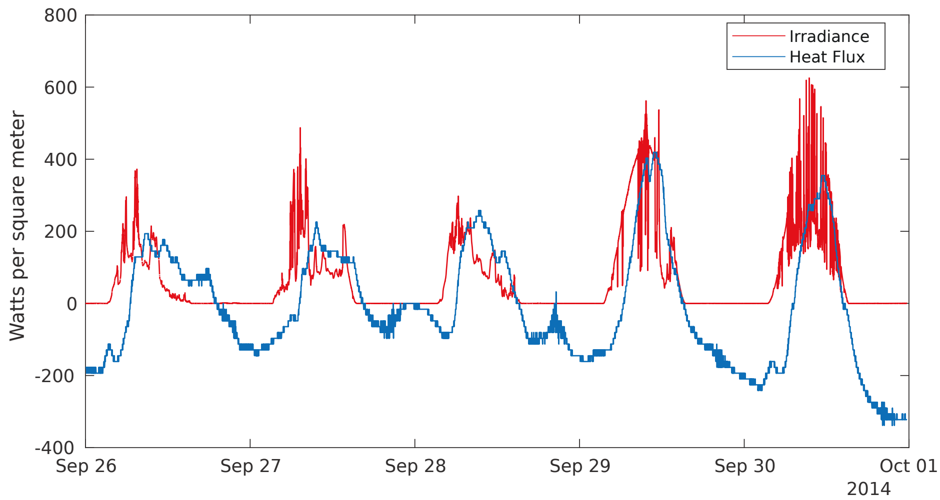

Average solar radiation $\overline{E}_e$	92 W/m^2
Average net heat flux $\overline{\phi}$	-27 W/m^2
Absorption ratio σ	-30%
Average positive heat flux $\overline{\phi}_p$	60 W/m^2
Absorption ratio, positive flux σ_p	65%

Figure 7. Instantaneous solar irradiation $\overline{E}_e$ [W/m^2] and heat flux $\overline{\phi}$ [W/m^2] from 26 Sep to 01 Oct 2014 (autumn) as a function of time and estimated average values as a function of time (day).

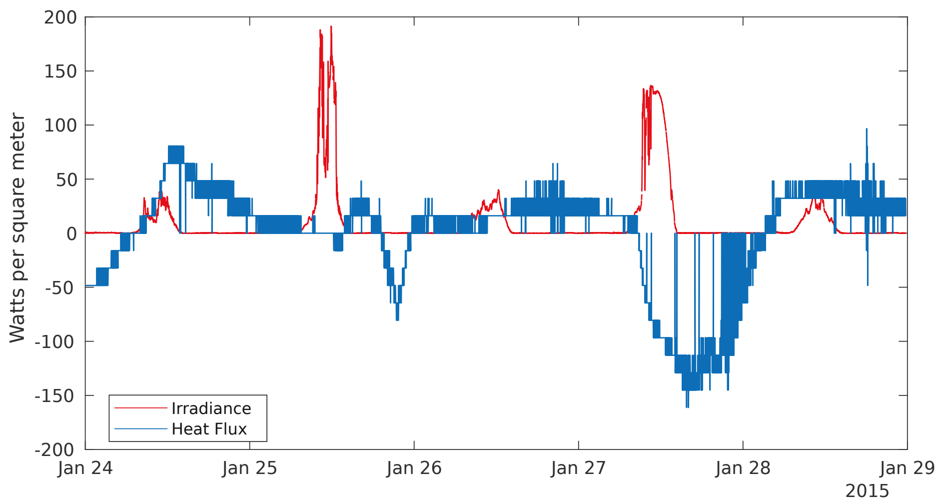

Average solar radiation $\overline{E}_e$	11 W/m^2
Average net heat flux $\overline{\phi}$	-1.9 W/m^2
Absorption ratio σ	-18%
Average positive heat flux $\overline{\phi}_p$	16 W/m^2
Absorption ratio, positive flux σ_p	150%

Figure 8. Instantaneous solar irradiation [W/m^2] and heat flux [W/m^2] from 24 to 29 Jan 2015 (winter), and their estimated average values as a function of time (day). Both irradiance and heat flux are negligible and heat flux is more dependent on the temperature than irradiance.

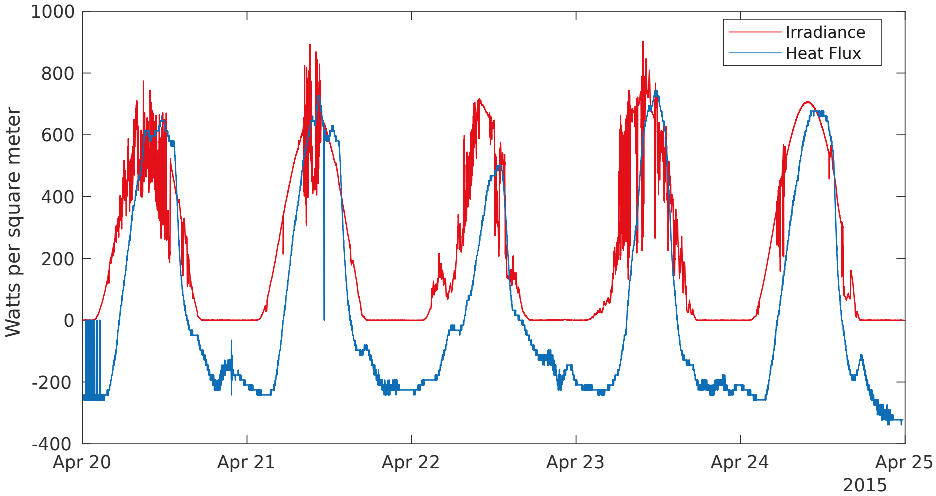

Average solar radiation $\overline{E}_e$	230 W/m^2
Average net heat flux $\overline{\phi}$	42 W/m^2
Absorption ratio σ	18%
Average positive heat flux $\overline{\phi}_p$	150 W/m^2
Absorption ratio, positive flux σ_p	67%

Figure 9. Instantaneous solar irradiation $\overline{E}_e$ [W/m^2] and heat flux [W/m^2] from 20 to 25 Apr 2015 (spring) as function of time (day) and their estimated average values.

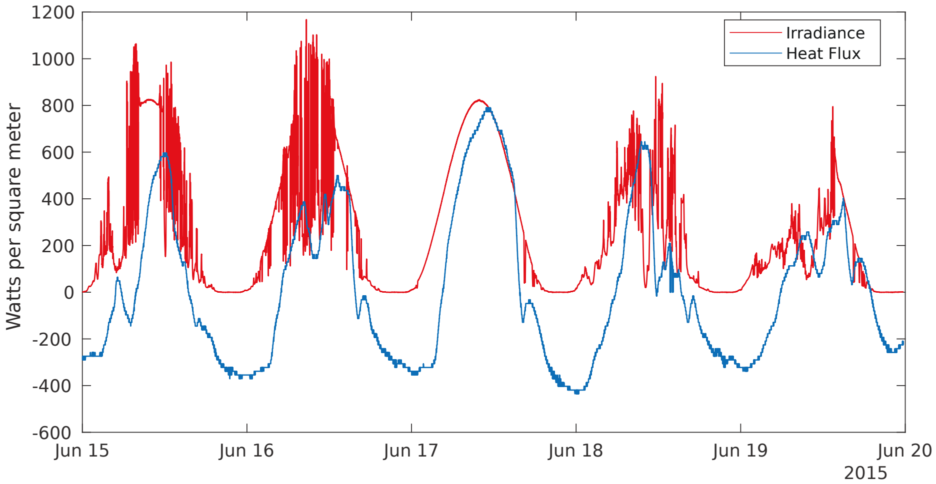

Average solar radiation $\overline{E}_e$	260 W/m^2
Average net heat flux $\overline{\phi}$	8.4 W/m^2
Absorption ratio σ	3.3%
Average positive heat flux $\overline{\phi}_p$	190 W/m^2
Absorption ratio, positive flux σ_p	53%

Figure 10. Instantaneous solar irradiation $\overline{E}_e$ [W/m^2] and heat flux $\overline{\phi}$ [W/m^2] from 15 to 20 Jun 2015 (summer) as a function of time (day) and their estimated average values.

Because thermal energy loss due to radiation and convection also occurs during daytime, the positive heat flux could be further improved by lowering the temperature of the surface during daytime hours; for example, by collecting and transferring thermal energy to seasonal storage. This would allow the utilization of this urban renewable energy even in cold climate regions. Further research is needed to find the full potential of the asphalt heat collection and storage system.

3.3. Temperature Distribution Measurements Using DTS

Using the DTS system, temperatures were measured periodically at certain depths. These measurements helped to analyze how the temperature below the surface is distributed. The selected measurement depths in this research are 0.5 m, 1 m, 1.5 m, 3 m, 5 m, and 10 m. Measurements for a period of one year are represented in Figure 11. From April to September, temperatures rise in the shallowest layers. Instead, from October to March the temperatures decrease. At the depth of 10 m the differences in temperature in the shallowest layers have no effect anymore.

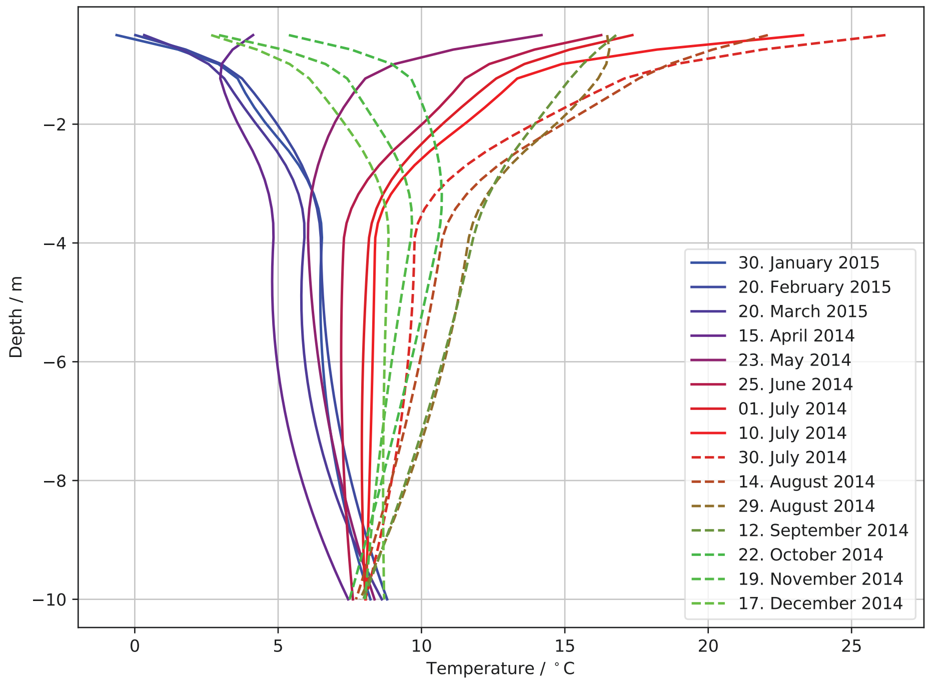

Figure 11. Seasonal soil temperatures at different depths from the surface according to the DTS measurements. During the summer (April–September) temperatures near the surface increase, and during winter months (October–March) the surface is the coldest. At 10 m depth the effect of the Sun is diminished.

Figure 12 represents the temperature changes of the upper layers of the ground from the surface down to 10 m. The data, acquired from the DTS system, clearly indicates that the deeper layers of the soil react to the heat flux with delay compared to the shallowest layers of the soil. This delay depends on soil type and heat conductivity, k. The curves for July and October show that the shallowest layers are already cooled down in October, but the temperatures of depths below 4 m tend to stay steady. The curves for October and December show that while the shallowest layers keep cooling down, the temperatures of deeper layers also drop. After the snow melts in April, the temperature of the shallowest layer begins to increase but the deeper layers are not affected. During May and the following months of summer, the temperatures continue to increase. Deeper layers are always more steady than the surface, and they absorb or release thermal energy much more slowly. The temperature change near the surface is positive between April and August and negative from the beginning of August until the beginning of March. The deeper layers of soil keep the thermal energy longer than the surface layer, and therefore, the cumulative thermal energy begins decreasing in the middle of October. When fast temperature increase occurs on the shallowest layers, some thermal energy can be delivered to the deeper layers to be stored.

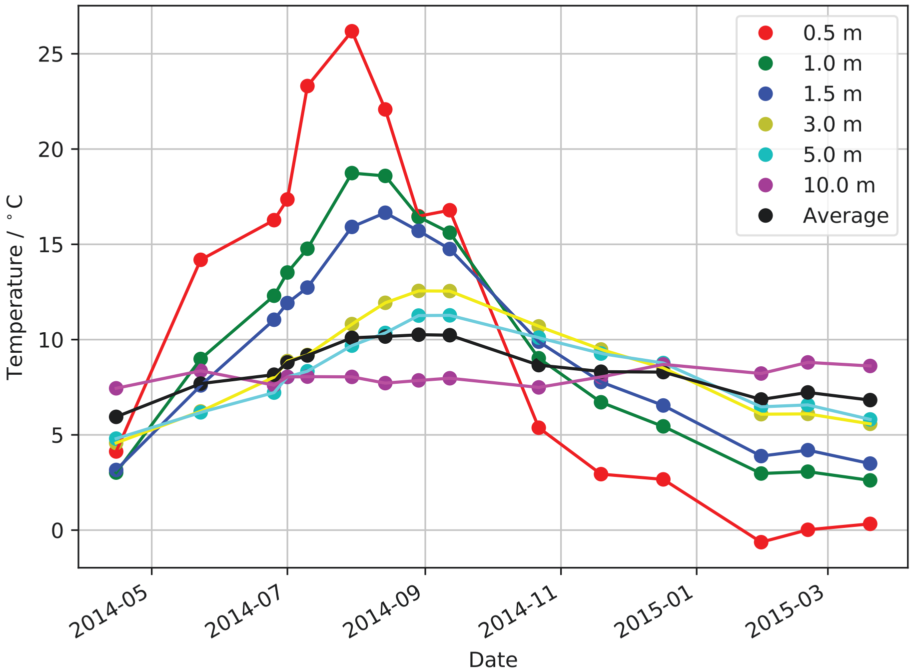

Figure 12. Soil temperatures measured at different depths (0.5 m, 1.0 m, ..., 10 m) and the weighted average temperature of the whole 10 m deep layer.

Figure 13 shows the solar irradiation and the cumulative heat flux from asphalt to the deeper soil layers. In addition to showing the net heat flux, the negative and positive parts of the heat flux are also integrated separately to obtain a better understanding of the flow. The cumulative net flow and the temperature of the soil are increasing until the 26th of September, when the cumulative irradiance is 870 kWh/m^2; cumulative positive, negative, and net flows are 610 kWh/m^2, 460 kWh/m^2, and 150 kWh/m^2, respectively. The positive, negative, and net flows correspond to 70%, 53%, and 17%, respectively, of the cumulative solar irradiance.

Figures 12 and 13 are not directly comparable, since they contain measurements taken in different years, but show similar results. Furthermore, the heat flux of the asphalt surface is not directly related to the internal heat exchanges inside the soil. Better conformance is obtained by comparing the cumulative heat flux with the average temperature through all soil layers, shown by the black line in Figure 12.

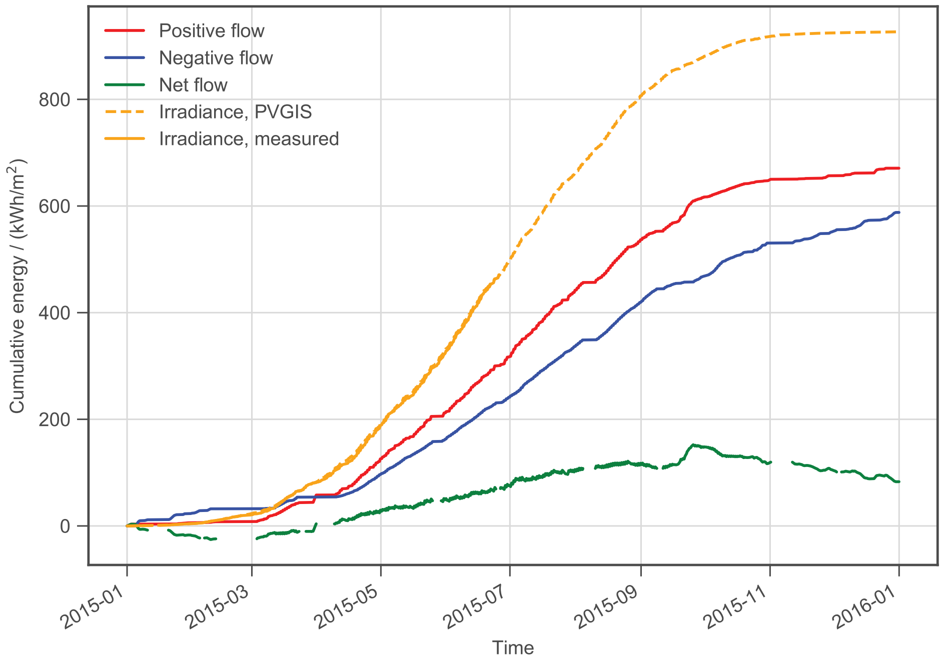

Figure 13. Hourly integrated cumulative irradiance and cumulative heat flux under the asphalt layer over an annual cycle. The net flow consists of the cumulative hourly positive flow into the ground and the cumulative hourly negative flow escaping from the ground. After the warming period, in 26th of September the positive flow is about 70% of the solar irradiance and the net flow is only about 17% of it. Irradiance PVGIS is the Solar irradiance estimated using the Photo Voltaic Geographical Information System [36,37].

4. Discussion and Conclusions

The data collected in this research make it possible to analyze the performance of the asphalt as a heat collection system during any time of the year. Selected periods of five-day data from every season of the year were analyzed and are represented in Figures 7–10.

When thermal energy is collected by the asphalt layer, the temperature rises, causing a temperature gradient that drives a heat flux through the soil, according to Fourier's law, $\phi = -k\nabla T$. Here k is the thermal conductivity $[k]$ = W/m K, and T is the temperature $[T]$ = K . The temperature distributions shown in Figure 11 reveal a high gradient in the topmost gravel layer and a gentler sloping gradient in the deeper layers, such as clay and bedrock. The same observation was seen in the preceding laboratory measurements as well, as reported in [14]. This structure is not desirable for solar energy storage. The thermal energy flowing through the asphalt is not efficiently distributed in the bigger soil volume because it is dissipated back to the atmosphere during the night until the thermal energy penetrates deeper layers (Figure 13). The heat loss can be eliminated by decreasing the soil surface temperature close to the ambient temperature by transferring the thermal energy from the surface. For this purpose, the model in which the energy is harvested from the surface and stored 6 m under the surface, expressed by Ho et al. [15], could be a working solution. The ground structure could be optimized by increasing the conductivity of the surface by changing the materials or by irrigation. According to Loomans et al. [6] the thermal energy could be harvested inside the asphalt, between two asphalt layers. In their model there are several layers—a thin asphalt layer on the surface, the asphalt pavement layer, and an asphalt layer with heat transfer tubes, and beneath them, asphalt layers again.

Figures 12 and 13 indicate that the net heat flux becomes positive during March or April, depending on the year, and turns back to negative in September or October. The surface reaches its peak temperature at the end of July but remains warm enough to continue driving positive net heat flux to the ground until the 26th of September. The average net heat flux is less than 15% of the available irradiance due to the nighttime thermal energy losses, while the average positive thermal energy is 64% of the irradiance. This positive heat flux could be more efficiently utilized by reducing nighttime losses, which were, according to Table 3, 3/4 of the positive heat flux during spring and summer, and even higher during autumn.

Table 3. Average solar irradiance, heat flux, and absorption ratios over five day periods in all seasons. The first three rows represent the average net heat collection values over the whole period and the next two rows represent the corresponding values for positive values.

Parameter	Autumn	Winter	Spring	Summer	Yearly Average
Average solar irradiance $\overline{E}_e$	92 W/m^2	11 W/m^2	230 W/m^2	260 W/m^2	148 W/m^2
Average net heat flux $\overline{\phi}$	−28 W/m^2	−1.9 W/m^2	42 W/m^2	8.4 W/m^2	9.5 W/m^2
Absorption ratio σ	−30%	−18%	18%	3.3%	6.4%
Average positive heat flux $\overline{\phi}_p$	60 W/m^2	16 W/m^2	150 W/m^2	190 W/m^2	104 W/m^2
Absorption ratio, positive flux σ_p	65%	145%	65%	73%	70%

The measurements revealed that the current efficiency of the asphalt pavement in absorbing solar irradiation during the soil warming period between 1st of January and 26th of September is about 17% (see Figure 13). If the nighttime escape of thermal energy can be eliminated, transferring thermal energy away from the surface, the efficiency could be up to 70% in the same time period (Table 3). The efficiency could also be increased by covering the asphalt field with insulating cover during the night. The cumulative irradiance, net heat flux, and positive heat flux in the asphalt field during the soil warming period were 870 kWh/m^2, 150 kWh/m^2, and 610 kWh/m^2, respectively. Cumulative irradiance, net heat flux, and positive heat flux during the whole year were 930 kWh/m^2, 83 kWh/m^2, and 670 kWh/m^2, respectively. These results imply that the asphalt layer could potentially collect up to 670 kWh/m^2 (see Figure 13), provided that the losses can be properly handled. The temperature of the surface layer is relatively low, exceeding +20 °C at 0.5 m depth only in the middle of the summer. The temperature of the heat collection liquid usually needs to be elevated using heat pumps before it can be used for heating purposes. In some applications, such as melting the snow on the asphalt field or making electricity by using thermocouples [38], it could be used without heat pumps. DTS measurements show (Figure 11) that the annual changes in the soil temperature, caused by the solar radiation, mostly occur within the first 10 m below the ground level. Identical results have been found by Ho et al. [15].

Some unexpected environmental factors occurred while taking the measurements, such as shadows of cars parking over the measurement area. The long time, which were needed to take the measurements, caused some interruption in data acquisition. These interruptions were mainly caused by battery depletion, software resets due to power shortages, and other unknown reasons. Measurement equipment could be developed by getting an instrument amplifier and backup power. In the future, these losses could be estimated and compensated for using Kalman filters and other estimation methods. In such a study, the asphalt and the layers below it are typically used in Finland. These results must not be generalized if the layers and the surroundings differ from those in this research. The data were acquired during a 1–2 year period, which is relatively short term taking into account the annual variation in weather.

In this research, the heat collecting properties of the existing asphalt fields were analyzed and some suggestions for improving the collection efficiency were made. Three independent methods were used to measure the solar irradiance, heat flux, and soil temperature, to explain the behavior of the asphalt pavement for collecting solar energy. This combination of methods was found to give valuable information for harvesting and storing of solar energy in cold climate region. Further research using thermal simulations and experiments is needed to study how much the active and passive heat transfer mechanisms, such as under-asphalt soil structures, could improve the net thermal energy collection efficiency in a practical case. Complementary information could be measured by using a radio net meter to measure the absorption and emission of the asphalt. [6] When the vertical temperature distribution (thermal gradient) in the soil is known, it can be used to optimize geothermal energy harvesting and storing applications in the future. An interesting model with which to apply the results of this study for a snow-melting system was proposed by Ho et al. [15]. The model consists of two pipe lines. The first one is embedded below the pavement and an another is located 6 m under the surface. The upper pipeline can be used to harvest heat in summer and for snow-melting in winter. Another pipeline can be used as a seasonal energy storage in summer and used for snow-melting in winter. The optimized asphalt pavements could act as solar collectors [1,39] and mitigate the urban heat island (UHI) effect [40].

Author Contributions: Software development, data curation, formal analysis C.Ç.; validation, C.Ç. and P.V.; methodology, investigation, writing–original draft preparation, visualization, C.Ç. and A.M.; resources, E.H.; writing–review and editing, A.M. and E.H.; supervision, P.V., E.H. and M.E. All authors have read and agreed to the published version of the manuscript.

Funding: This research received no external funding.

Acknowledgments: The authors gratefully acknowledge the financial support of the City of Vaasa and the Graduate School of the University of Vaasa.

Conflicts of Interest: The authors declare no conflict of interest.

References

1. Bobes-Jesus, V.; Pascual-Muñoz, P.; Castro-Fresno, D.; Rodriguez-Hernandez, J. Asphalt solar collectors: A literature review. *Appl. Energy* **2013**, *102*, 962–970. [CrossRef]
2. Bijsterveld, W.T.V.; Houben, L.J.M.; Scarpas, A.; Molenaar, A.A.A. Using Pavement as Solar Collector: Effect on Pavement Temperature and Structural Response:. *Transp. Res. Rec.* **2001**. [CrossRef]
3. Li, C.; Shang, J.; Cao, Y. Discussion on energy-saving taking urban heat island effect into account. In Proceedings of the 2010 International Conference on Power System Technology, Hangzhou, China, 24–28 October 2010; pp. 1–3. [CrossRef]
4. Mäkiranta, A.; Hiltunen, E. Utilizing Asphalt Heat Energy in Finnish Climate Conditions. *Energies* **2019**, *12*, 2101. [CrossRef]
5. Majorowicz, J.; Grasby, S.E.; Skinner, W.R. Estimation of Shallow Geothermal Energy Resource in Canada: Heat Gain and Heat Sink. *Nat. Resour. Res.* **2009**, *18*, 95–108. [CrossRef]
6. Loomans, M.; Oversloot, H.; De Bondt, A.; Jansen, R.; Van Rij, H. Design tool for the thermal energy potential of asphalt pavements. In Proceedings of the Eighth International IBPSA Conference, Eindhoven, The Netherlands, 11–14 August 2003; pp. 745–752.
7. Hailu, G.; Hayes, P.; Masteller, M. Long-Term Monitoring of Sensible Thermal Storage in an Extremely Cold Region. *Energies* **2019**, *12*, 1821. [CrossRef]
8. Mehrpooya, M.; Hemmatabady, H.; Ahmadi, M.H. Optimization of performance of Combined Solar Collector-Geothermal Heat Pump Systems to supply thermal load needed for heating greenhouses. *Energy Convers. Manag.* **2015**, *97*, 382–392. [CrossRef]
9. Hesaraki, A.; Holmberg, S.; Haghighat, F. Seasonal thermal energy storage with heat pumps and low temperatures in building projects—A comparative review. *Renew. Sustain. Energy Rev.* **2015**, *43*, 1199–1213. [CrossRef]
10. Sibbitt, B.; McClenahan, D.; Djebbar, R.; Thornton, J.; Wong, B.; Carriere, J.; Kokko, J. The Performance of a High Solar Fraction Seasonal Storage District Heating System—Five Years of Operation. *Energy Procedia* **2012**, *30*, 856–865. [CrossRef]
11. Lund, J.W.; Freeston, D.H.; Boyd, T.L. Direct utilization of geothermal energy 2010 worldwide review. *Geothermics* **2011**, *40*, 159–180. [CrossRef]
12. Mesquita, L.; McClenahan, D.; Thornton, J.; Carriere, J.; Wong, B. Drake Landing Solar Community: 10 Years of Operation. In *Proceedings of SWC2017/SHC2017*; International Solar Energy Society: Abu Dhabi, UAE, 2017; pp. 1–12. [CrossRef]

13. Haq, H.M.K.U.; Hiltunen, E. An inquiry of ground heat storage: Analysis of experimental measurements and optimization of system's performance. *Appl. Therm. Eng.* **2019**, *148*, 10–21. [CrossRef]
14. Martinkauppi, J.B.; Mäkiranta, A.; Kiijärvi, J.; Hiltunen, E. Thermal Behavior of an Asphalt Pavement in the Laboratory and in the Parking Lot. *Sci. World J.* **2015**, *2015*. [CrossRef]
15. Ho, I.H.; Dickson, M. Numerical modeling of heat production using geothermal energy for a snow-melting system. *Geomech. Energy Environ.* **2017**, *10*, 42–51. [CrossRef]
16. File: Fennoscandia.png—Wikimedia Commons, the Free Media Repository. 2019. Available Online: https://commons.wikimedia.org/w/index.php?title=File:Fennoscandia.png&oldid=365664646 (accessed on 14 January 2020).
17. Finnish Meteorological Institute FMI: Heating Degree Days. Available online: https://en.ilmatieteenlaitos.fi/heating-degree-days (accessed on 13 January 2020).
18. Finnish Meteorological Institute FMI: Monthly Average Air Temperature Data 2014–2016, Klemettilä, Vaasa. Available online: https://ilmatieteenlaitos.fi/havaintojen-lataus#! (accessed on 28 January 2019).
19. Hall, M.R.; Dehdezi, P.K.; Dawson, A.R.; Grenfell, J.; Isola, R. Influence of the Thermophysical Properties of Pavement Materials on the Evolution of Temperature Depth Profiles in Different Climatic Regions. *J. Mater. Civ. Eng.* **2012**, *24*, 32–47. [CrossRef]
20. Strzelczyk, P.; Szewczyk, M.; Gałek, R.; Gil, P. Measurement of solar radiation properties and thermal energy of the atmosphere in Rzeszow. In *Zeszyty Naukowe Politechniki Rzeszowskiej. Mechanika*; z. 90 [298], nr 4; Rzeszow University of Technology: Rzeszow, Poland, 2018.
21. Van den Box, K. Hukseflux User Manual LP02, Second Class Pyranometer. 2015. Available online: https://www.hukseflux.com/uploads/product-documents/LP02_manual_v1606.pdf (accessed on 12 September 2019).
22. Hoeksema, E. User Manual, HFP01 & HFP03, Heat Flux Plate/Heat Flux Sensor. 2015. Available Online: https://www.hukseflux.com/uploads/product-documents/HFP01_HFP03_manual_v1721.pdf (accessed on 12 September 2019).
23. Zhu, K.; Blum, P.; Ferguson, G.; Balke, K.D.; Bayer, P. The geothermal potential of urban heat islands. *Environ. Res. Lett.* **2010**, *5*, 044002. [CrossRef]
24. Fisher, A.T.; Mankoff, K.D.; Tulaczyk, S.M.; Tyler, S.W.; Foley, N.; WISSARD Science Team. High geothermal heat flux measured below the West Antarctic Ice Sheet. *Sci. Adv.* **2015**, *1*, e1500093. [CrossRef]
25. Ouyang, L.B.; Belanger, D. Flow Profiling via Distributed Temperature Sensor (DTS) System—Expectation and Reality. In Proceedings of the Society of Petroleum Engineers, SPE Annual Technical Conference and Exhibition, Houston, TX, USA, 26–29 September 2004. [CrossRef]
26. Coleman, T.I.; Parker, B.L.; Maldaner, C.H.; Mondanos, M.J. Groundwater flow characterization in a fractured bedrock aquifer using active DTS tests in sealed boreholes. *J. Hydrol.* **2015**, *528*, 449–462. [CrossRef]
27. Henninges, J.; Zimmermann, G.; Büttner, G.; Schrötter, J.; Erbas, K.; Huenges, E. Fibre-optic temperature measurements in boreholes. In Proceedings of the 7th FKPE-Workshop "Bohrlochgeophysik and Gesteinsphysik", GeoZentrum Hannover, Hannover, Germany, 23–24 October 2003; pp. 23–24.
28. *Oryx DTS User Manual v4*; Sensornet Ltd.:, London, UK, 2007.
29. Ukil, A.; Braendle, H.; Krippner, P. Distributed Temperature Sensing: Review of Technology and Applications. *IEEE Sens. J.* **2012**, *12*, 885–892. [CrossRef]
30. Sayde, C.; Gregory, C.; Gil-Rodriguez, M.; Tufillaro, N.; Tyler, S.; Giesen, N.V.d.; English, M.; Cuenca, R.; Selker, J.S. Feasibility of soil moisture monitoring with heated fiber optics. *Water Resour. Res.* **2010**, *46*. [CrossRef]
31. Xu, Q.; Solaimanian, M. Modeling temperature distribution and thermal property of asphalt concrete for laboratory testing applications. *Constr. Build. Mater.* **2010**, *24*, 487–497. [CrossRef]
32. Valtanen, E. *The Handbook of Math and Physics*, *Matematiikan ja Fysiikan Käsikirja*, 2 ed.; Genesis-kirjat Oy: Jyväskylä, Finland, 2007.
33. Engineering Toolbox. Densities and Heat Capacities of Materials. Available Online: https://www.engineeringtoolbox.com (accessed on 15 December 2019).
34. Blocon, A. EED Earth Energy Designer-Vertical Borehole Design Program for. 2015. Available online: https://www.buildingphysics.com/manuals/EED3.pdf (accessed on 20 October 2019).
35. Ronkainen, N. *Properties of Finnish Soil Types*; Finnish Environment Institute: Helsinki, Finland, 2012. Available online: https://core.ac.uk/download/pdf/14927376.pdf (Accessed on 5 December 2019).

36. Gracia, A.M.; Huld, T.; European Commission; Joint Research Centre; Institute for Energy and Transport. *Performance Comparison of Different Models for the Estimation of Global Irradiance on Inclined Surfaces: Validation of the Model Implemented in PVGIS*; Publications Office: Luxembourg, 2013.
37. European Comission, J.R.G. Photovoltaic Geographical Information System. 2014. Available Online: http://re.jrc.ec.europa.eu/pvgis (accessed on 21 September 2019).
38. Datta, U.; Dessouky, S.; Papagiannakis, A.T. Thermal Energy Harvesting from Asphalt Roadway Pavement. In *Advancement in the Design and Performance of Sustainable Asphalt Pavements*; Mohammad, L., Ed.; Sustainable Civil Infrastructures; Springer International Publishing: Cham, Switzerland, 2018; pp. 272–286. Available online: https://link.springer.com/chapter/10.1007/978-3-319-61908-8_20 (accessed on 20 February 2020)
39. Basheer Sheeba, J.; Krishnan Rohini, A. Structural and Thermal Analysis of Asphalt Solar Collector Using Finite Element Method. *J. Energy* **2014**, *2014*, 602087. [CrossRef]
40. Pascual-Muñoz, P.; Castro-Fresno, D.; Serrano-Bravo, P.; Alonso-Estébanez, A. Thermal and hydraulic analysis of multilayered asphalt pavements as active solar collectors. *Appl. Energy* **2013**, *111*, 324–332. [CrossRef]